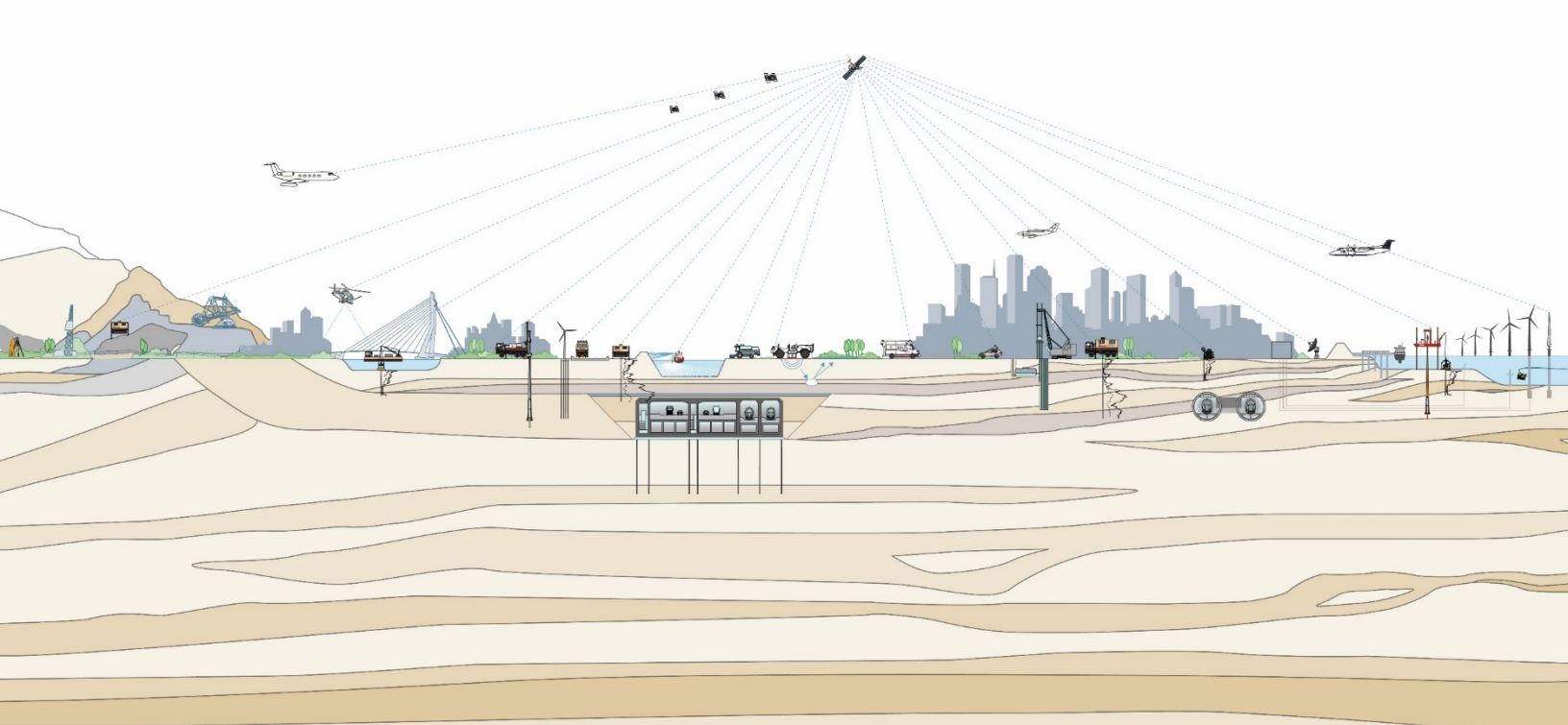


EFFECTS OF CYCLIC LOADING ON SUCTION BUCKET FOUNDATIONS FOR OFFSHORE WIND TURBINES

Prepared for:
Bureau of Safety and
Environmental Enforcement

August 2016
Project No. 04.76160003





FUGRO CONSULTANTS, INC.

August 26, 2016
Project No. 04.76160003

Bureau of Safety and Environmental Enforcement
Acquisition Operations Branch
45600 Woodland Road, VAE-AMD
Sterling, Virginia 20166-9216

Attention: Mr. Altan Aydin

Subject: Effects of Cyclic Loading on Suction Bucket Foundations for Offshore Wind Turbines

Dear Mr. Aydin:

Fugro Consultants, Inc. (Fugro) is pleased to present this report documenting the methodology, results, and recommendations from the study performed to assess the effects of cyclic loading on suction bucket foundations for offshore wind turbines. Our services are being provided in accordance with Contract No. E16PC00004, dated February 8, 2016. We thank you for the opportunity to work on this project and are looking forward to continuing providing our services in the future.

Sincerely,

FUGRO CONSULTANTS, INC.

A handwritten signature in blue ink that reads "Connor Hayden".

Connor Hayden, Ph.D., P.E.
Senior Staff Engineer

A handwritten signature in blue ink that reads "Weiyu Chen".

Weiyu Chen, Ph.D., P.E. G.E.
Principal Geotechnical Engineer

A handwritten signature in blue ink that reads "Dan Dolan".

Dan Dolan, P.E.
Principal Structural Engineer
(Moffatt & Nichol)

A handwritten signature in blue ink that reads "Thaleia Travararou".

Thaleia Travararou, Ph.D., P.E., G.E.
Principal Geotechnical Engineer



CONTENTS

	Page
1.0 INTRODUCTION.....	1-1
1.1 Project Description and Background.....	1-1
1.2 Work Authorization	1-2
1.3 Scope and Organization	1-2
1.4 Summary and Findings.....	1-2
1.5 Limitations of this Study.....	1-4
2.0 LITERATURE REVIEW.....	2-1
2.1 Design Practice and Guidelines.....	2-1
2.2 Laboratory Soil Element Experiments.....	2-2
2.3 Small Scale Laboratory Model Experiments	2-3
2.4 Large Scale Field experiments	2-5
2.5 Numerical Simulations of Suction Bucket Foundations	2-5
2.6 Wind Turbine Projects Using Suction Bucket Foundations	2-7
3.0 ADVANCED NUMERICAL MODELING METHODOLOGY.....	3-1
3.1 Introduction.....	3-1
3.2 Loading Conditions.....	3-2
3.2.1 Background.....	3-2
3.2.2 Foundations	3-3
3.2.3 Assumptions	3-3
3.2.4 Loads.....	3-3
3.3 Soil Degradation Models.....	3-4
3.3.1 Clay	3-4
3.3.2 Dense Sand	3-6
3.4 Stepping Procedure.....	3-6
3.5 Strength Degradation	3-7
3.6 Estimation of System Fundamental Frequency.....	3-8
4.0 ADVANCED NUMERICAL MODELING ANALYSES RESULTS.....	4-1
4.1 Introduction.....	4-1
4.2 Cyclic Loading on Mono-bucket Foundation	4-1
4.2.1 Uniform Clay (soft and stiff).....	4-1
4.2.2 Stiff Clay	4-2
4.2.3 Dense Sand	4-2
4.2.4 Interlayered.....	4-3
4.3 Cyclic Loading on Multi-Bucket Foundation	4-3
4.3.1 Soft Clay	4-3
4.3.2 Stiff Clay	4-4
4.3.3 Dense Sand	4-4



4.3.4	Interlayered.....	4-5
4.4	Summary.....	4-5
5.0	DEVELOPMENT OF PRELIMINARY DESIGN GUIDELINES	5-1
5.1	Cyclic Design Considerations.....	5-1
5.1.1	Subsurface Conditions and Soil Properties	5-1
5.1.2	Loading Conditions	5-2
5.1.3	Foundation Type	5-2
5.2	Foundation Performance Checklist.....	5-3
5.2.1	Cyclic Stability of Suction Bucket Foundation.....	5-3
5.2.2	Cyclic Settlement and Displacement.....	5-3
5.2.3	Cyclic Foundation Stiffness and Frequency	5-3
5.2.4	Cyclic Soil Reactions on Skirt and Top Plate.....	5-4
5.2.5	Design Considerations	5-4
6.0	RECOMMENDATIONS FOR LABORATORY TESTING AND FUTURE STUDIES	6-1
6.1	Limitations of Existing Studies and Data Gaps	6-1
6.2	Recommendations for Future Laboratory Testing.....	6-1
6.2.1	Elemental Cyclic Soil Behavior.....	6-2
6.2.2	Laboratory Model Experiments	6-3
6.3	Recommendations for Additional Analytical Studies	6-4
6.3.1	Design Soil-Load Combinations	6-4
6.3.2	Definition of “Threshold” Limits.....	6-4
6.3.3	Assessment of Degradation for Actual Foundations.....	6-4
6.3.4	Assessment of Cyclic Wind Loads	6-4
7.0	REFERENCES.....	7-1

TABLES

	Page
Table 2.1-1: Available Design Guidance for Offshore Wind Turbine.....	2-1
Table 2.2-1: Element Level Laboratory Cyclic Soil Tests	2-3
Table 2.3-1: Small-scale Laboratory Experiments for Offshore Foundations.....	2-4
Table 2.4-1: Suction Bucket Field Experiments.....	2-5
Table 2.6-1: OWT Projects with Suction Bucket Foundation	2-7
Table 3.1-1. Foundation System Dimensions.....	3-1
Table 3.1-2. Idealized Soil Properties for FLAC ^{3D} Analyses	3-2
Table 3.2-1: Wave, Current and Wind Load Parameters.....	3-3
Table 3.6-1. Hypothetical Tower Properties for f_n Calculations.....	3-8
Table 4.1-1. Analysis Cases Presented	4-1
Table 4.4-1. Initial Key Response Values.....	4-6
Table 4.4-2. Percent Change in Key Response Values during Storm Loading.....	4-7



Table 4.4-3. Percent Change in Key Response Values during Normal Sea State Loading.....	4-7
Table 5.2-1: Cyclic Suction Bucket Foundation Design Considerations.....	5-4
Table 6.2-1: Soil Classification Properties for US East Coast Offshore Wind Turbine Projects	6-2
Table 6.2-2: Recommendation for Laboratory Cyclic Soil Elemental Tests	6-3
Table 6.2-3: Recommendation for Laboratory Model Experiments.....	6-3

FIGURES

Dimensions of Caisson Foundation Systems and FLAC3D Model	3.1-1
Monocaisson Foundation Loading Time History.....	3.2-1
Tetrapod Foundation Loading Time History	3.2-2
Comparison of Vucetic and Dobry (1988) to Degradation Data.....	3.3-1
Degradation Parameter Form Used in this Study	3.3-2
Example Degradation Index Curves for Varying Shear Strains	3.3-3
Example Approach to Variable Shear Strains	3.3-4
Example of Finn/Byrne Model for Three Strain Levels	3.3-5
Example of Stepping Procedure.....	3.4-1
Validation of Stepping Approach – Contours After 900 Cycles.....	3.4-2
Validation of Stepping Approach – Rotation After 900 Cycles	3.4-3
Illustration of Stiffness Reduction Impact on Global Fundamental Frequencies	3.6-1
Degradation Index Contours – Monocaisson, Soft Clay	4.2-1
Rotational Stiffness vs. Time – Monocaisson, Soft Clay.....	4.2-2
Global Fundamental Frequency vs. Time – Monocaisson, Soft Clay.....	4.2-3
Maximum Total Rotation vs. Time – Monocaisson, Soft Clay.....	4.2-4
Degradation Index Contours – Monocaisson, Stiff Clay	4.2-5
Rotational Stiffness vs. Time – Monocaisson, Stiff Clay.....	4.2-6
Global Fundamental Frequency vs. Time – Monocaisson, Stiff Clay.....	4.2-7
Maximum Total Rotation vs. Time – Monocaisson, Stiff Clay	4.2-8
Degradation Index Contours – Monocaisson, Dense Sand	4.2-9
Rotational Stiffness vs. Time – Monocaisson, Dense Sand.....	4.2-10
Global Fundamental Frequency vs. Time – Monocaisson, Dense Sand.....	4.2-11
Maximum Total Rotation vs. Time – Monocaisson, Dense Sand.....	4.2-12
Degradation Index Contours – Monocaisson, Interlayered	4.2-13
Rotational Stiffness vs. Time – Monocaisson, Interlayered	4.2-14
Global Fundamental Frequency vs. Time – Monocaisson, Interlayered	4.2-15
Maximum Total Rotation vs. Time – Monocaisson, Interlayered	4.2-16
Degradation Index Contours – Tetrapod, Soft Clay	4.3-1
Rotational Stiffness vs. Time – Tetrapod, Soft Clay	4.3-2
Global Fundamental Frequency vs. Time – Tetrapod, Soft Clay	4.3-3
Maximum Total Rotation vs. Time – Tetrapod, Soft Clay	4.3-4



Degradation Index Contours – Tetrapod, Stiff Clay	4.3-5
Rotational Stiffness vs. Time – Tetrapod, Stiff Clay.....	4.3-6
Global Fundamental Frequency vs. Time – Tetrapod, Stiff Clay	4.3-7
Maximum Total Rotation vs. Time – Tetrapod, Stiff Clay.....	4.3-8
Degradation Index Contours – Tetrapod, Dense Sand.....	4.3-9
Rotational Stiffness vs. Time – Tetrapod, Dense Sand	4.3-10
Global Fundamental Frequency vs. Time – Tetrapod, Dense Sand	4.3-11
Maximum Total Rotation vs. Time – Tetrapod, Dense Sand	4.3-12
Loading Mechanism – Monocaisson vs. Multicaisson	5.1-1

SECTION 1.0



1.0 INTRODUCTION

1.1 PROJECT DESCRIPTION AND BACKGROUND

Suction buckets have widely been used as foundations for offshore oil and gas platforms; however, there have been limited applications in Offshore Wind Turbine (OWT) projects. For the OWT foundation, in addition to the design requirements on capacity and displacement, the foundation and overall system frequencies can only operate within a narrow range, which is different from the typical oil and gas platform. Due to limited data and case histories, this research study was requested by the Bureau of Safety and Environmental Enforcement (BSEE) to assist in assessing the feasibility of suction bucket foundations for OWT projects. This report presents the results from advanced numerical analyses performed to assess the effect of cyclic loading on the response of Offshore Wind Turbines (OWT) founded on suction bucket foundations. In particular, the primary goal of this study is to provide insight with respect to the effect of soil stiffness and strength degradation on the response of OWT founded on suction bucket foundations when subjected to a large number of loading cycles. Of primary interest is the assessment of the effect of the soil stiffness and strength degradation on the foundation stiffness and associated fundamental period of the OWT system to ensure appropriate foundation design and avoidance of potential resonance phenomena.

Throughout the design life of an offshore wind turbine (typically 20 – 30 years), the foundation will be subjected to permanent, cyclic, and extreme loads including, but not limited to: 1) environmental loads (wind, wave, and current), 2) structure-associated loads, and 3) other loads (accidental and operating loads). These different loading mechanisms excite the system with a wide range of frequencies adding complexity to the foundation response. For the cyclic foundation design, environmental loads, including wind and wave loads, and their impacts towards foundation performance are of the highest importance and are the main focus of this study. When subjected to cyclic loads, cyclic displacement of the suction bucket foundation would affect adjacent soils, which in return affect the cyclic foundation behavior through soil-foundation interaction effects. Under cyclic loads, soil strength can degrade, which is an issue under both operating and extreme loading conditions. Additionally, soil stiffness can degrade and result in excess deformation and change in natural frequency, which could be an issue due to the potential for resonant response under the operating conditions of the turbine.

The cyclic response of the wind turbine system can change with the load amplitudes and number of loading cycles owing to changes in foundation stiffness during cyclic loading. Laboratory tests have shown that wind turbines founded in relatively dense sands exhibited near-field soil densification, generally resulting in an increase in foundation stiffness and associated fundamental frequency of response. By contrast, when founded in clay, the foundation stiffness has been generally shown to decrease due to cyclic soil strength and stiffness degradation. The change in dynamic foundation stiffness due to cyclic loading may result in resonance between the foundation response and the rotor or blade passing frequency, which should be avoided. This issue becomes all the more important considering the very tight tolerance in operational specifications (i.e., allowable range of system frequency).

The potential benefits of using suction buckets instead of the more conventional pile foundations are related to cost efficiencies and reduced environmental impacts. However, only a limited number of



OWT projects are currently founded on suction bucket foundations ([Table 2.6-1](#)). The acceptable performance of this foundation concept for OWT has not yet been fully demonstrated due to limited number of studies (both numerical and experimental) and case histories. To make suction bucket foundations attractive for offshore wind applications, additional information is required to demonstrate their feasibility, particularly with respect to the effect of cyclic loading and potential soil stiffness and strength degradation on the dynamic response of these systems. To this end, this study presents the results from advanced numerical analyses performed for a selected idealized cases to provide insight regarding the cyclic response of OWT founded on suction bucket foundations. Based on the analytical results, recommendations for design considerations and future laboratory testing were also developed and presented here.

1.2 WORK AUTHORIZATION

Fugro is providing engineering consulting services to the Bureau of Safety and Environmental Enforcement (BSEE) on the effect of cyclic loading on suction bucket foundations for OWT. The work was performed in general accordance with the scope of work outlined in Fugro's proposal titled "Cyclic Loading of Suction Bucket Foundations", dated September 3, 2015 which was submitted in response to Broad Agency Announcement (BAA) E15PS00085 "Research for Renewable Energy" Topic 4. The work was performed in accordance with the contract terms and conditions under BSEE Award/Contract No. E16PC00004.

1.3 SCOPE AND ORGANIZATION

The scope of work for this study included the following tasks:

- Task 1 – Review of Available Research and State of Practice;
- Task 2 – Advanced Numerical Analyses;
- Task 3 – Development of Preliminary Design Guidance for Suction Bucket Foundation;
- Task 4 – Development of Recommendations for Laboratory Testing Program;
- Task 5 – Meetings and Teleconferences; and
- Task 6 – Reporting.

Following this introductory section, [Section 2.0](#) presents a literature review of the current state of practice in terms of design guidelines, available laboratory testing, small and large scale experiments, actual renewable projects using suction bucket foundations, and analytical studies. [Section 3.0](#) describes the analytical framework employed in this study. [Section 4.0](#) presents the results of advanced numerical analyses performed for single and tetrapod bucket foundations on idealized sand and clay profiles. [Section 5.0](#) discusses preliminary design considerations based on the analytical results of this study. Finally, [Section 6.0](#) presents recommendations for future laboratory and small scale testing and additional analytical studies.

1.4 SUMMARY AND FINDINGS

A summary of the work performed and findings of numerical analyses is provided below. Advanced numerical analyses were performed for the following cases:



- Foundation concept: a) a single bucket with 16-meter diameter and 12-meter penetration, and b) a tetrapod foundation with 10-m diameter and 6-meter penetration for each bucket. These geometries were generally based on design information from actual projects (e.g., Icebreaker);
- Subsurface conditions: four idealized profiles were analyzed: a) soft clay, b) stiff clay, c) dense sand, and d) interlayered of dense sand overlying stiff clay. These idealized conditions were generally based on typical subsurface conditions from an overview of Fugro's database of OWT projects in the US; and
- Environmental loads: a) 1-year return period storm (wind and wave), and b) 30-year return period storm were considered.

Analyses were performed considering both stiffness and strength degradation within soils due to cyclic loading and their effects on the system response. Qualitative observations from the analytical results are summarized as follows:

- Soil stiffness and strength degradation is more prominent in cohesive soils (clays) than cohesionless soils (sands);
- For clays, soil stiffness degradation results in a decrease in the system fundamental frequency and increase in cyclic foundation displacements (horizontal and vertical displacement and rotation) over time;
- Strength degradation in clays does not appear to significantly affect the rotational stiffness and hence fundamental frequency of the system; however, it contributes to larger permanent foundation deformations, which may result in instability;
- The amount of potential stiffness degradation in sands depends primarily on the sand relative density and drainage conditions;
- For dense sands under fully drained conditions, cyclically induced soil densification results in a slight increase in the system fundamental frequency; and
- The effect of soil and hence foundation stiffness degradation on the system frequency is more important when the foundation and structural stiffness are within about one order of magnitude. If the foundation is too soft, or too stiff compared to the superstructure, the effect of soil degradation on system frequency may be negligible.

Quantitative results from the cases analyzed in terms of foundation performance, including maximum displacement and rotation, change in foundation stiffness, and change in natural frequencies, are presented in [Section 4.0](#) and summarized in [Tables 4.4-1](#) and [4.4-2](#). In summary:

- Overall, for the combinations of foundation geometry, subsurface conditions, and loading analyzed here, the effects of soil stiffness and strength degradation were relatively small and resulted in small changes in foundation stiffness and associated system frequency;
- For the mono-bucket, the peak foundation rotations within different soils generally do not increase significantly over time. However, if strength degradation is considered within the soft clay, peak foundation rotations can increase by 70 percent for the foundation analyzed;
- For the mono-bucket, the fundamental frequencies can decrease by 2 percent (soft clay with strength reduction) or increase by 1 percent (sand and interlayered) over its design life;



- For the tetrapod buckets, the change in foundation peak rotations and fundamental frequencies are generally less compared to the mono-bucket. In addition, for the tetrapod in soft clay (with strength degradation), the peak foundation rotation does not increase during the design life; and
- From the performance standpoint, the tetrapod system seemed to provide more stable performance compared to the mono-bucket. However, related cost for fabrication and installation are also higher.

The above quantitative observations are based on the particular foundation geometries, idealized soil profiles, and loading combinations analyzed and the findings above should not be generalized. Also, the focus of this study is to evaluate the effect of cyclic loading; foundation installation and static capacity/dimension analyses are not part of the work scope. Additional analytical studies are recommended to examine a wider range of cases and allow for generalization and formulation of design recommendations.

1.5 LIMITATIONS OF THIS STUDY

This report has been prepared for the exclusive use of the Bureau of Safety and Environmental Enforcement and its agents for the specific application of the effects of cyclic loading on suction bucket foundation on offshore wind turbines. In our opinion, the findings, conclusions, professional opinions and recommendations presented herein were prepared in accordance with generally accepted state of practice.

This study examined a limited number of cases to explore the effect of cyclic soil stiffness and strength degradation on foundation stiffness, stability and system response. The results of this study are applicable for conditions and assumptions similar to the cases analyzed and should not be generalized.

Although information contained in this report may be of some use for other purposes, it may not contain sufficient information for other parties or uses. If any changes are made to the project as described in this report, the conclusions and recommendations in this report shall not be considered valid unless the changes are reviewed and the conclusions and recommendations of this report are modified or validated in writing by Fugro.

SECTION 2.0



2.0 LITERATURE REVIEW

A review of available published journal and conference papers, research reports, and in-house projects related to offshore suction bucket foundations is presented in the following sections. In particular, we have reviewed available literature on design guidelines, laboratory, and field model tests, large scale tests, existing and future wind farm projects, and analytical studies. The findings from this review were used to formulate the state of knowledge and practice in relation to the key attributes and response characteristics of suction bucket foundations for Offshore Wind Turbines (OWT).

2.1 DESIGN PRACTICE AND GUIDELINES

Design standards and guidelines for OWT have been developed by different organizations; however, no standard has yet been officially adopted for use by U.S. regulatory agencies. The majority of the guidelines were developed for conventional driven piles, shallow gravity base foundations (i.e., footings), and anchors (for floating structures), with very little or no design guidance on suction bucket foundations. The suction bucket is mentioned in the DNV-OS-J101 guideline (2014); however, it suggests suction buckets be designed with gravity base specifications.

Table 2.1-1 lists the documents that make mention of cyclic degradation among all documents reviewed. However, none of these documents currently provide specific guidance on how to incorporate soil degradation phenomena in design.

Table 2.1-1: Available Design Guidance for Offshore Wind Turbine

Organization	Guidelines
Det Norske Veritas (DNV) - Norway	DNVGL-ST-0126 (Support structures for wind turbines, 2016) DNV-OS-J101 (Offshore wind turbine structures, 2014)
International Electrotechnical Commission (IEC)	IEC 61400-1 (Design Requirements, 2005) IEC 61400-3 (Offshore wind turbines, 2009)
Germanischer Lloyd (GL) – Germany	Guideline for the Certification of Offshore Wind Turbines (2005)
American Bureau of Shipping (ABS) – US	ABS #176 (Bottom-fixed wind turbines) ABS #195 (Floating wind turbines)
Nippon Kokan Koji (NKK) - Japan	Floating wind turbine structures
Bundesamt für Seeschifffahrt und Hydrographie (BSH) - Germany	Standard: Design of Offshore Wind Turbine Structures (2015) Standard for Geotechnical Site and Route Surveys (2014)
Danish Energy Agency (DEA) - Denmark	Recommendation for technical approval of offshore wind turbines (2001)

Among the available design guidelines, DNVGL-ST-0126 is the most recent and is the only one that provides any specific direction about cyclic degradation. The effects of cyclic loading are particularly relevant for the ULS and SLS limit states. Specifically, Section 7.4.4 requires that the effects of cyclic loading on soil properties be considered in foundation design, emphasizing that the concern relates to the effect of cyclic degradation of soil properties (i.e., both stiffness and strength). This section goes on to explain that cyclic loading may lead to an increase in pore pressure, accompanied with large permanent shear strains and reductions in soil shear strength. These effects shall be accounted for in



the assessment of permanent foundation rotations. In the SLS design condition, soil's shear modulus degradation due to cyclic loading shall be accounted for when calculating the foundation's performance (fundamental vibration frequency, settlement, and lateral displacement).

The DNVGL-ST-0126 design standard (Section 7.7) states that the suction bucket foundation concept is not covered by current available codes, thus a case-to-case evaluation is required. Thorough literature study should be performed prior to the design, and information based on former experience should be exploited. Soil strength degradation from cyclic loads shall be considered. There are potential favorable and unfavorable consequences of the rate effect found from cyclic tests, therefore the loading mechanism should be well understood. Last, this standard suggests that finite element analyses or scale model tests be performed to better assess the possible failure modes, drainage mechanism, and soil reactions on the bucket due to cyclic loading.

Overall, current design guidelines exist for more conventional gravity and pile foundations, which generally have very different aspect ratios and response than suction buckets. DNVGL-ST-0126 recognized the difference between suction bucket with respect to those foundations as well as the limitation of understanding. Overall, detailed methodology and recommendations on how to incorporate cyclic loading effects in the design of OWT founded on suction bucket foundations are not provided due to limited knowledge in relation to these effects. This highlights the limited state of knowledge regarding the cyclic response of these systems and need for additional studies to enhance the industry's level of understanding.

2.2 LABORATORY SOIL ELEMENT EXPERIMENTS

Table 2.2-1 lists the laboratory cyclic soil experiments with a relatively large number of cycles (generally over 1000 cycles) available in the public domain. Throughout the years, Fugro has also developed a database for cyclic soil tests for windfarm projects in the North Sea. Although the actual data cannot be presented in this report, insights gained from those data were applied when developing the idealized cyclic soil models for this research. For clays, both stiffness and strength tend to degrade with increasing number of loading cycles primarily due to the development of excess pore pressures and changes in the soil's structure. The undrained shear strength and shear modulus generally decrease with increasing shear strain/stress amplitude and number of cycles (Andersen 1988). For biased loading, permanent strains also increased with increasing number of cycles (Guo et al. 2013). However, if excess pore pressure was allowed to dissipate, the undrained shear strength was found to increase as clay underwent consolidation (Yasuhara et al. 1982, 1992). In addition, the magnitude of strength/stiffness degradation was also dependent on the features of cyclic shear loads – two-way cyclic loading accompanied by principal stress axis reversal induced the cyclic failure more rapidly than one-way cyclic loading. This is likely due to higher excess pore pressures and residual shear strains for the case of cyclic stress reversal compared to no reversal (Yasuhara et al. 1992). In general, both stress- and strain-controlled, cyclic triaxial and simple shear tests have been used to characterize the stiffness and strength degradation in clays. Vucetic and Dobry (1988) developed a criterion to model degradation of the backbone curve in clays based on a series of strain-controlled cyclic simple shear tests. This model, which has been used in the numerical analyses presented in this study, represents the stiffness and strength degradation by means of a degradation index (δ) and a degradation parameter (t). The authors also found that degradation is dependent on the Over-Consolidation Ratio (OCR) and Plasticity



Index (PI). In general, both higher OCR and PI values are associated with smaller degradation compared to lower OCR and/or PI.

For dense sands (Andersen & Berre 1999), the number of cycles to failure, the cyclic shear strength, and the failure mode (i.e., combination of average and cyclic shear strains at failure) of dense sand under cyclic loading was governed by the stress path, combination of average and cyclic shear stresses, and drainage conditions.

For medium dense sands (Wichtmann 2010), the laboratory cyclic triaxial tests showed that excess pore pressure (if undrained) and/or volumetric strain (if drained) can occur when sand samples were subjected to cyclic loading. Magnitudes of the pore pressures and densification were dependent on the number of cycles and confining pressure. Therefore, it is important to “replicate” the actual in-situ stress state when conducting laboratory sand experiments.

Table 2.2-1: Element Level Laboratory Cyclic Soil Tests

Reference	Soil Type	D/U	PI	Relative Density (Rd)	Cyclic Test Type	Stress/Strain Control	# of cycles	Loading Frequency (Hz)
Andersen 1988	Clay	U	27	-	CTX, CSS	stress	10,000	0.1
Guo et al. 2013	Clay	U	36	-	CTX	stress	50,000	1
Yasuhara et al. 1982	Clay	U	58	-	CTX	stress	3,600	0.1~1
Yasuhara et al. 1992	Clay	D/U	70	-	CTX	strain	538,200	0.1~1
Fugro 2014	Clay	U	30	-	CTX, CSS	stress/strain	1,500	0.25
Vucetic & Dorby 1988	Clay	U	27-57	-	CSS	strain	~100	0.2
Andersen & Berre 1999	Sand	D/U	-	95	CTX, CSS	stress	1,500	0.1
Wichtmann 2010	Sand	D/U	-	60	CTX	stress	1,000	unknown

2.3 SMALL SCALE LABORATORY MODEL EXPERIMENTS

A limited number of small-scale (1-g and centrifuge) laboratory experiments have been conducted by researchers to shed light on the behavior of suction bucket foundations under cyclic loading conditions. [Table 2.3-1](#) provides a summary of the key published experiments along with their testing setup and key observations.



Table 2.3-1: Small-scale Laboratory Experiments for Offshore Foundations

Reference	Test	Soil	Relative Density	Foundation		Cyclic Loading		General Observation
				Type	Dimension (prototype)	Type	# cycles	
Cox et al. 2014	Centrifuge	Dry Sand	85%	Mono-Bucket	Dia. 16 m	H, M	12,000	<ul style="list-style-type: none"> Rotational stiffness ↑ with # of cycles
Kim et al. 2014	Centrifuge	Sat. Sand	60% ~ 70%	Mono-; Tripod	Dia. 15.5 m; Dia. 6.5 m	H, M	50	<ul style="list-style-type: none"> Saturated sand appeared to be fully drained Accumulated uplift ↑ with # of cycles Cyclic stiffness ↑ with # of cycles
Dyvik et al. 1989	1-g	Sat. Clay	-	Gravity Foundation	Dia. 0.4 m	H, M	200	<ul style="list-style-type: none"> Cyclic stiffness ↓ with # of cycles Cyclic stiffness ↓ with load magnitude
Zhu et al. 2013	1-g	Dry Sand	20%	Mono-Bucket	Dia. 0.2 m	H, M	100,000	<ul style="list-style-type: none"> Stiffness ↑ with # of cycles
Bhattachar et al. 2013	1-g	Dry Sand	28%	Tetrapod	Dia. 0.07 m	H, M	1.2 million	<ul style="list-style-type: none"> Stiffness ↑ with less than 5e5 cycles Stiffness ↓ after over 5e5 cycles
Byrne et al 2004	1-g	Sat. Sand	76% and 92%	Mono-Bucket	Dia. 0.15 m	V, H, M	100	<ul style="list-style-type: none"> Excess pore pressure was generated Stiffness ↓ with load magnitude
Kelly et al 2006	Pressure Chamber	Sat. Sand	53% ~ 82%	Mono-Bucket	Dia. 0.28 m	V	1,000	<ul style="list-style-type: none"> Vertical stiffness ↑ with # of cycles (partial drainage condition)

Overall, there are a larger number of tests performed for sand compared to clay, likely because of the increased difficulties of handling clay, particularly in the centrifuge. The relative density of the sands in the experiments ranged between as low as 20 percent to as high as 92 percent. Additionally, there are only a few number of studies performed for a large number of cycles (e.g., larger than 1,000).

In general, for the experiment founded in clay (performed for a gravity foundation rather than suction bucket), cyclic loads resulted in a gradual reduction of stiffness and increase of hysteresis after 200 cycles of loading. Gapping was found at the side of the bucket under very large amplitude cycles.



Permanent displacements (vertical and horizontal) and rotations were observed at the end of cyclic loading.

For the suction bucket founded in dry sand, the laboratory results generally showed small increase in stiffness, primarily due to the densification effect attributed to cyclic loading. However, the experiment performed by Bhattachar et al. (2013) showed that foundation stiffness could decrease after large number of cycles, probably due to irreversible damages in soil fabric (Andersen 2015).

The experiments performed in saturated sands suggested that excess pore pressure can develop due the large number of cyclic loading. As a result, foundation stiffness decreased with larger number of cycles (Byrne et al 2004). However, if drainage was allowed to occur (Kelly et al. 2006, Kim et al. 2014), the foundation behaved more similar to foundations in dry sand. Bye et al. (1995) discuss two scale model tests performed for suction bucket foundations in dense sand for a gas treatment platform. Excess pore pressures were developed due to the rapid loading conditions imposed in these tests despite the high relative density of the sand, indicating the potential for local liquefaction. These observations suggest the importance of drainage conditions in sand which depend on both the relative density and frequency of loading, among other things.

2.4 LARGE SCALE FIELD EXPERIMENTS

A very small number of large-scale field experiments are available in the published literature. In general, the findings from large-scale field experiments are similar to small-scale laboratory experiments. [Table 2.4-1](#) lists published experiments along with their testing setup and key experimental observations.

Table 2.4-1: Suction Bucket Field Experiments

Reference	Test	Soil	Foundation		Cyclic Loading		General Observation
			Type	Dimension	Type	# cycles	
Houlsby et al. 2005	Field	Sat. Clay	Mono-Bucket	Dia. 1.5 m and 3 m	V, H, M	100	<ul style="list-style-type: none"> Cyclic stiffness ↓ with # of cycles Cyclic stiffness ↓ with # load magnitude
Houlsby et al. 2005	Field	Sat. Sand	Mono-Bucket	Dia. 1.5 m and 3 m	V, H, M	100	<ul style="list-style-type: none"> Cyclic stiffness ↓ with # of cycles Cyclic stiffness ↓ with # load magnitude
Liingaard 2006	Field	Sat. Sand	Mono-Bucket	Dia. 12 m	Actual environmental loads.		<ul style="list-style-type: none"> Field installed bucket Observed data (system frequency) was compared with numerical analyses.

2.5 NUMERICAL SIMULATIONS OF SUCTION BUCKET FOUNDATIONS

In recent years, numerical analyses have been performed more often to evaluate the cyclic loading effects on offshore foundations (Andersen 2009, 2015, Erbrich et al. 2016, Lee et al. 2016).



Compared to the conventional limit-equilibrium analyses, the numerical simulations can provide better details on time-dependent model behavior rather than just the foundation capacity. However, applying the cyclic loading time histories in finite element or finite difference software with a large number of cycles can be very time consuming and therefore not practical. An equivalent cycle (N_{eq}) approach was proposed (Andersen 2015, Erbrich et al. 2016) to estimate the degraded soil properties and then used for design. The approach consists of three steps: In the first step, dynamic analyses are conducted with the initial soil properties to calculate the dynamic soil stress time histories in each soil element. In the second step, the irregular soil stress time histories are transformed to a number of cyclic load parcels. Each load parcel constitutes a uniform cyclic stress with different number of cycles using the rain flow counting method (Andersen 2015). The load parcels are then “plotted” on the cyclic stress vs. N of cycles plot to estimate the accumulated pore pressures or shear strains. A degraded stress-strain soil curve can then be derived from the soil stress-strain-N charts. The chart can be developed either primarily from past experience from similar soils (Andersen 2015) or from site-specific cyclic experiments (Erbrich et al. 2016). In the third step, dynamic analyses are conducted again, but with degraded soil properties. This approach is based on a number of key assumptions:

- Dynamic analyses with only the initial soil properties (Step 1) can provide correct stress time histories;
- Irregular stress time histories can be idealized to uniform stress time histories with equivalent stress;
- Pore pressure or shear strain can be accumulated over load parcels;
- Cyclic soil behavior is “assigned” to each individual element by means of chart solutions (Andersen 2015) or interpolation from laboratory test results (Erbrich et al. 2016);
- Load parcels with large number of cycles and lower shear stress can generate the same amount of pore pressure/shear strain compared to load parcels with smaller number of cycles and higher shear stress;
- The equivalent number of shear cycles and shear stress can represent the complete loading time history; and
- Dynamic analyses with the already-degraded soil properties (Step 3) can provide reasonable representation for the actual gradually-degraded soil behavior

This approach has been used to predict displacement and capacity assuming a constant N_{eq} for all the elements in the soil volume (Andersen and Hoeg, 1991). However, the assumption of a constant N_{eq} within the soil volume may underestimate the effects of stress redistribution and progressive failure (Andersen 2015). Subsequently NGI developed a more detailed model which allowed different N_{eq} be applied at different soil elements through iterations on calculated shear stress within different elements.

For the current study we have developed a new approach to simulate a large number of cycles directly in time domain, thus allowing for the recording of time histories of foundation displacements and rotations. Cyclic soil behavior is simulated directly by means of a constitutive model and cycle-by-cycle changes in foundation stiffness and displacements are explicitly modeled. Details of this approach are described in [Section 3.0](#).



2.6 WIND TURBINE PROJECTS USING SUCTION BUCKET FOUNDATIONS

Table 2.6-1 provides a list of offshore wind turbine projects with suction bucket foundations. Mono-bucket foundation was typically adopted for shallow water (<20 m) and multi-bucket foundation was used at deeper waters. The diameters for mono-bucket ranged between 12 m to 18 m with the skirt length from 6 m to 15 m. For the multi-bucket foundation in the Borkum Riffgrund 1 wind farm in Germany, the diameter was 8 m with the skirt length of 8 m. The majority of the projects are located in Europe (i.e., Germany, Denmark and the UK), whereas there is only one project in the United States, which will be constructed in a lake rather than a sea or ocean environment.

Table 2.6-1: OWT Projects with Suction Bucket Foundation

Project	Location	Water Depth	Foundation		Soil	General Observation
			Type	Dimension		
Frederikshavn	Denmark, 2002	1~4 m	Mono-Bucket	D=12 m L=6 m	Clay	3.0 MW Prototype. Installed in ~4 m of water. Instrumented with details presented in Liingaard (2006).
Wilhelmshaven	Germany, 2005	~18 m	Mono-Bucket	D=16 m L=15 m	Sand	4.5 MW. Hit by barge during installation and failed due to buckling.
Horns Rev 2 Met Mast	Denmark, 2009	9~17 m	Mono-Bucket	D=12 m L=6 m	Interlayer	Total Height: 38 m. Weight: 165 tones. Decommissioned in 2015.
Dogger Bank	UK, 2013	~18 m	Mono-Bucket	D=14 m L=8 m	unknown	Met mast.
Borkum Riffgrund 1	Germany, 2014	~25 m	Tripod	D=8 m L=8 m	Sand	3.6 MW Turbines
Icebreaker	Lake Erie, USA	~20 m	Mono-Bucket	D= 18 L=12 m	Interlayer	Not yet constructed. Six, 3 MW turbines. Significant foundation icing conditions, but small wave loads due to location (lake).

SECTION 3.0



3.0 ADVANCED NUMERICAL MODELING METHODOLOGY

3.1 INTRODUCTION

Analyses were conducted in FLAC^{3D} (Itasca, 2015), a finite difference software developed for geotechnical/structural analyses with strong capabilities in non-linear, dynamic problems. The soil and suction bucket were combined in an integrated 3-D model allowing analysis of the soil-bucket interaction. The wind and wave loads acting on the superstructure were converted into equivalent loads acting at the top of the bucket. Hence, the superstructure was not modeled in FLAC^{3D}. The FISH scripting language incorporated into FLAC^{3D} allowed several custom functions to model clay and sand degradation to be developed.

The range of potential site conditions and foundation designs is significant, so it is beyond the scope of this study to attempt to encompass the full range of designs and site conditions that may be defined for any given site. The project team accessed the data available within the public domain along with prior experience to characterize environmental loading and foundation configurations representing a reasonable basis for this study. Elastic shell elements were used to represent the bucket. The bucket skirt was assumed to be 4.25 cm thick steel. Table 3.1-1 summarizes the key dimensions of the mono-bucket and tetrapod foundation systems analyzed. Figure 3.1-1 illustrates the dimensions of the buckets for the mono-bucket and tetrapod system, which had a 17.2 m center-to-center distance between the four pods. It is important to note that these bucket dimensions were developed to merely to capture overall trends in foundation stiffness degradation. They are not “designed” to the four soil cases analyzed. Hence, the bucket may be overly large in the sand case, for example.

Table 3.1-1. Foundation System Dimensions

Foundation	Diameter (m)	Skirt length (m)	Wall Thickness (cm)	Bucket Center-to-Center Distance (m)
Mono-bucket	16	12	4.25	N/A
Tetrapod	10	6	4.25	17.2

Given the symmetry of the bucket and applied loading direction, a half model (i.e., one half of the bucket and the surrounding soil) effectively models the mono-bucket system while significantly reducing computational time. In the tetrapod model, a half bucket was modeled in FLAC^{3D}, and the response of the individual bucket was converted to the overall tetrapod system response assuming an idealized rigid connection between each bucket. However, depending on the properties of the tetrapod jacket, the rigidity of the connections may be important to consider. Quiet boundaries applied to the base and three sides of the model limited the impact of bucket-induced waves propagating through the soil and reflecting off of the model boundaries back toward the bucket. Free-field boundaries were installed to allow for wave passing and avoid unwanted wave reflection from the boundaries. The fourth side of the model, representing the line of symmetry with respect to the loading conditions, was fixed in the normal direction. The bucket shell element nodes along this line of symmetry were fixed against translation and rotation in the appropriate directions.



The idealized soil conditions selected represent the general soil conditions encountered in the US east coast offshore environment. Table 3.1-2 summarizes the four idealized soil conditions considered. Soil strength was modeled with the Mohr-Coloumb failure criteria. Cyclic loading- induced changes in the clay and sand stiffness were modeled using user-implemented routines through FISH, a scripting language integrated into FLAC^{3D}.

Table 3.1-2. Idealized Soil Properties for FLAC^{3D} Analyses

Case	Submerged Unit Weight (kN/m ³)	Initial Shear Modulus (MPa)	Poisson's Ratio	Friction Angle (deg.)	Undrained Shear Strength (MPa)	Plasticity Index (PI)
Soft Clay	10	$G_{max}/S_u = 600$	0.45	N/A	0.04	30
Stiff Clay	10	$G_{max}/S_u = 600$	0.45	N/A	0.15	30
Dense Sand	10	64	0.30	35	N/A	N/A
Sand over Soft Clay	Case considers dense sand with a thickness of ½ the bucket skirt length over soft clay using properties above					

3.2 LOADING CONDITIONS

3.2.1 Background

The environmental loads developed for the analysis included the wave, current, and wind loads. Wave and current loads were defined for generic mono-bucket and jacket support structures. The wind loads were defined based on published wind load data from various turbine manufactures. Cyclic loading is generated both by wave and wind loads on offshore wind turbines and their support structures. Cyclic wave loads can be classified in terms of their frequency of occurrence (e.g., extreme storms, which are rare or operating waves, which occur continuously), period of oscillation, and load amplitude. Assessing the effect of cyclic degradation under these different loading regimes is important as it is possible that limit states may be effected by different combination of load amplitudes and cycles. The cyclic loading during a 50-year storm, which might occur once during the life of the facility, could subject the foundation to hundreds of high amplitude load cycles. The normal wave environment could induce millions of loading cycles, but with much smaller amplitudes. The loading conditions used for this analysis focused on this relationship between load amplitude and cycle exposure.

The cyclic loads generated by wind acting on the wind turbine during power generation are quite complex and generates another regime of cyclic loading. Wind load fluctuations occur normally due to wind gusts and turbulence. In addition, cyclic loads are generated by the normal rotation of the turbine, which is transverse to the wind direction and also due to the aerodynamic interaction of the blades and the support tower. These loads tend to generate cyclic forces within the foundation that are much smaller than those discussed above for wave loads, but with approximately 10 times the number of cycles, depending on the site specific conditions.

The definition of cyclic wind loads requires a more extensive analysis of a specific turbine and its support condition to properly represent the dynamic response of the system. Given that the load amplitudes are small, this study focused on the definition of degradation for the higher amplitude wave loads. The wind loads were therefore applied statically throughout the whole time period analyzed. The



approach was intended to establish the effects of degradation for the two regimes of wave load which could then provide an indication of reduced potential for wind load degradation if the effects of cyclic degradation under normal wave loading was found to be small.

3.2.2 Foundations

The wave loads were generated for the 1-year and 50-year return period storm conditions for a typical mono-bucket configuration. These loads were developed through direct computation using standard API methodology. The total load (force and overturning moment) from the mono-bucket foundation model was resolved into a shear force and axial tension-compression force couple for various legs of the tetrapod foundation. A site-specific explicit wave load analysis of a jacket structure was not performed at this stage.

3.2.3 Assumptions

1. The wave load was generated from a single sinusoidal wave.
2. The wind load derived at the turbine interface was assumed to be constant.
3. The wind load on the foundation was not included.
4. The wave, wind, and current load were assumed to be collinear.
5. The total load (wind, wave and current) on the foundations – mono-bucket, and tetrapod was assumed to be constant and hence isolate the effect of the external load from the analysis of the suction bucket for different foundation configurations.

3.2.4 Loads

Table 3.2-1 presents the parameters used to generate the wave, current, and wind load for the suction bucket. The wave and current parameters were used in EDP (structural analysis software) to generate the wave and current load. The wind load from the turbine and foundation interface was assumed to be constant.

Table 3.2-1: Wave, Current and Wind Load Parameters

Description	1-year Return Period	50-year Return Period
Wave Loads		
Water Depth (m)	27	27
Wave Height, Hmax (m)	10	13
Wave Period, T (s)	10	11
Current Velocity (m/s) w.r.t. depth		
Depth 0-m	0.9	1.2
Mudline	0.3	0.6
Turbine Loads at Interface		
Base Shear (kN)	850	1470
Overturning Moment (kN-m)	53000	91000



The wave, current, and turbine loads were resolved into a force and overturning moment (or tension compression force couple) at mudline. Design loads associated with storm and normal sea state conditions were considered in the analyses. The load acting on the superstructure was converted into an overturning moment and shear that was applied to the bucket top in the FLAC^{3D} model. Figure 3.2-1 compares the loading time history for one cycle of normal sea state loading to a cycle of storm loading for the mono-bucket, with the overturning moment shown on the left axis and the base shear on the right. The storm loading has a higher cyclic amplitude as well as a higher static bias. The period of loading is 11 s and 10 s for the storm and normal sea state conditions, respectively. Figure 3.2-2 presents the loading cycle for the tetrapod system applied to the top of each bucket. In this case, the moment at the base of the tower superstructure can be translated to a vertical load applied to each bucket. Due to the assumed static horizontal wind load acting on the superstructure, Leg 1 and Leg 2 on Figure 3.2-2 will be in tension, while Leg 3 and Leg 4 will be in compression. Again, the storm loads have higher cyclic amplitudes as well as higher static biases. The same period of loading applied to the mono-bucket also applied to the tetrapod. A vertical gravity load of 7.5 MN applied statically to the mono-bucket and divided among the four buckets of the tetrapod represented the weight of the superstructure. The foundations were first subjected to one week of storm loading followed by 30 years of normal sea state loading. The 30 years of normal sea state loading represents around 96 million cycles.

3.3 SOIL DEGRADATION MODELS

3.3.1 Clay

This study focused on the effects of cyclic loading on the fundamental frequency of the wind turbine system. Hence, the degradation of soil surrounding each bucket is of critical importance. Cyclic degradation of clay was quantified by the degradation index (δ), which is the shear modulus after a given number of cycles over the shear modulus during the initial cycle. Figure 3.3-1 compares the Vucetic and Dobry (1988) relationship to data from several Fugro projects. Additionally, the Drammen Clay from the North Sea was adapted from the contour diagrams presented in Andersen (2015). The Vucetic and Dobry (1988) degradation model was selected for this study as it fell within the range of available data, and the OCR and PI values were similar to those typical of the Eastern US offshore environment. This model estimates the degradation index (δ) as a function of the number of cycles (N) and the degradation parameter (t) through the following relationship:

$$\delta = N^{-t} \quad \text{Equation 3-1}$$

The degradation parameter (t) depends on the cyclic shear strain (γ) as well as the properties of the clay (e.g., OCR or PI). For the purpose of this study, the degradation parameter was based on the Venezuelan North of Paria clay from Vucetic and Dobry (1988) for and OCR of 1. Figure 3.3-2 illustrates a curve fit to this curve from Vucetic and Dobry (1988) resulting in the following equation:

$$t = 0.062\gamma^{0.59} \quad \text{Equation 3-2}$$

One should note that Figure 3.3-2 contains no data below shear strains (γ) of around 0.5 percent, and hence, there is considerable uncertainty in the extrapolation in this range. Degradation at smaller strains could be the focus of future research. Combining Equations 3-1 and 3-2 results in the following



expression, which relates the degradation parameter (δ) to the number of cycles (N) and the cyclic shear strain (γ):

$$\delta = N^{-0.062\gamma^{0.59}} \quad \text{Equation 3-3}$$

Equation 3-3 was implemented in a custom FISH function to update the shear modulus of each element in the FLAC^{3D} model after each loading cycle. In this case, the cyclic shear strain was represented by the square root of the sum of the squares of the cyclic amplitudes of each component of shear strain. [Figure 3.3-3](#) illustrates the change in degradation index versus number of cycles for various strain levels. As Vucetic and Dobry (1988) based their relationship on data up to 100 cycles, the dashed curves beyond this point indicated extrapolation beyond the data. The lower limit of the degradation index was capped at 0.35, below which there is no further degradation. There is limited data on an appropriate limiting value, which could be examined through future testing. Mortezaie and Vucetic (2016) analyzed threshold strains (below which cyclic degradation may not occur) for cyclic degradation with a limited number of cycles (e.g., 10) and summarized the findings of other researchers, which suggest that a threshold strain on the order of 0.01 percent may be a reasonable initial estimate. For the purpose of this study, a threshold strain was not incorporated into our model, which likely resulted in slightly conservative degradation estimates. For example, applying 100 million cycles at 0.005 percent cyclic shear strain results in a degradation index of around 0.95. For smaller strains, there would be even less degradation, and hence, less importance in applying a threshold strain.

Equation 3-3 is for a constant shear strain; however, the cyclic shear strain will change during the analyses when the loading changes from storm to normal sea state. Additionally, even with a constant cyclic loading amplitude, the cyclic shear strain will change during loading due to shear modulus degradation in each zone. To capture the effect of these evolving cyclic shear strains, the strain was monitored during each cycle, and the degradation index was converted to a representative number of cycles at the current cyclic shear strain. [Figure 3.3-4](#) provides a hypothetical example of the process, which ignores small changes in shear strain due to shear modulus degradation, and includes the following steps:

1. The degradation index starts at 1.0 (i.e., no degradation), and after four cycles at 0.25 percent shear strain, the degradation index (δ) is calculated per Equation 3-3 to be 0.963.
2. The cyclic shear strain then increases to 1.0 percent (e.g., due to an increased cyclic load on the turbine). The degradation index (δ) from the previous cycles of loading (0.963) corresponds to 1.8 cycles (N) at a cyclic shear strain of 1.0 percent.
3. After the soil is subjected to three additional cycles at 1.0 percent cyclic shear strain, the new degradation index can be calculated using Equation 3-3 with a representative number of cycles (N) equal to 4.8 (i.e., 1.8 + 3), leading to a degradation index of 0.907.
4. The cyclic shear strain then decreases back to 0.25 percent, and the previous degradation index of 0.907 corresponds to 35 cycles (N) at 0.25 percent shear strain.
5. The degradation index after 40 additional cycles at 0.25 percent shear strain can be calculated with Equation 3-3 using a representative number of cycles equal to 75 (i.e., 35 + 40).
6. The process continues.

3.3.2 Dense Sand

The change in the shear stiffness of sand should depend on the initial density as well as the drainage conditions. In this study, the sand was assumed to be fully drained, so excess pore pressure generation was not considered. Densification of a sand leads to an increased shear modulus. Wichtmann and Triantafyllidis (2004) present a relationship between void ratio (e) and initial shear modulus (G_0):

$$G_0(p = 80 \text{ kPa}) = 65 \text{ MPa} \frac{(1.88 - e)^2}{1 + e} \quad \text{Equation 3-4}$$

The 65 MPa constant in Equation 3-4 was modified from 113 MPa as presented by Wichtmann and Triantafyllidis (2004) to arrive at the targeted initial shear modulus for the sand in this study. In the numerical simulations, the change in void ratio was related to the volumetric strain, which was estimated following the Finn/Byrne model. The Finn/Byrne model estimates the volumetric strain cycle-by-cycle as a function of the shear strain and the volumetric strain at the end of the previous cycle. Byrne (1991) describes the formulation used in this study. Figure 3.3-5 illustrates the behavior of the Finn/Byrne model for three shear strain levels. It is important to note that the Finn/Byrne model was developed for earthquake loading (i.e., relatively low number of loading cycles). Thus, the dashed lines on Figure 3.3-5 indicate there is uncertainty when extrapolating beyond the range of data used to develop their model. Additional studies examining the densification of sand subjected to many shear cycles could help reduce this uncertainty.

The Mohr-Coulomb (M-C) constitutive model was used in this study for both clay and sand. We recognize there are certain limitations on the M-C model: 1) stress-strain behavior is linear elastic – perfectly plastic, and 2) no post-failure strength degradation. In the beginning of this study, a fully-nonlinear hyperbolic soil model was also used to compare the results with the M-C model. It was found that for the bucket dimension and loading condition analyzed, the two different constitutive models provided essentially the same results. Therefore, M-C model was adopted for its much shorter analytical time required. It is noted here that M-C soil model may not be applicable for different bucket dimension and/or loading condition, comparison and verification between different approaches will be required for any site-specific study.

3.4 STEPPING PROCEDURE

When performed on a relatively recent CPU (Intel Core i7-4790K @3.6GHz), around 20 minutes are required to run one 11.1 s cycle (model time) in FLAC^{3D}, depending on the exact FLAC^{3D} model. Hence, directly performing millions of cycles is not feasible. Therefore, a technique needed to be developed to model the effect of millions of loading cycles without explicitly running each cycle in FLAC^{3D}.

The clay degradation model depends on the cyclic shear strains and the number of cycles. If the superstructure is subjected to cyclic loading of constant amplitude, the cyclic shear strains will still tend to increase slightly with each cycle of loading due to shear modulus degradation. Therefore, an iterative approach should be taken. However, when the percent change in the strain in each zone in FLAC^{3D} is small, it is reasonable to use a single cycle in FLAC^{3D} to represent the degradation due to many “real”



cycles by using Equation 3-3. Initially, each FLAC^{3D} cycle represents one “real” cycle. However, when the maximum (of all zones) percent change in shear strain between a FLAC^{3D} cycle and the preceding cycle is less than a target shear strain value taken equal to 2 percent for the purpose of this study, the number of “real” cycles that each FLAC^{3D} cycle represents is increased by a factor of 10. These criteria were developed after testing various combinations to balance the accuracy of the stepping procedure and computation time.

Figure 3.4-1 illustrates this methodology implemented in FLAC^{3D}. The left y-axis shows the number of “real” cycles that each FLAC^{3D} cycle represents. The right y-axis shows the maximum percent change in the cyclic shear strain from the preceding cycle to the current cycle. Initially, each FLAC^{3D} cycle represents just one “real” cycle. During the first two cycles, the maximum percent change was greater than 2 percent; however, during the 3rd cycle, the percent change dropped below 2 percent, thus the fourth cycle in FLAC^{3D} was assumed to represent 10 real cycles. The max percent change remained less than 2 percent during the fourth cycle, so the fifth cycle was assumed to represent 100 additional real cycles. However, during the fifth cycle, the percent change in the strain was greater than 2 percent, so the sixth cycle remained representing only 100 additional cycles.

Applying this technique of representing multiple “real” cycles by a single FLAC^{3D} cycle permitted the stiffness degradation of the bucket subjected to millions of cycles to be assessed in a reasonable amount of computational time. To validate the approach, Figure 3.4-2 compares a soft clay model run cycle-by-cycle for 900 cycles with an identical model using the stepping procedure described (14 FLAC^{3D} cycles required to represent 900 real cycles). This figure illustrates that the spatial patterns of the degradation index (900th cycle shear modulus divided by the first cycle shear modulus) between the two approaches are essentially identical. As an additional check, Figure 3.4-3 compares the bucket rotation time history from 900th cycle from the cycle-by-cycle approach to the 14th FLAC^{3D} cycle (representing the 900th real cycle) from the stepping approach. Again, the two techniques provide essentially identical results. The rotation from the second cycle serves as a reference, illustrating the increase in the amplitude of cyclic rotation after 900 cycles.

The densification in the sand model, and thus increase in shear modulus, depends on the cyclic shear strains, similar to the clay degradation model. Hence, the stepping procedure described for clay was also adopted when modeling sand behavior under cyclic loading. As performing the iterative Finn/Byrne calculations for tens of millions of cycles of loading for thousands of zones in the FLAC^{3D} model would take several days to complete, an additional extrapolation method was developed, verified, and applied.

3.5 STRENGTH DEGRADATION

This study focused on the change in the fundamental frequency of the combined bucket and superstructure system. Hence, the degradation of the shear modulus in soils surrounding the bucket was the primary focus. However, strength degradation, particularly for clays, may be an additional concern. This strength degradation could be due to a combination of soil fabric breakdown or excess pore pressure generation. As not the focus of this study, separate models of strength degradation were not developed; however, several sensitivity studies were performed with the strength of the clay assumed to degrade at twice the rate of shear modulus degradation (e.g., a shear modulus degradation of 20 percent was assumed to correspond to a strength degradation of 40 percent). Again, the intention



was to examine general trends due to strength degradation through the sensitivity analyses presented in [Section 4.0](#), not to provide realistic values.

3.6 ESTIMATION OF SYSTEM FUNDAMENTAL FREQUENCY

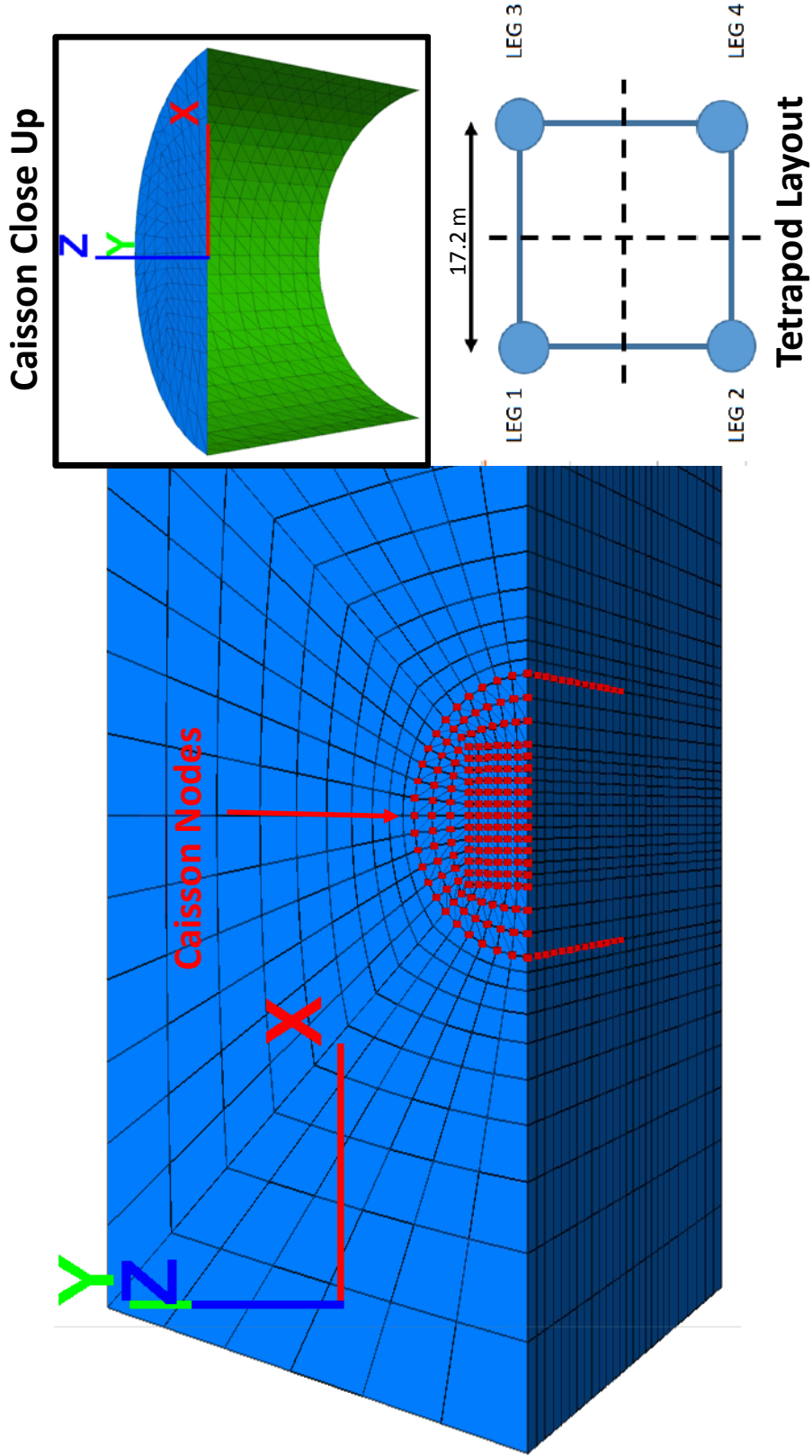
The effect of cyclic loading on the global tower fundamental frequency is the primary focus of this study. However, the modeling focuses on the bucket alone, whereas the fundamental frequency depends on both the bucket stiffness and tower properties. The fundamental frequency can be estimated by representing the superstructure as a simple single degree of freedom system (with properties E , I , L , and m) and the foundation as a rotational spring (stiffness of k). The results of the FLAC^{3D} analyses provide the rotational stiffness (k) of the mono-bucket. However, no hypothetical superstructure was developed as part of this project. Therefore, results are primarily provided in terms of rotational stiffness (k), which can then be related to the fundamental frequency depending on the representative properties of the superstructure. However, the example calculations provided in [Section 4.0](#) to illustrate the process used the assumed properties in [Table 3.6-1](#).

Table 3.6-1. Hypothetical Tower Properties for f_n Calculations

Property	Value
Young's Modulus, E (Pa)	2×10^{11}
Second Moment of Inertia, I (m^4)	21.6
Length of Tower above Bucket (m)	90
Lumped Mass (kg)	1×10^6

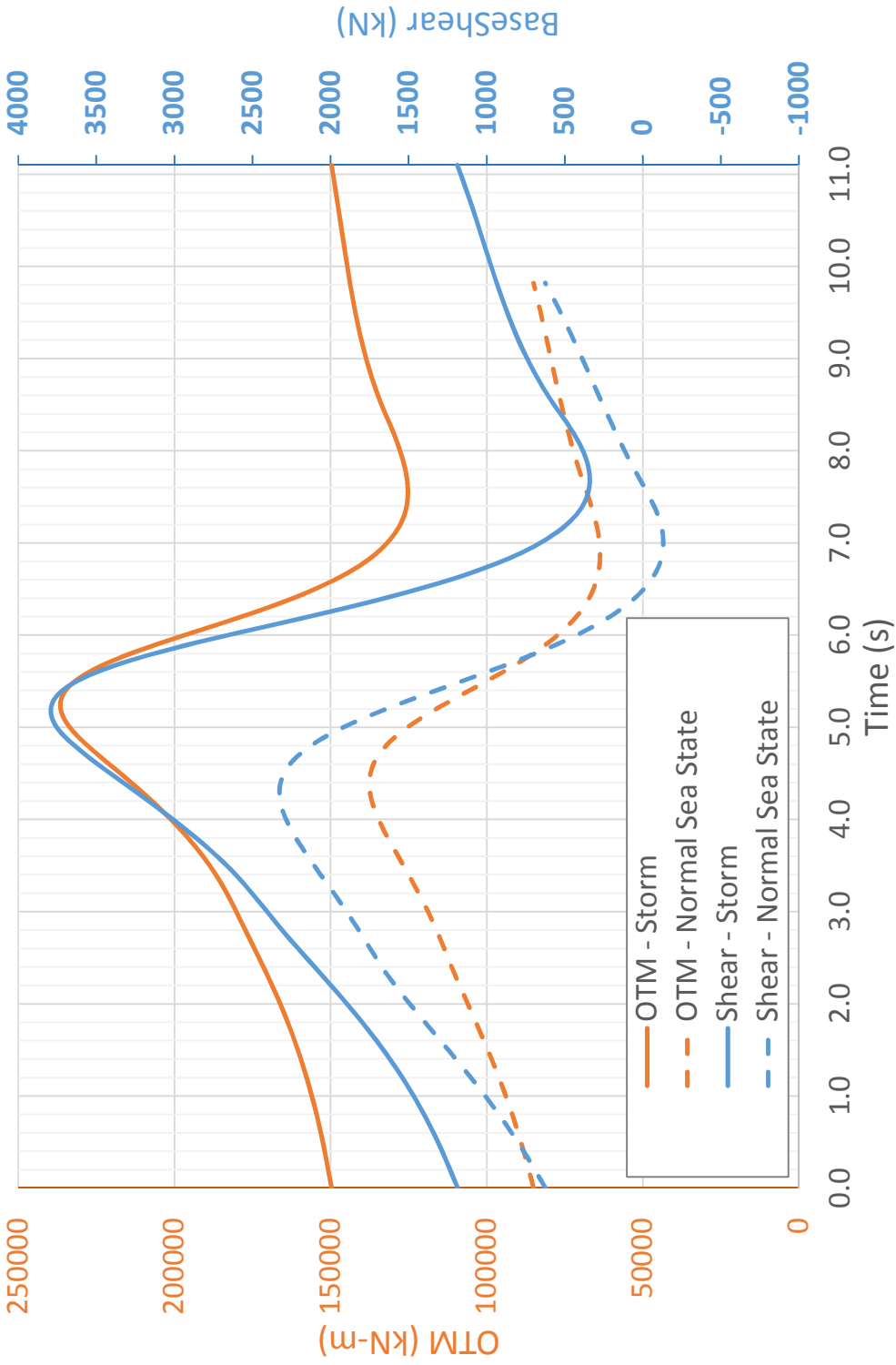
[Figure 3.6-1](#) illustrates the fundamental frequency as a function of the ratio of the initial rotational stiffness of the bucket (k) to the tower properties represented by $3EI/L$, using the properties from [Table 3.6-1](#). The various curves show the impact of degradation of the bucket rotational stiffness on the frequency of the bucket-tower system. Depending on the allowable frequency range, different degrees of foundation stiffness degradation can be allowed. Also, it appears that the effect of soil, and hence foundation stiffness degradation on the system frequency, is more important when the foundation and structural stiffness are within about one order of magnitude. If the foundation is too soft or too stiff compared to the structure, the effect of soil degradation on the frequency of the system is limited.

In the case of the tetrapod, k represents the rotational stiffness of the entire tetrapod foundation. One half of one of the 4 buckets that comprise the tetrapod system was modeled in FLAC^{3D}. Therefore, the rotation of the tetrapod foundation was estimated by relating the vertical displacements of each bucket to the rotation of the system, assuming (for this study) the buckets were rigidly connected. Similarly, the vertical loads shown on [Figure 3.2-2](#) applied to each bucket were converted to an equivalent moment acting at the base of the tower. The rotational stiffness of the complete tetrapod foundation is this equivalent moment divided by the rotation of the tetrapod system.



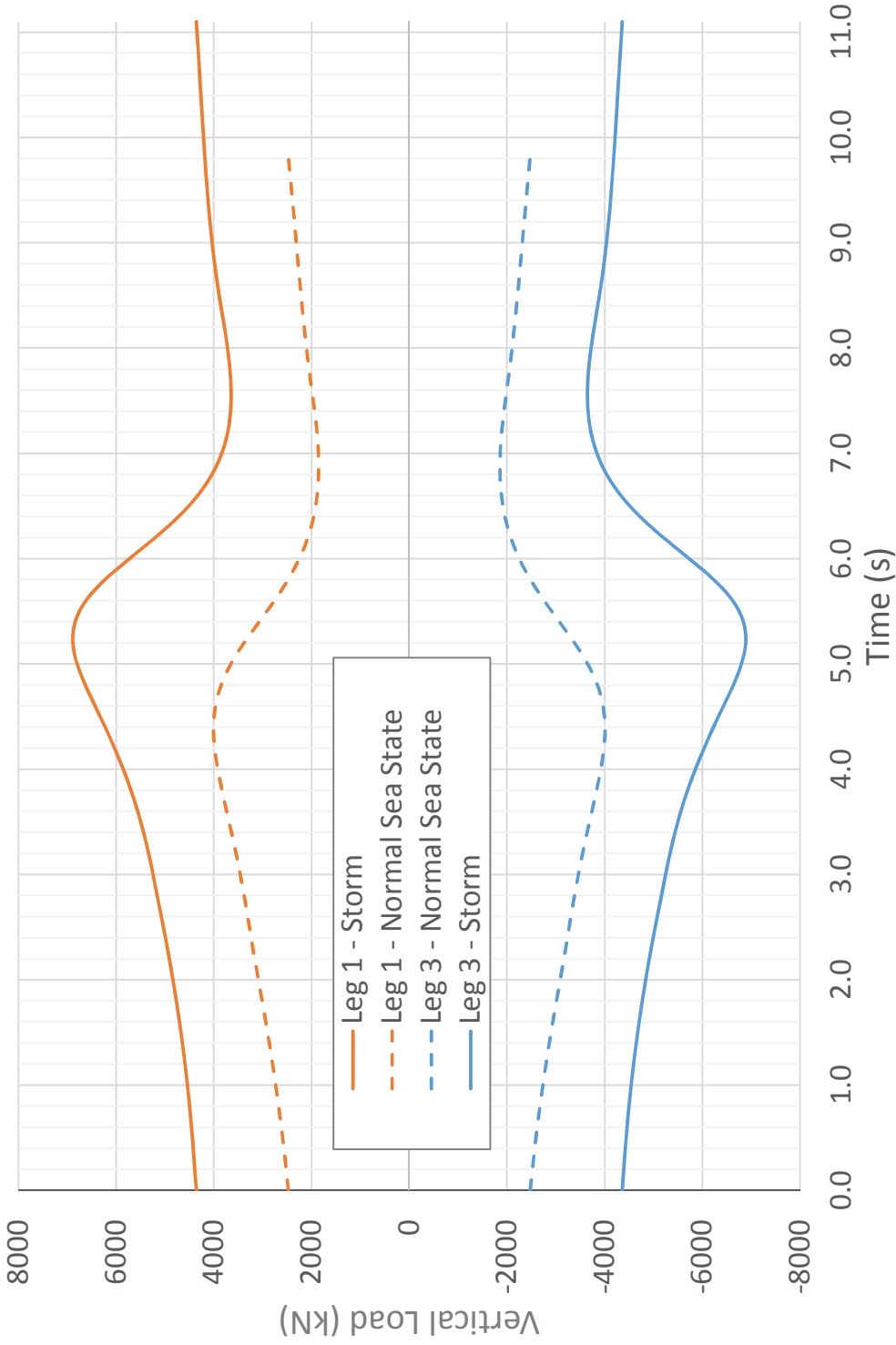
DIMENSIONS OF CAISSON FOUNDATION SYSTEMS AND FLAC3D MODEL
 Cyclic Loading Effects on Suction Bucket Foundations
 Offshore Wind Turbines

FIGURE 3.1-1



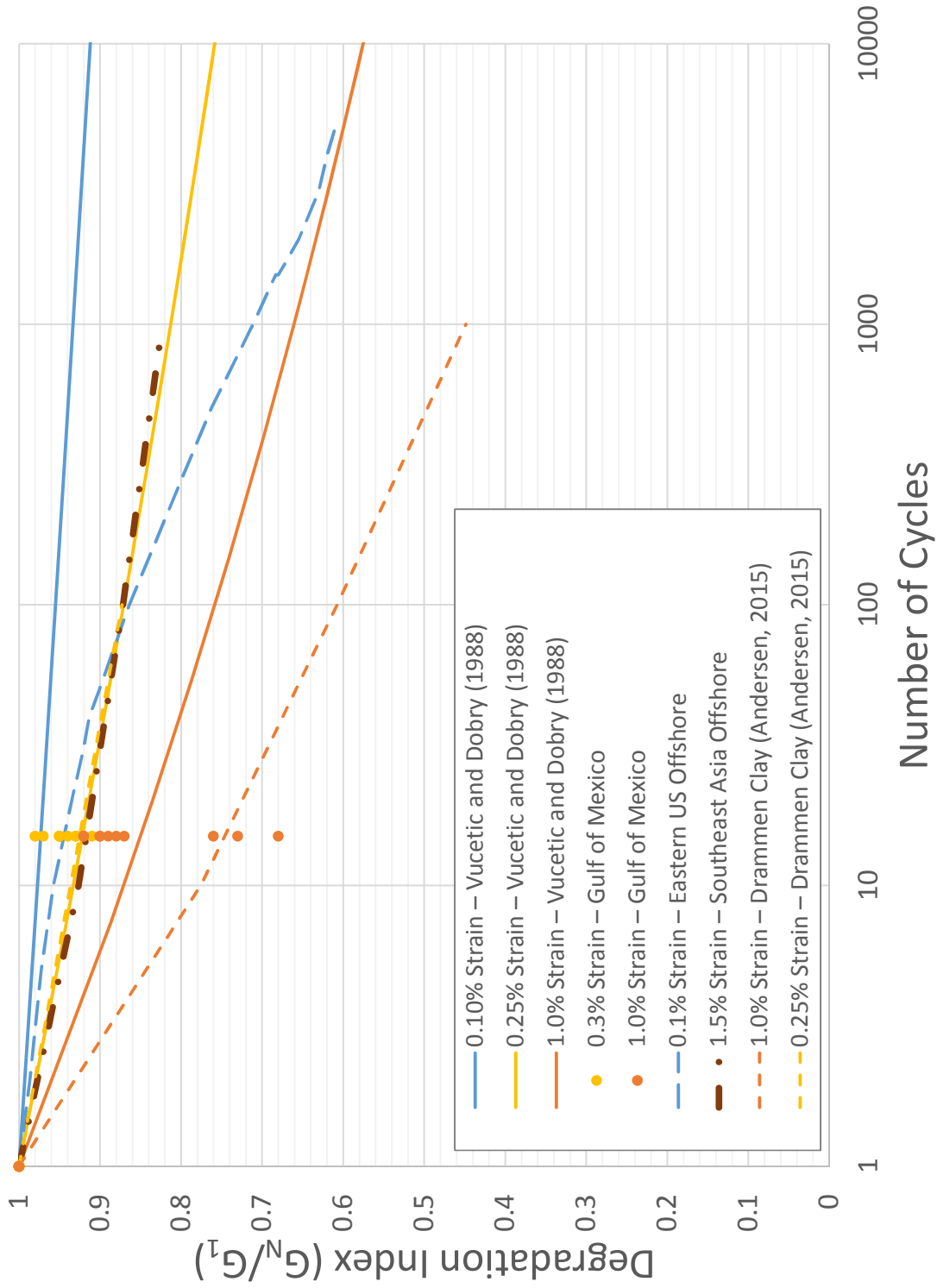
MONOCAISSON FOUNDATION LOADING TIME HISTORY
 Cyclic Loading Effects on Suction Bucket Foundations
 Offshore Wind Turbines

FIGURE 3.2-1



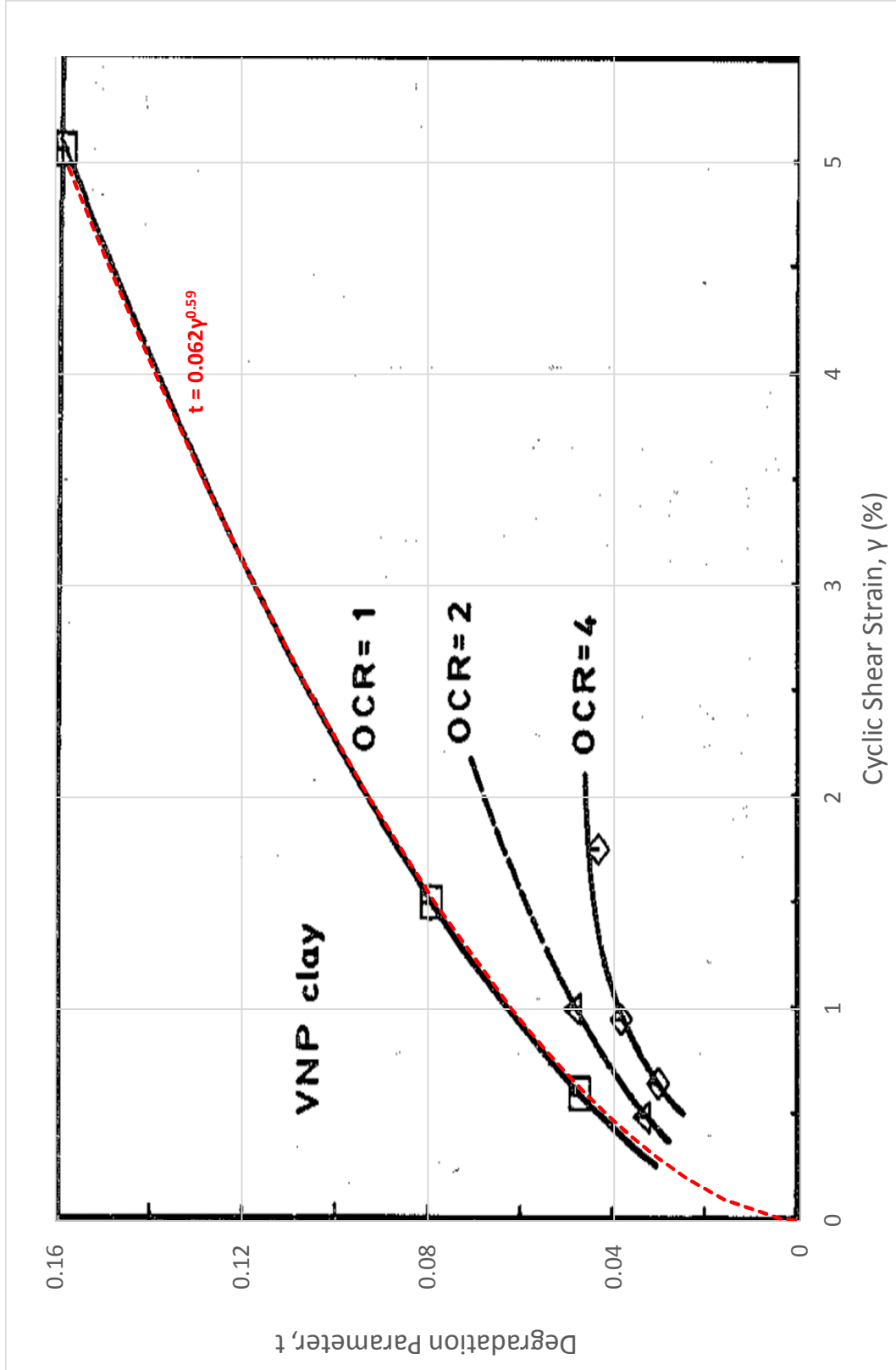
TETRAPOD FOUNDATION LOADING TIME HISTORY
Cyclic Loading Effects on Suction Bucket Foundations
Offshore Wind Turbines

FIGURE 3.2-2



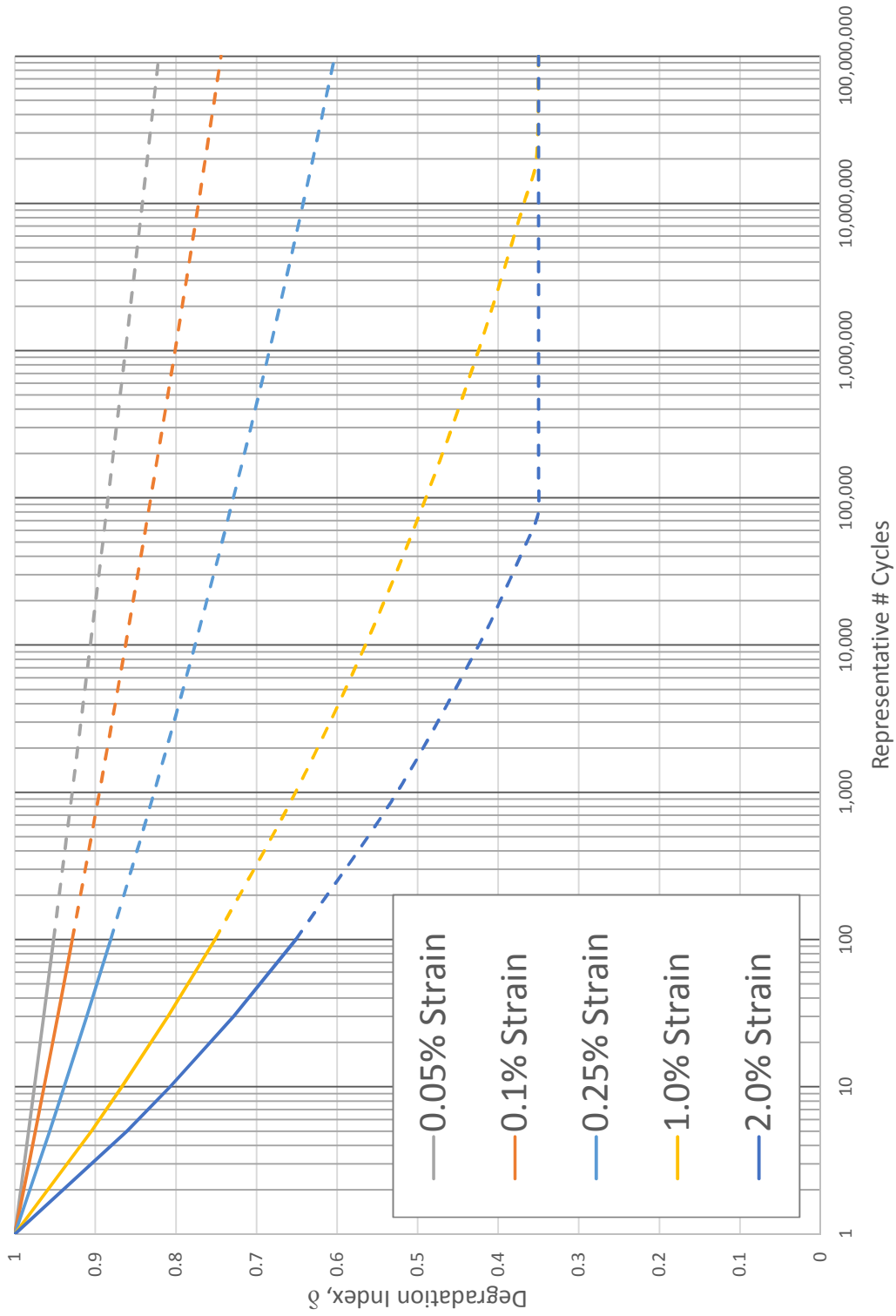
COMPARISON OF VUCETIC AND DOBRY (1988) TO DEGRADATION DATA
 Cyclic Loading Effects on Suction Bucket Foundations
 Offshore Wind Turbines

FIGURE 3.3-1



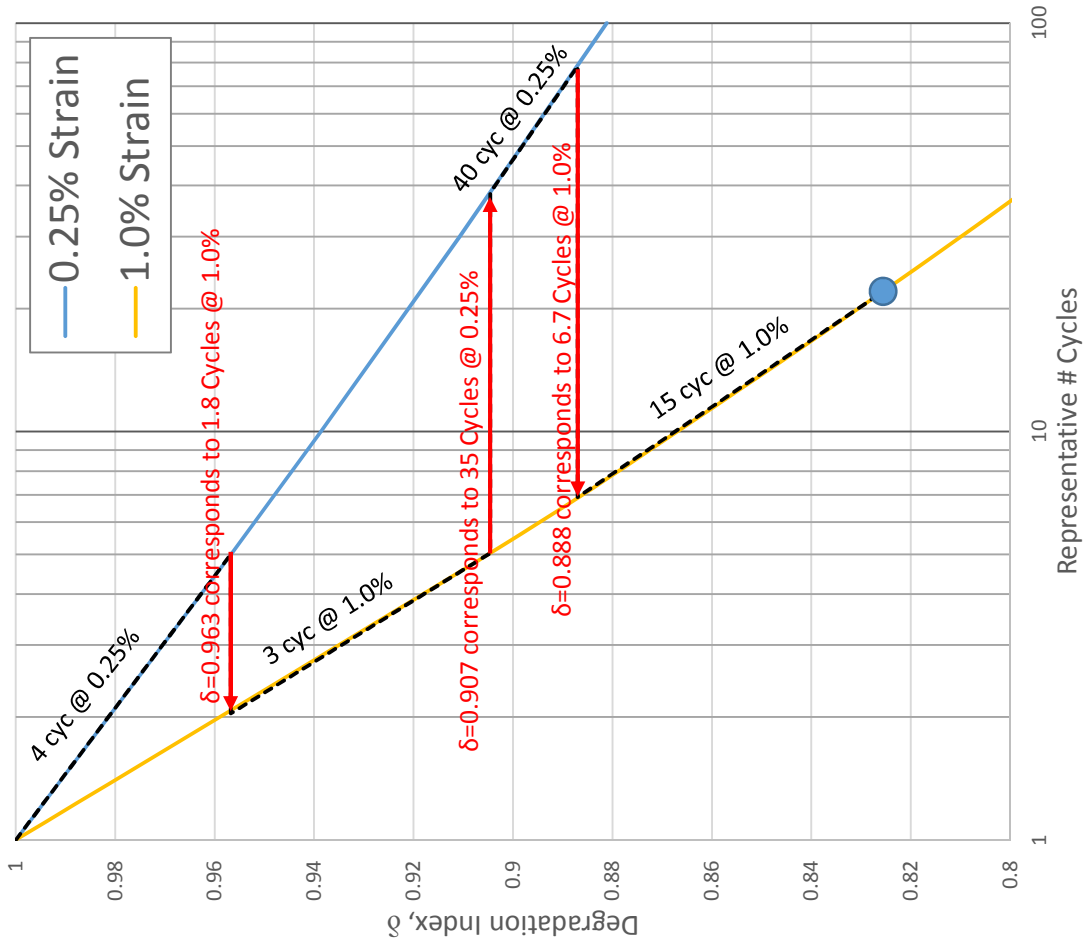
DEGRADATION PARAMETER FORM USED IN THIS STUDY
 Cyclic Loading Effects on Suction Bucket Foundations
 Offshore Wind Turbines

FIGURE 3.3-2



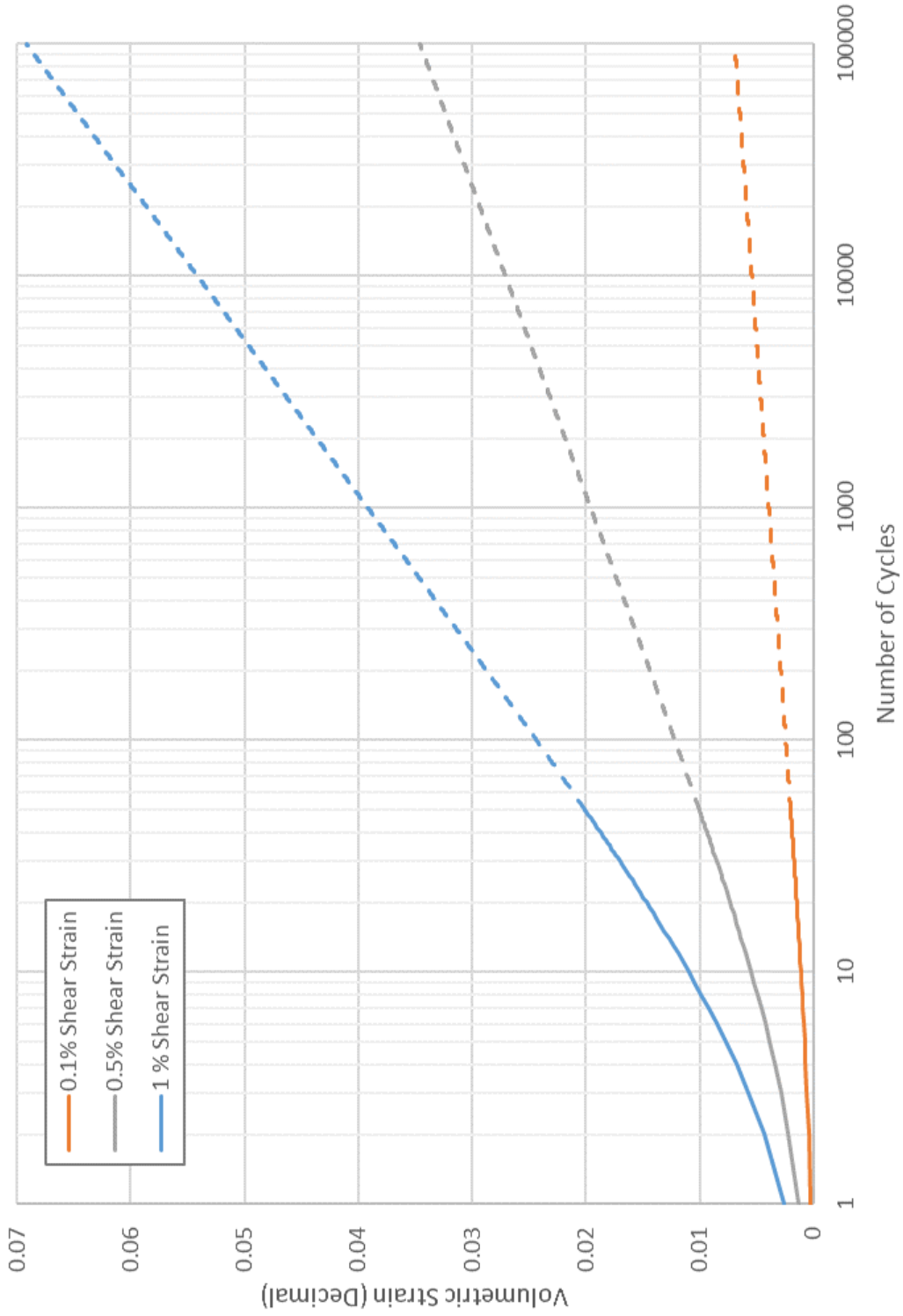
EXAMPLE DEGRADATION INDEX CURVES FOR VARYING SHEAR STRAINS
 Cyclic Loading Effects on Suction Bucket Foundations
 Offshore Wind Turbines

FIGURE 3.3-3



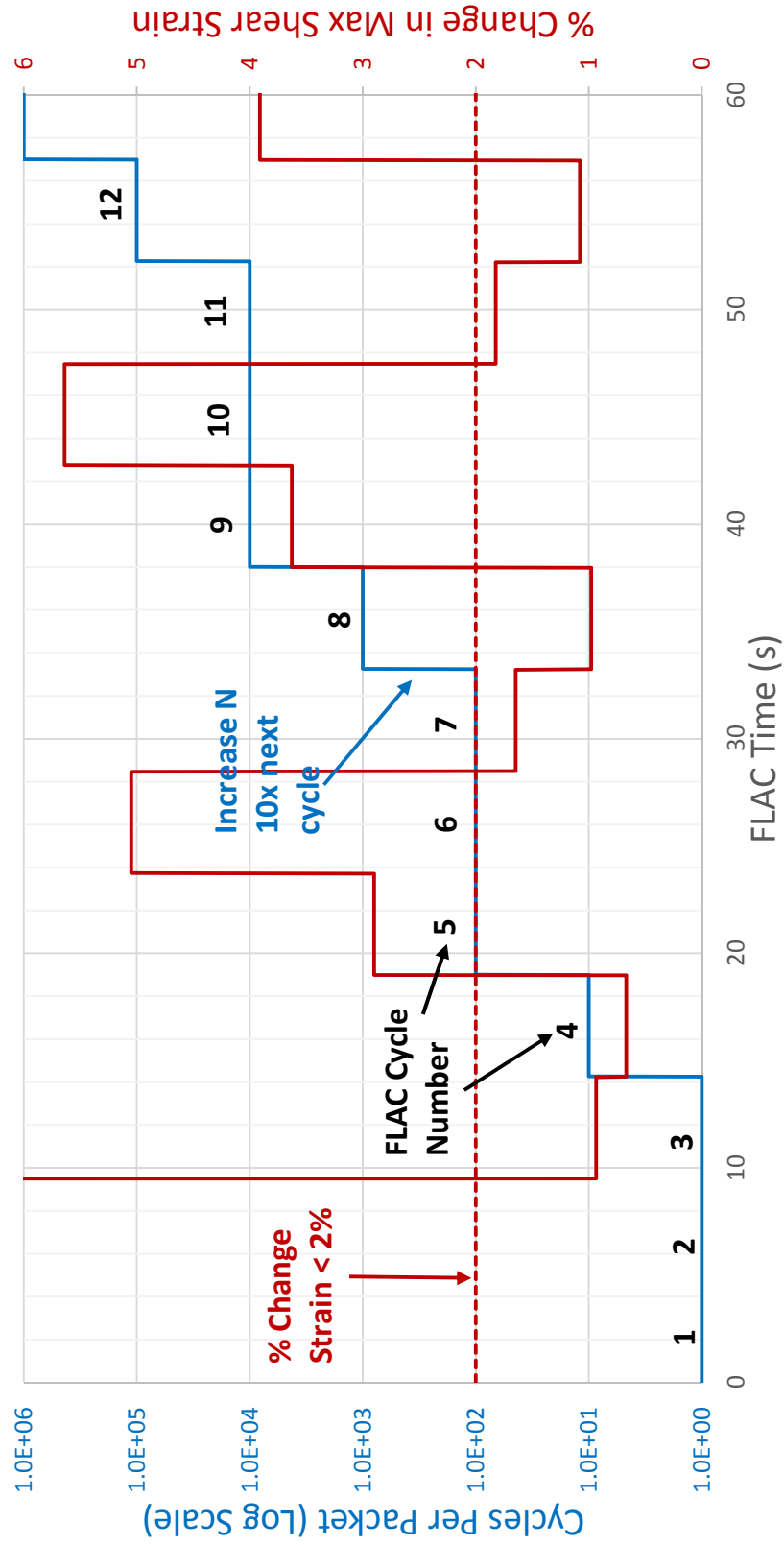
EXAMPLE APPROACH TO VARIABLE SHEAR STRAINS
Cyclic Loading Effects on Suction Bucket Foundations
Offshore Wind Turbines

FIGURE 3.3-4



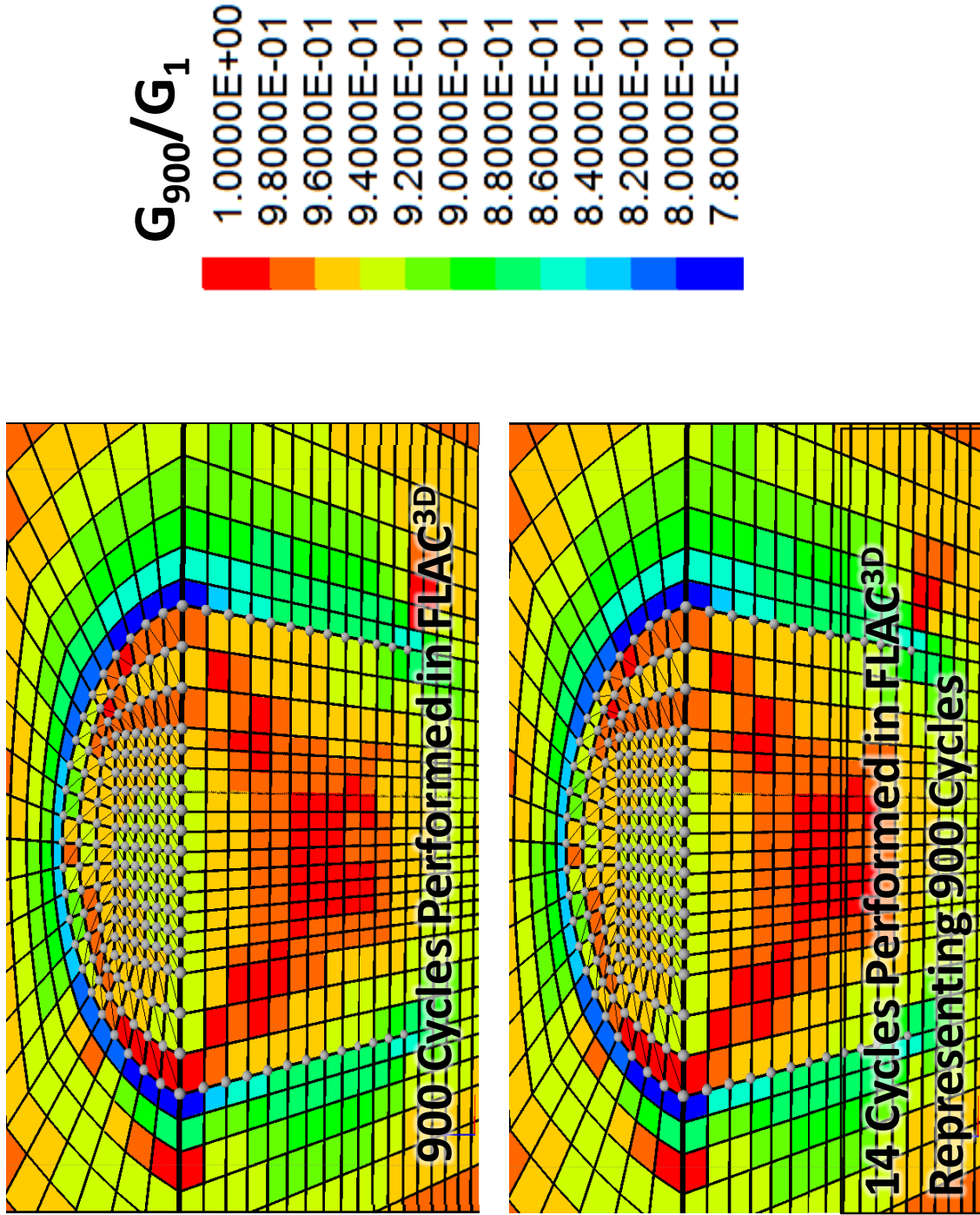
EXAMPLE OF FINN/BYRNE MODEL FOR THREE STRAIN LEVELS
 Cyclic Loading Effects on Suction Bucket Foundations
 Offshore Wind Turbines

FIGURE 3.3-5



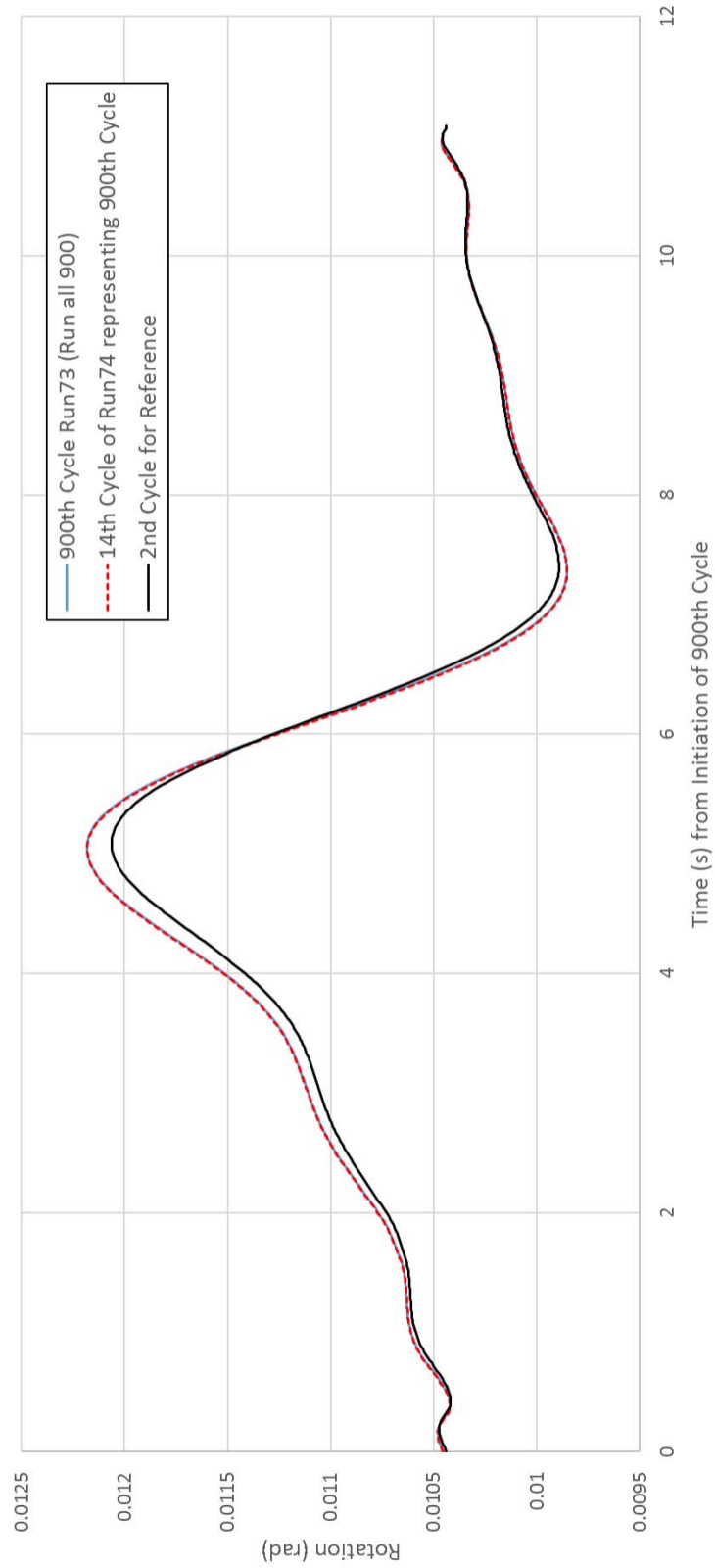
EXAMPLE OF STEPPING PROCEDURE
 Cyclic Loading Effects on Suction Bucket Foundations
 Offshore Wind Turbines

FIGURE 3.4-1



VALIDATION OF STEPPING APPROACH – CONTOURS AFTER 900 CYCLES
 Cyclic Loading Effects on Suction Bucket Foundations
 Offshore Wind Turbines

FIGURE 3.4-2



VALIDATION OF STEPPING APPROACH – ROTATION AFTER 900 CYCLES
Cyclic Loading Effects on Suction Bucket Foundations
Offshore Wind Turbines

FIGURE 3.4-3

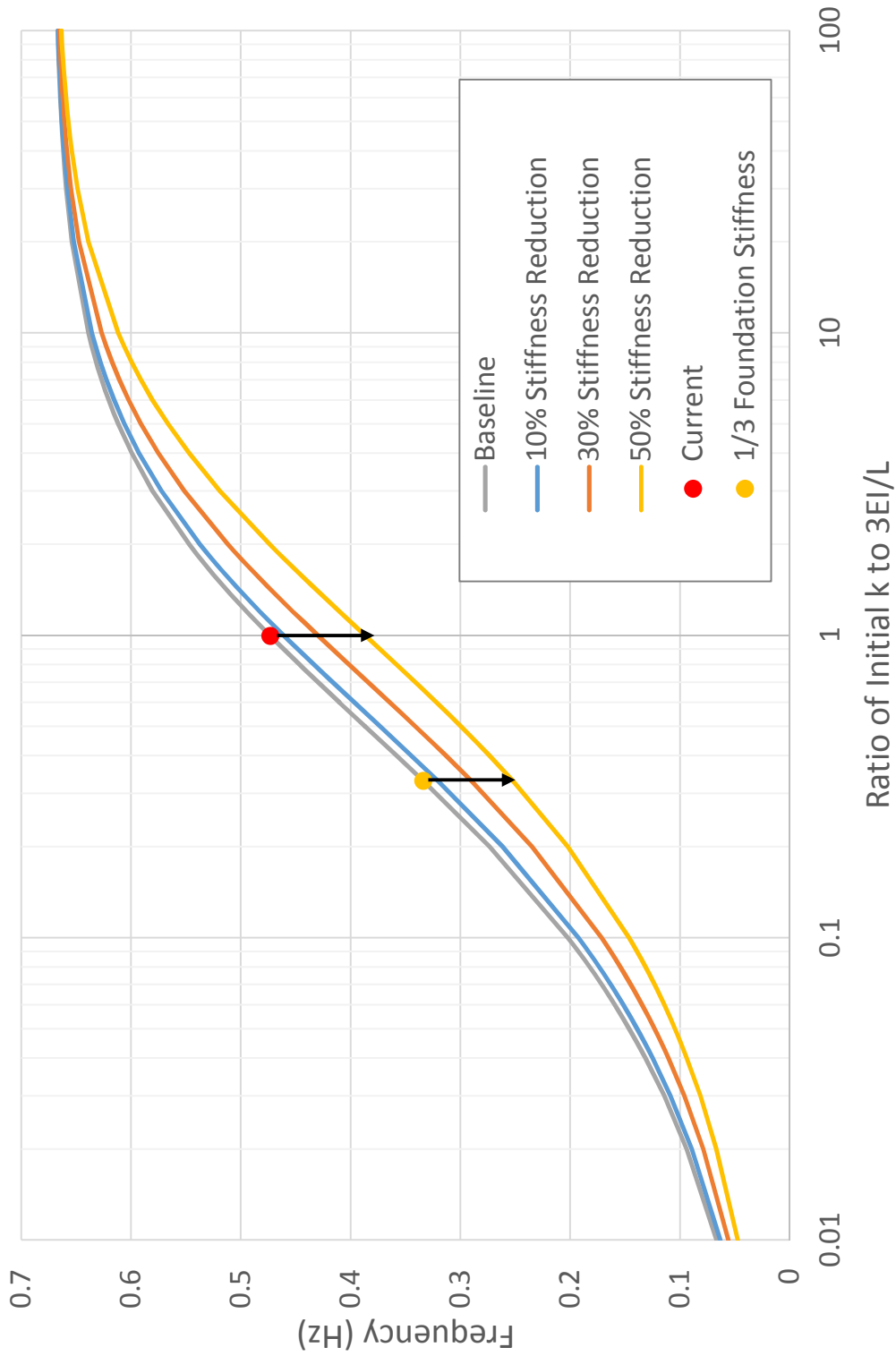


ILLUSTRATION OF STIFFNESS REDUCTION IMPACT ON GLOBAL FUNDAMENTAL FREQUENCIES
 Cyclic Loading Effects on Suction Bucket Foundations
 Offshore Wind Turbines

FIGURE 3.6-1

SECTION 4.0



4.0 ADVANCED NUMERICAL MODELING ANALYSES RESULTS

4.1 INTRODUCTION

This section presents the results from the analyses performed following the methodology outlined in [Section 3.0](#). [Table 4.1-1](#) summarizes the cases presented.

Table 4.1-1. Analysis Cases Presented

Case	Mono-bucket	Tetrapod
Soft Clay	X ¹	X ¹
Stiff Clay	X	X
Dense Sand	X	X
Interlayered	X	X

Note: 1) Sensitivity analyses performed with strength degradation.

4.2 CYCLIC LOADING ON MONO-BUCKET FOUNDATION

4.2.1 Uniform Clay (soft and stiff)

[Figure 4.2-1](#) illustrates the degradation index after one week of storm loading followed by 30 years of normal sea state loading. The small black cubes indicate the nodes of the bucket structural elements. The maximum amount of degradation occurred near the top edge of the bucket where the degradation index reached a low of around 75 percent. The amount of degradation decreased with depth, with degradation indices of around 90 percent in the soil zones adjacent to the bucket skirt.

[Figure 4.2-2](#) shows the rotational stiffness of the bucket as a function of time. When plotted on a logarithmic time scale, the rotational stiffness decreased more rapidly during the storm loading than normal sea state, which is consistent with the larger storm load amplitudes. The overall decrease in the rotational stiffness is moderate.

[Figure 4.2-3](#) provides an example of the global fundamental frequency of the bucket-superstructure system, using the example superstructure properties presented previously in [Table 3.5-1](#). As the frequency depends on the rotational stiffness of the bucket, it follows a similar shape as that observed in [Figure 4.2-2](#). However, as the frequency also depends on the superstructure properties, the percent change in the frequency over 30 years is less than the percent change in the rotational stiffness.

[Figure 4.2-4](#) presents the maximum rotation reached during a given cycle as a function of time. The baseline case, assuming no strength degradation, shows a very minor increase during the storm loading and a significant drop after the reduction to normal sea state loading, as expected. In contrast, the sensitivity analysis that included strength degradation shows a significant increase in the maximum rotation during the course of storm loading. This indicates that the strength degradation may be important to consider in future research, particularly when the total rotation of the tower is of concern. However, incorporating strength degradation had very minimal impact on the rotational stiffness and fundamental frequency, which was the focus of this study.



4.2.2 Stiff Clay

Figure 4.2-5 illustrates the degradation index after one week of storm loading followed by 30 years of normal sea state loading. The small black cubes indicate the nodes of the bucket structural elements. The maximum amount of degradation occurred near the top edge of the bucket where the degradation index reached a low of around 85 percent. The amount of degradation decreased with depth, with degradation indices of around 95 percent in the soil zones adjacent to the bucket skirt.

Figure 4.2-6 shows the rotational stiffness of the bucket as a function of time. When plotted on a logarithmic time scale, the rotational stiffness decreased more rapidly during the storm loading than normal sea state, which is consistent with the larger storm load amplitudes. The overall decrease in the rotational stiffness is moderate.

Figure 4.2-7 provides an example of the global fundamental frequency of the bucket-superstructure system, using the example superstructure properties presented previously in Table 3.5-1. As the frequency depends on the rotational stiffness of the bucket, it follows a similar shape as that observed in Figure 4.2-6. However, as the frequency also depends on the superstructure properties, the percent change in the frequency over 30 years is less than the percent change in the rotational stiffness.

Figure 4.2-8 presents the maximum rotation reached during a given cycle as a function of time. There is a very minor increase during the storm loading and a significant drop after the reduction to normal sea state loading, as expected. The analysis for this case does not include strength degradation.

4.2.3 Dense Sand

Figure 4.2-9 illustrates the degradation index after one week of storm loading followed by 30 years of normal sea state loading. The small black cubes indicate the nodes of the bucket structural elements. The maximum amount of densification occurred near the top edge of the bucket where the “degradation” index increased to a maximum of around 1.05. The amount of densification decreased rapidly with depth and was negligible below the top few meters.

Figure 4.2-10 shows the rotational stiffness of the bucket as a function of time. During storm loading, the rotational stiffness increased slightly due to the densification-induced shear modulus increase. However, there is a sudden, significant increase in the rotational stiffness when changing to the smaller normal sea state load. This indicates that, for the sand, the stiffness depends on the loading amplitude. This is in contrast to the clay where there is not a sharp discontinuity.

Figure 4.2-11 provides an example of the global fundamental frequency of the bucket-superstructure system, using the example superstructure properties presented previously in Table 3.5-1. As the frequency depends on the rotational stiffness of the bucket, it follows a similar shape as that observed in Figure 4.2-10. However, as the frequency also depends on the superstructure properties, the percent change in the frequency over 30 years is less than the percent change in the rotational stiffness.

Figure 4.2-12 presents the maximum rotation reached during a given cycle as a function of time. The increase during the storm loading is negligible and a significant drop occurs after the reduction to normal sea state loading, as expected.



4.2.4 Interlayered

Figure 4.2-13 illustrates the degradation index after one week of storm loading followed by 30 years of normal sea state loading. The small black cubes indicate the nodes of the bucket structural elements. The sharp discontinuity between the contours occurs at a depth of 6 m, at the interface between the sand and clay. The clay degrades to a minimum degradation index of around 0.88. Whereas there is a slight increase in the “degradation” index in the sand at the top edge of the bucket. However, at almost no densification occurs below the top meter of sand.

Figure 4.2-14 shows the rotational stiffness of the bucket as a function of time. During storm loading, the rotational stiffness initially increased but then slightly decreased due to counteracting effects of densification in sand and degradation in clay. However, there is a sudden, significant increase in the rotational stiffness when changing to the smaller normal sea state load. This indicates that, for the interlayered case, the stiffness depends on the loading amplitude. This is in contrast to the stiff or soft clay models where there is not a sharp discontinuity.

Figure 4.2-15 provides an example of the global fundamental frequency of the bucket-superstructure system, using the example superstructure properties presented previously in Table 3.5-1. As the frequency depends on the rotational stiffness of the bucket, it follows a similar shape as that observed in Figure 4.2-14. However, as the frequency also depends on the superstructure properties, the percent change in the frequency over 30 years is less than the percent change in the rotational stiffness.

Figure 4.2-16 presents the maximum rotation reached during a given cycle as a function of time. The increase during the storm loading is small and a significant drop occurs after the reduction to normal sea state loading, as expected.

4.3 CYCLIC LOADING ON MULTI-BUCKET FOUNDATION

4.3.1 Soft Clay

Figure 4.3-1 illustrates the degradation index after one week of storm loading followed by 30 years of normal sea state loading. The small black cubes indicate the nodes of the bucket structural elements. The maximum amount of degradation occurred near the top edge of the bucket where the degradation index reached a low of around 85percent. The amount of degradation decreased with depth, with degradation indices of around 90percent in the soil zones adjacent to the bucket skirt.

Figure 4.3-2 shows the rotational stiffness of the tetrapod system as a function of time. The rotational stiffness was back-calculated from the vertical stiffness to represent the overall tetrapod behavior. When plotted on a logarithmic time scale, the rotational stiffness decreased more rapidly during the storm loading than normal sea state, which is consistent with the larger storm load amplitudes. The overall decrease in the rotational stiffness is moderate.

Figure 4.3-3 provides an example of the global fundamental frequency of the bucket-superstructure system, using the example superstructure properties presented previously in Table 3.5-1. As the frequency depends on the rotational stiffness of the bucket, it follows a similar shape as that observed in Figure 4.3-2. However, as the frequency also depends on the superstructure properties, the percent change in the frequency over 30 years is less than the percent change in the rotational stiffness.



Figure 4.3-4 presents the maximum rotation reached during a given cycle as a function of time. The baseline case, assuming no strength degradation, shows a negligible increase during the storm loading and a significant drop after the reduction to normal sea state loading, as expected. The sensitivity analysis that included strength degradation shows a small increase in the maximum rotation during the course of storm loading. This indicates that the strength degradation may be important to consider in future research, particularly when the total rotation of the tower is of concern. However, incorporating strength degradation had very minimal impact on the rotational stiffness and fundamental frequency, which was the focus of this study.

4.3.2 Stiff Clay

Figure 4.3-5 illustrates the degradation index after one week of storm loading followed by 30 years of normal sea state loading. The small black cubes indicate the nodes of the bucket structural elements. The maximum amount of degradation occurred near the top edge of the bucket where the degradation index reached a low of around 93 percent. The amount of degradation decreased with depth, with degradation indices of around 96 percent in the soil zones adjacent to the bucket skirt.

Figure 4.3-6 shows the rotational stiffness of the bucket as a function of time. When plotted on a logarithmic time scale, the rotational stiffness decreased more rapidly during the storm loading than normal sea state, which is consistent with the larger storm load amplitudes. The overall decrease in the rotational stiffness is small.

Figure 4.3-7 provides an example of the global fundamental frequency of the bucket-superstructure system, using the example superstructure properties presented previously in Table 3.5-1. As the frequency depends on the rotational stiffness of the bucket, it follows a similar shape as that observed in Figure 4.3-6. However, as the frequency also depends on the superstructure properties, the percent change in the frequency over 30 years is less than the percent change in the rotational stiffness.

Figure 4.3-8 presents the maximum rotation reached during a given cycle as a function of time. There is a negligible increase during the storm loading and a significant drop after the reduction to normal sea state loading, as expected. The analysis for this case does not include strength degradation.

4.3.3 Dense Sand

Figure 4.3-9 illustrates the degradation index after one week of storm loading followed by 30 years of normal sea state loading. The small black cubes indicate the nodes of the bucket structural elements. The maximum amount of densification occurred near the top edge of the bucket where the “degradation” index increased to a maximum of less than 1.01. The amount of densification decreased even further with depth.

Figure 4.3-10 shows the rotational stiffness of the bucket as a function of time. The change in stiffness is negligible and is so small that the exact shape of the curve may not be meaningful. Figure 4.3-11 provides an example of the global fundamental frequency of the bucket-superstructure system, using the example superstructure properties presented previously in Table 3.5-1. As the frequency depends on the rotational stiffness of the bucket, it follows a similar shape as that observed in Figure 4.3-10. Again, the change is negligible.



Figure 4.3-12 presents the maximum rotation reached during a given cycle as a function of time. The increase during the storm loading is negligible and a significant drop occurs after the reduction to normal sea state loading, as expected.

4.3.4 Interlayered

Figure 4.3-13 illustrates the degradation index after one week of storm loading followed by 30 years of normal sea state loading. The small black cubes indicate the nodes of the bucket structural elements. The sharp discontinuity between the contours occurs at a depth of 6 m, at the interface between the sand and clay. The clay degrades to a minimum degradation index of around 0.88. The densification of sand was negligible and led to an increase in the “degradation” index to less than 1.01.

Figure 4.3-14 shows the rotational stiffness of the bucket as a function of time. During storm loading, the rotational stiffness initially increased but then slightly decreased due to counteracting effects of densification in sand and degradation in clay. However, there is a sudden, significant increase in the rotational stiffness when changing to the smaller normal sea state load. This indicates that, for the interlayered case, the stiffness depends on the loading amplitude. This is in contrast to the stiff or soft clay models where there is not a sharp discontinuity.

Figure 4.3-15 provides an example of the global fundamental frequency of the bucket-superstructure system, using the example superstructure properties presented previously in Table 3.5-1. As the frequency depends on the rotational stiffness of the bucket, it follows a similar shape as that observed in Figure 4.3-14. However, as the frequency also depends on the superstructure properties, the percent change in the frequency over 30 years is less than the percent change in the rotational stiffness.

Figure 4.3-16 presents the maximum rotation reached during a given cycle as a function of time. The increase during the storm loading is small and a significant drop occurs after the reduction to normal sea state loading, as expected.

4.4 SUMMARY

Table 4.4-1 presents a summary of the initial (i.e., from the first loading cycle) key response values from the analyses performed. The peak rotation is the maximum rotation reached during a cycle of loading. Of course, the initial values of the baseline soft clay (no strength degradation) vs. soft clay with strength degradation are identical, but are provided for subsequent comparison. In general, the rotational stiffness was as follows, from stiffest to softest: stiff clay, sand, interlayered, and soft clay. The tetrapod system was overall stiffer than the mono-bucket.



Table 4.4-1. Initial Key Response Values

Foundation	Property	Soft Clay	Soft Clay w/ Strength Degradation	Stiff Clay	Sand	Interlayered
Mono-bucket	Peak Rotation (deg)	0.17	0.17	0.04	0.09	0.23
	Rotational Stiffness (kN-m/rad)	1.43E+08	1.42E+08	3.88E+08	2.43E+08	1.58E+08
	Fundamental Frequency (Hz) ¹	0.47	0.47	0.57	0.53	0.49
Tetrapod System	Peak Rotation (deg)	0.09	0.09	0.03	0.02	0.04
	Rotational Stiffness (kN-m/rad)	4.62E+08	4.62E+08	1.32E+09	8.66E+08	4.48E+08
	Fundamental Frequency (Hz) ¹	0.59	0.59	0.64	0.62	0.58

Notes: 1) Using example superstructure properties in [Table 3.5-1](#)

[Table 4.4-2](#) presents a summary of the percent change in key response values during the storm loading. Similarly, [Table 4.4-3](#) presents a summary of the percent change in key response values during the normal sea state loading (i.e., the beginning of normal sea state loading is taken as the initial value in the percent change calculation). It is important to note that the order these loading scenarios are applied will affect the results. As described in Section 3.2, the foundations were subjected to storm loading followed by normal sea state loading in this study. Key observations include the following:

- Degradation of clay led to a decrease in the rotational stiffness and fundamental frequency, whereas densification of drained sands led to an increase in rotational stiffness and fundamental frequency.
- The percent change in the stiffness (and thus frequency) from largest to smallest were soft clay, stiff clay, interlayered, and sand, respectively.
- The mono-bucket generally underwent more change in all three response values (peak rotation, rotational stiffness, and fundamental frequency) than the tetrapod system.
- The percent change in peak rotation was generally around 1 percent or less, except for the mono-bucket with soft clay including strength degradation, in which case a significant increase in peak rotation occurred.
- The addition of strength degradation to the soft clay analyses did not significantly affect the rotational stiffness and hence fundamental frequency, which was the focus of this study.



Table 4.4-2. Percent Change in Key Response Values during Storm Loading

Foundation	Property	Soft Clay	Soft Clay w/ Strength Degradation	Stiff Clay	Sand	Interlayered
Mono-bucket	Peak Rotation (deg)	1.1%	69.7%	0.9%	0.5%	1.0%
	Rotational Stiffness (kN-m/rad)	-5.5%	-5.1%	-3.0%	1.2%	0.9%
	Fundamental Frequency (Hz) ¹	-1.4%	-1.3%	-0.4%	0.2%	0.1%
Tetrapod System	Peak Rotation (deg)	-0.7%	1.7%	-0.4%	-0.2%	-0.3%
	Rotational Stiffness (kN-m/rad)	-2.6%	-2.6%	-1.3%	-0.1%	-1.4%
	Fundamental Frequency (Hz) ¹	-0.3%	-0.3%	-0.1%	0.0%	-0.2%

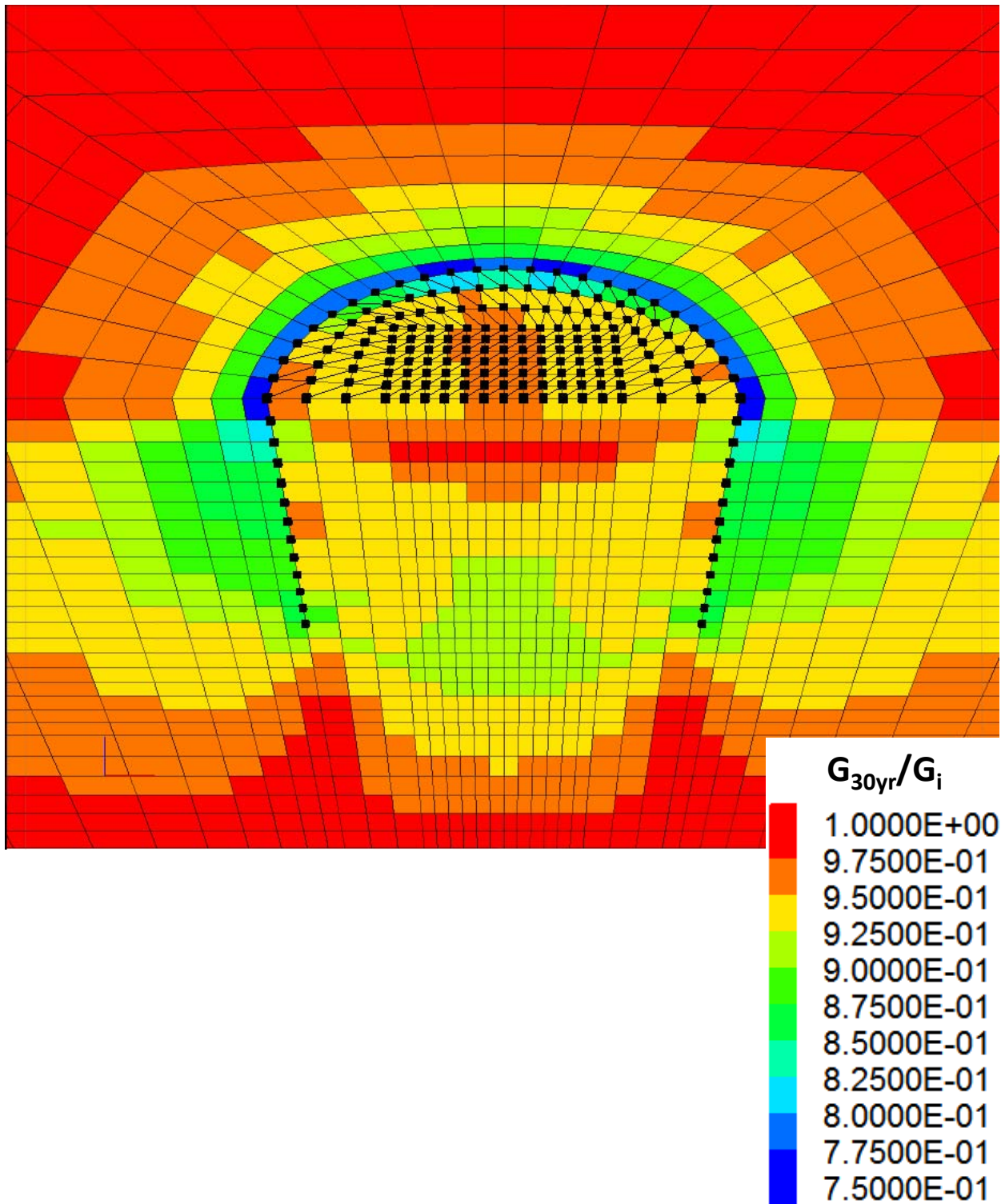
Notes: 1) Using example superstructure properties in [Table 3.5-1](#)

Table 4.4-3. Percent Change in Key Response Values during Normal Sea State Loading

Foundation	Property	Soft Clay	Soft Clay w/ Strength Degradation	Stiff Clay	Sand	Interlayered
Mono-bucket	Peak Rotation (deg)	0.4%	0.0%	0.4%	0.0%	0.0%
	Rotational Stiffness (kN-m/rad)	-2.0%	-2.6%	-1.1%	0.1%	-0.7%
	Fundamental Frequency (Hz) ¹	-0.5%	-0.7%	-0.1%	0.0%	-0.2%
Tetrapod System	Peak Rotation (deg)	-1.0%	-0.9%	-0.6%	0.0%	-1.2%
	Rotational Stiffness (kN-m/rad)	-1.0%	-1.0%	-0.5%	0.0%	-0.7%
	Fundamental Frequency (Hz) ¹	-0.1%	-0.1%	0.0%	0.0%	-0.1%

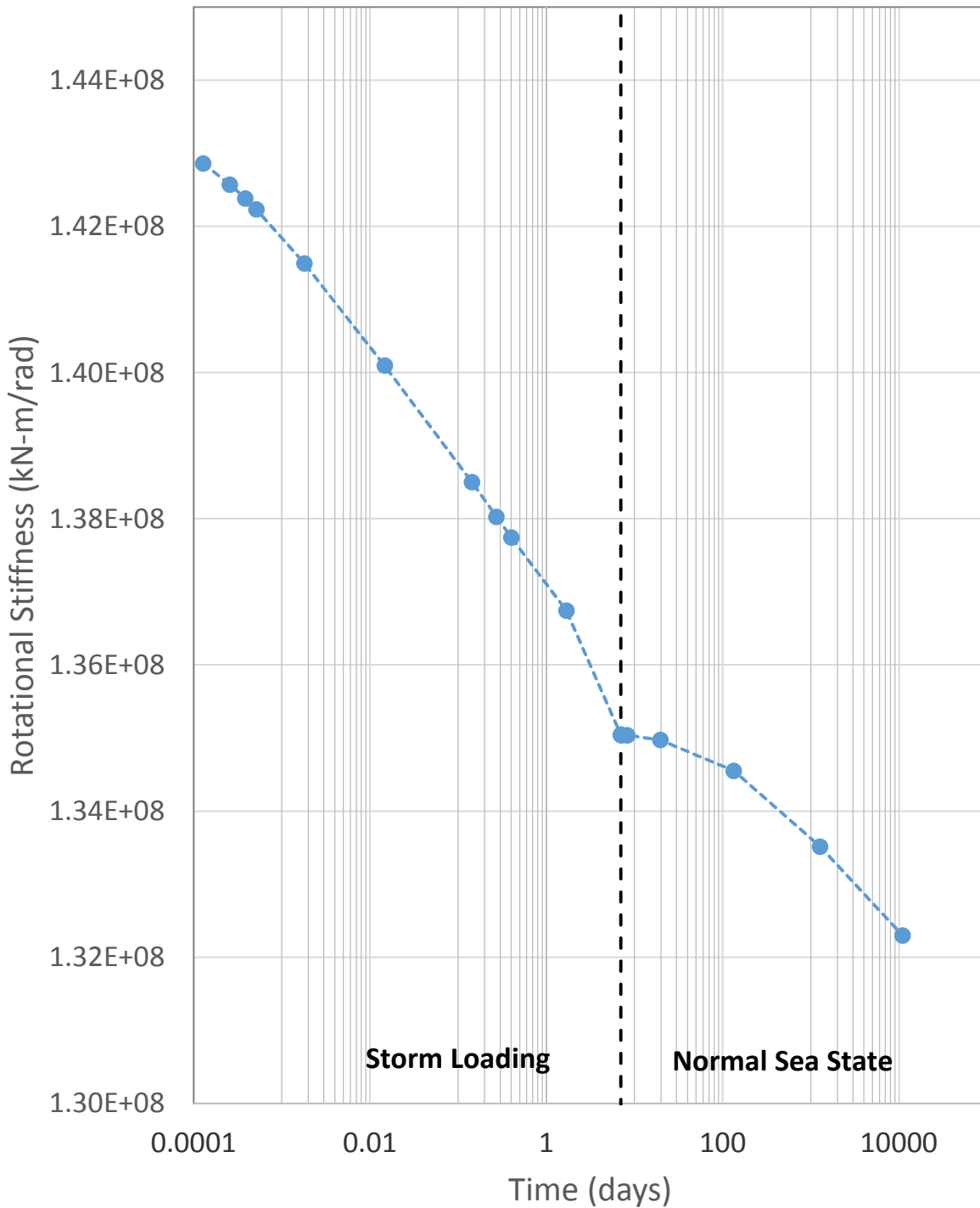
Notes: 1) Using example superstructure properties in [Table 3.5-1](#)

It is important to note that the conclusions presented above and the trends from [Tables 4.4-1, 4.4-2, and 4.4-3](#), are applicable to the scenarios analyzed, but may be different if a wider combination of soil conditions, loading scenarios, and bucket designs are considered. For example, in this study, a single sized mono-bucket was used for all soil types. Hence, the dimensions are likely conservative for the sand and stiff clay cases. We recommend that additional evaluations be performed for buckets with dimensions specifically developed for each type of soil condition considered (e.g., the mono-bucket in sand should be smaller than a mono-bucket in clay, assuming the same loading conditions).

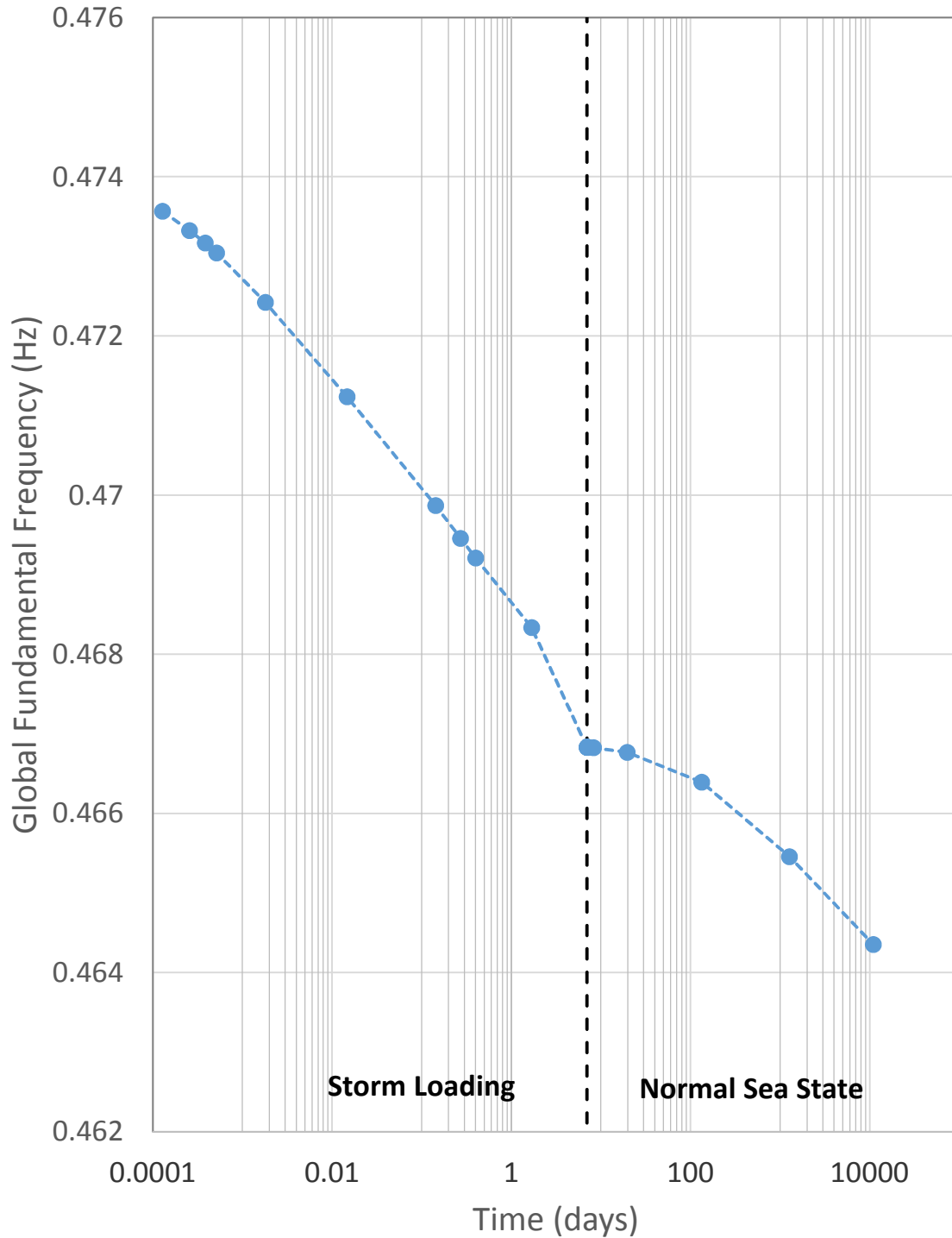


DEGRADATION INDEX CONTOURS – MONOCAISSON, SOFT CLAY
Cyclic Loading Effects on Suction Bucket Foundations
Offshore Wind Turbines

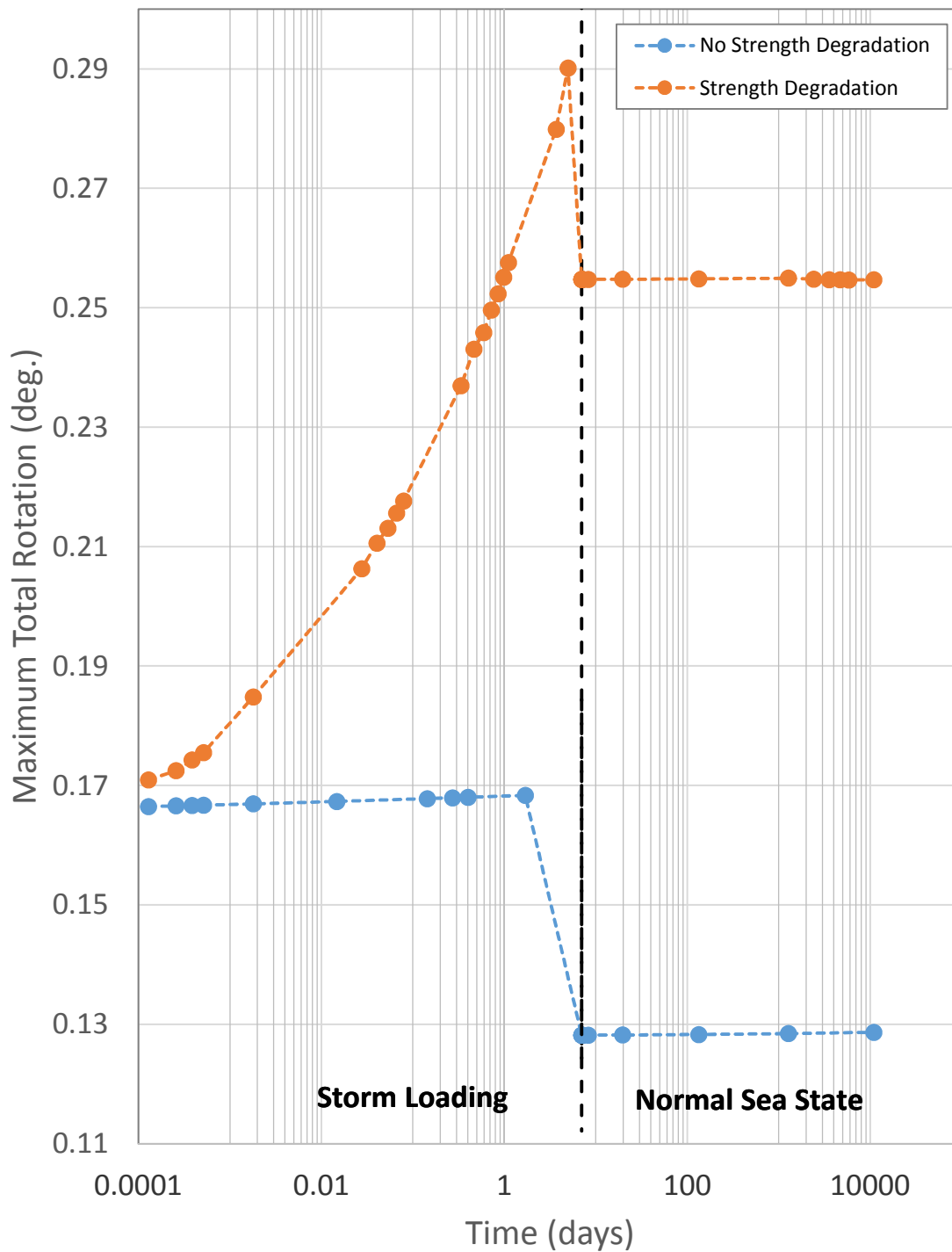
FIGURE 4.2-1



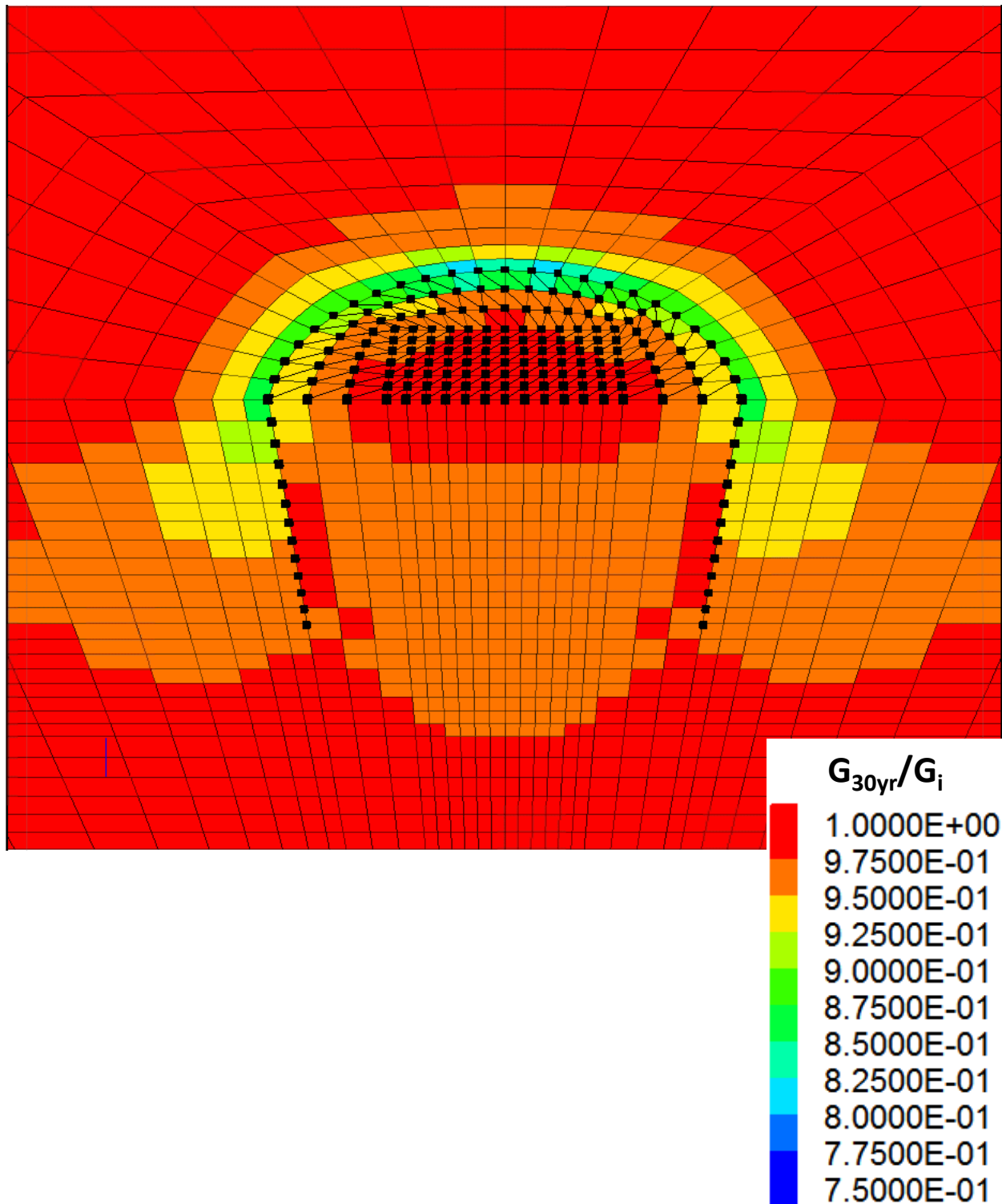
ROTATIONAL STIFFNESS VS. TIME – MONOCAISSON, SOFT CLAY
Cyclic Loading Effects on Suction Bucket Foundations
Offshore Wind Turbines



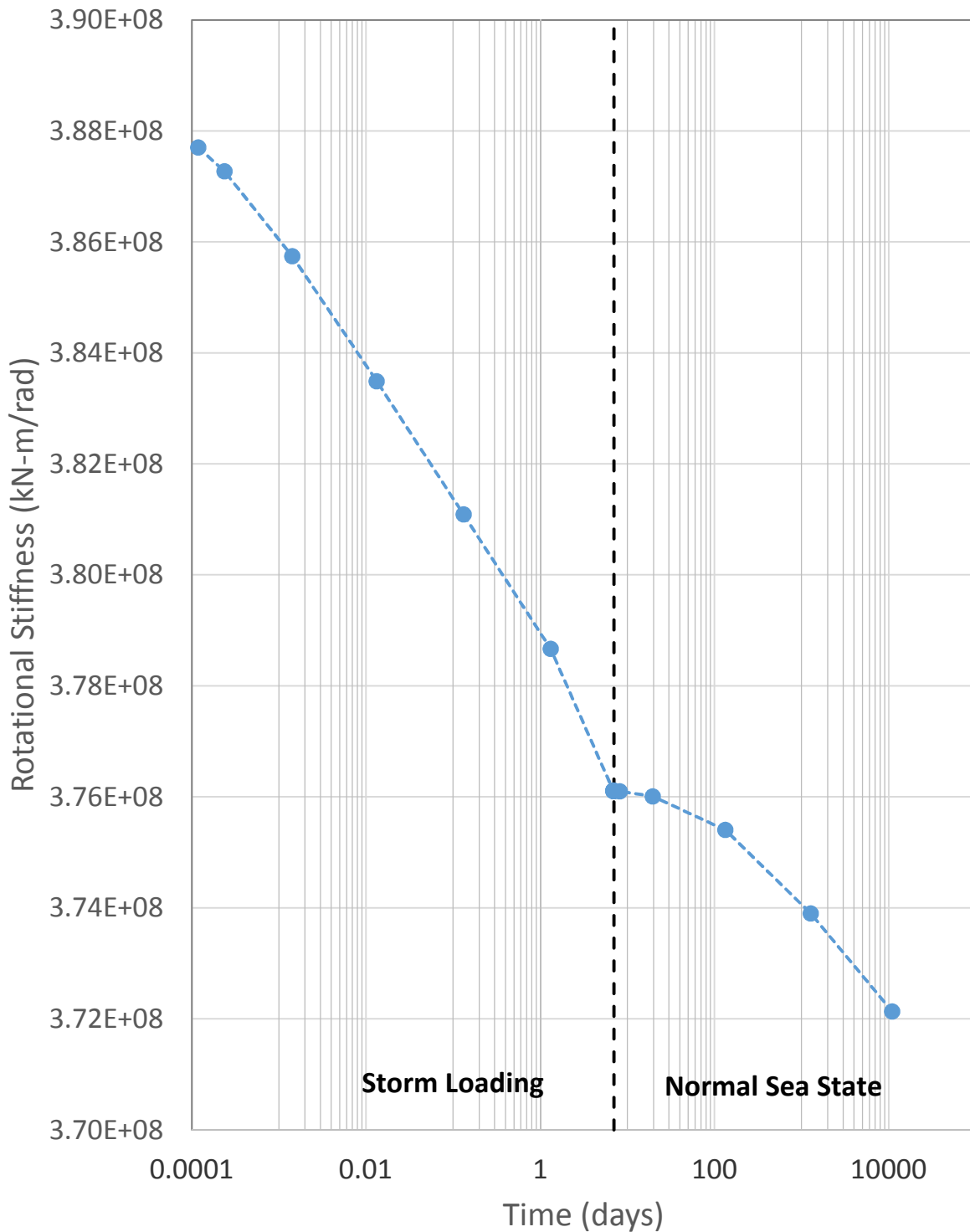
GLOBAL FUNDAMENTAL FREQUENCY VS. TIME – MONOCAISSON, SOFT CLAY
Cyclic Loading Effects on Suction Bucket Foundations
Offshore Wind Turbines



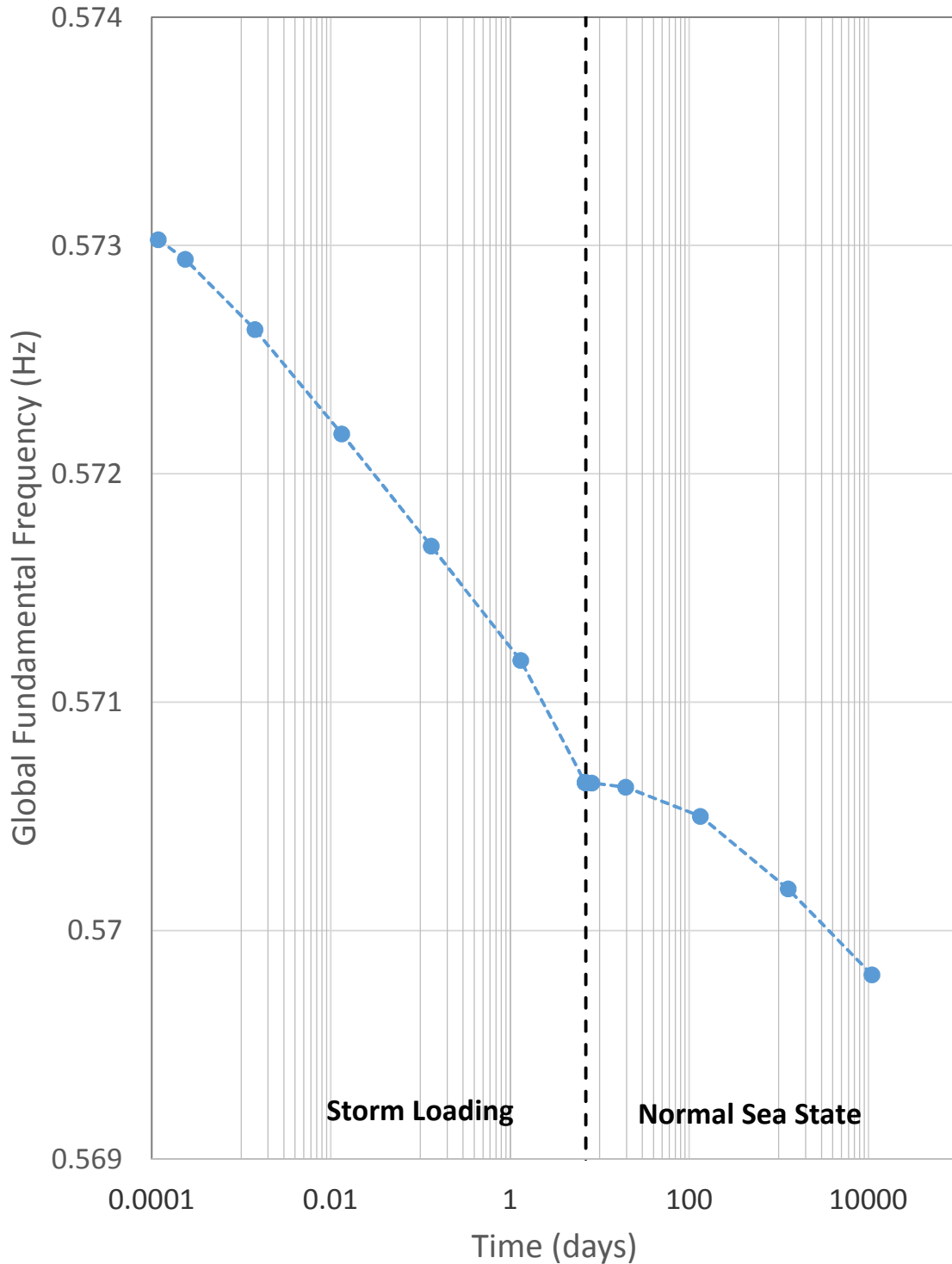
MAXIMUM TOTAL ROTATION VS. TIME – MONOCAISSON, SOFT CLAY
Cyclic Loading Effects on Suction Bucket Foundations
Offshore Wind Turbines



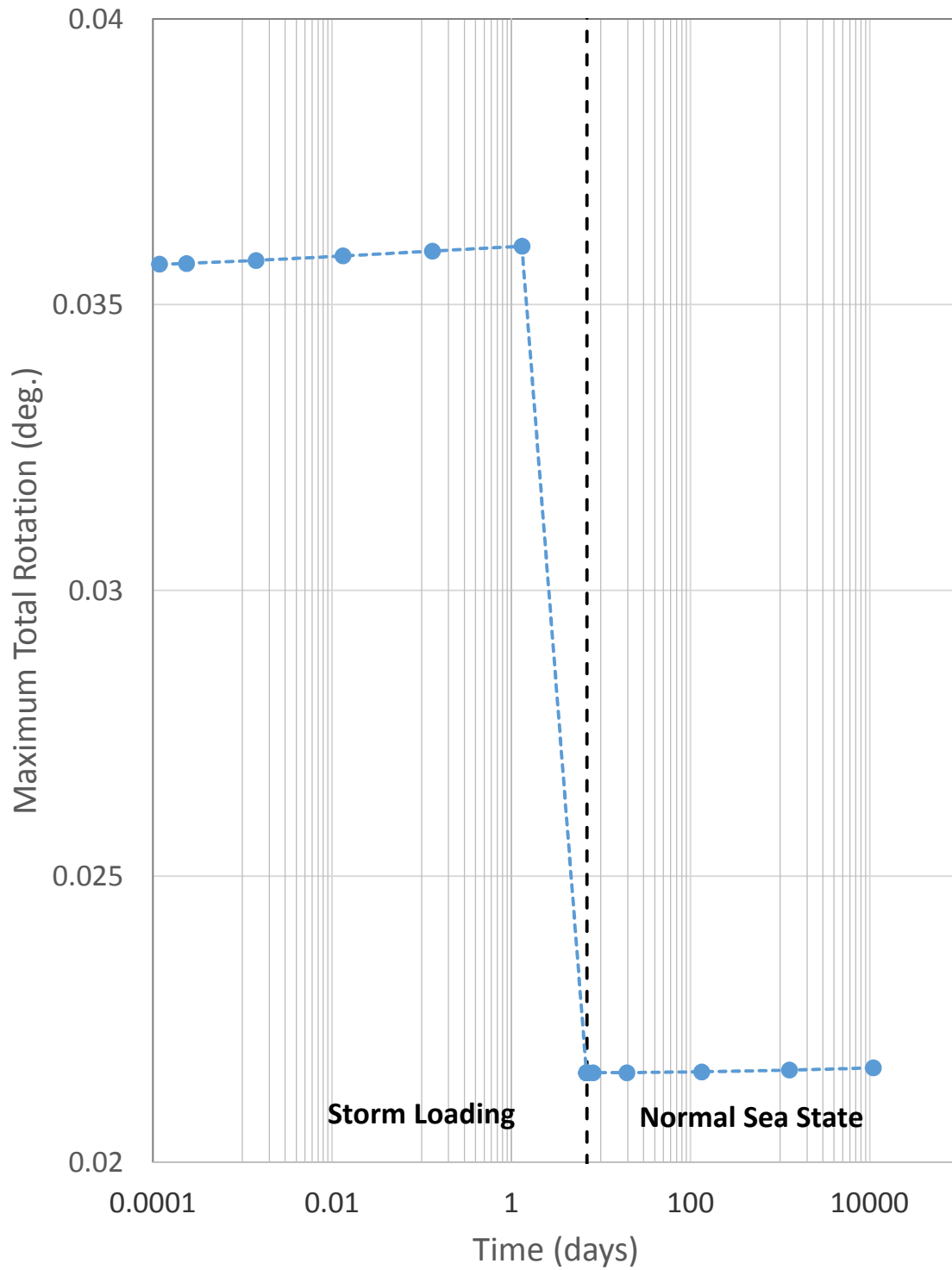
DEGRADATION INDEX CONTOURS – MONOCAISSON, STIFF CLAY
Cyclic Loading Effects on Suction Bucket Foundations
Offshore Wind Turbines



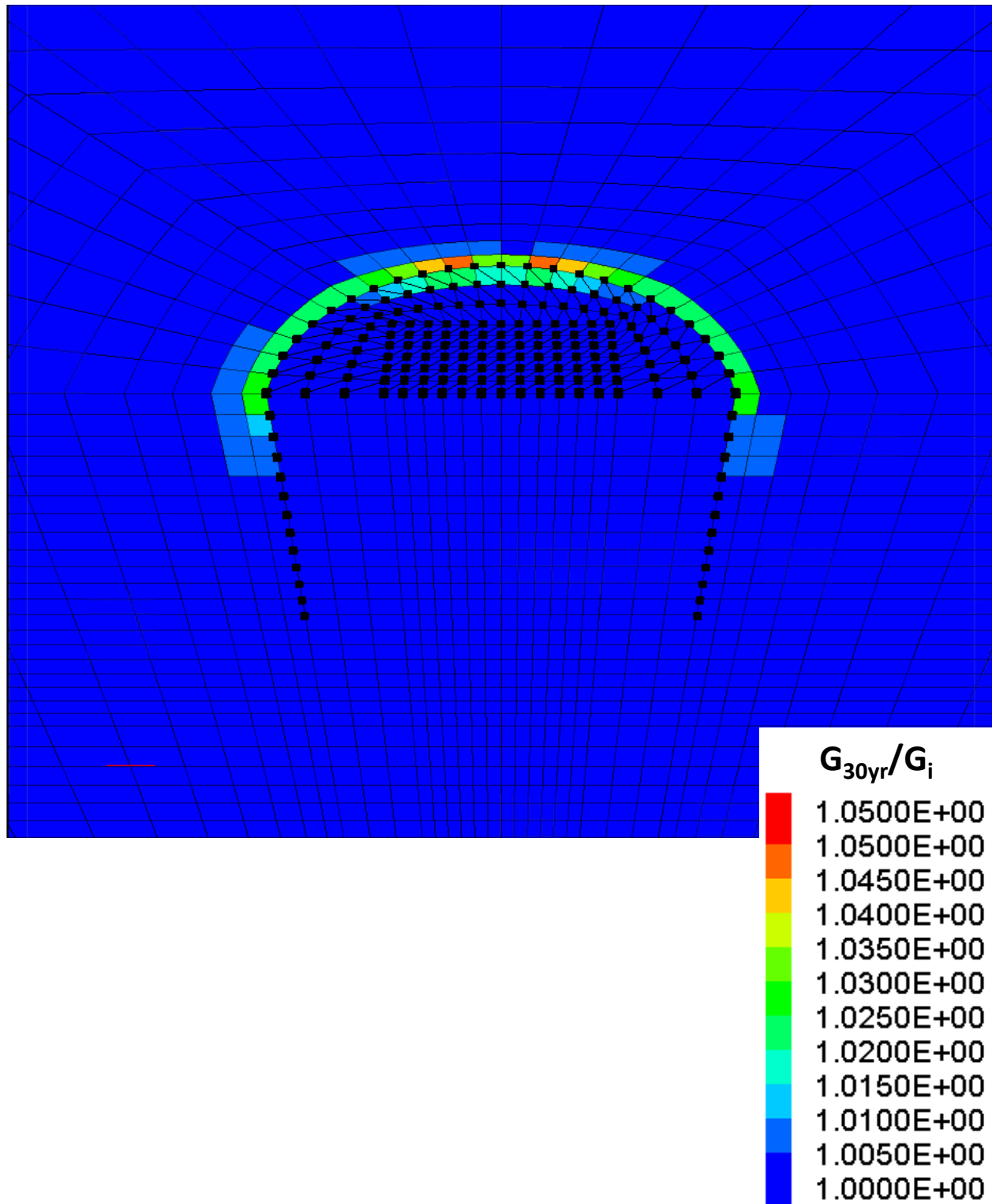
ROTATIONAL STIFFNESS VS. TIME – MONOCAISSON, STIFF CLAY
Cyclic Loading Effects on Suction Bucket Foundations
Offshore Wind Turbines



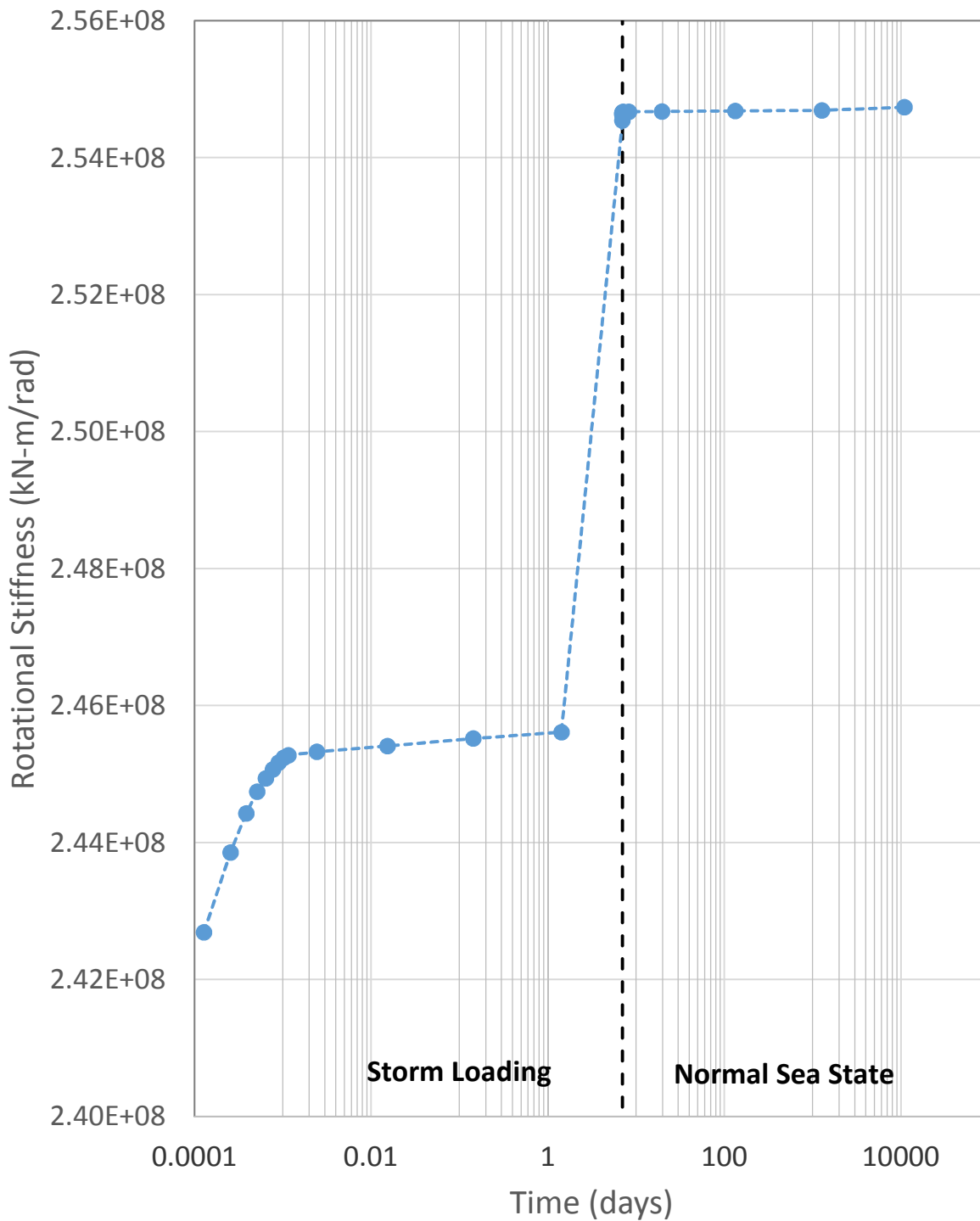
GLOBAL FUNDAMENTAL FREQUENCY VS. TIME – MONOCAISSON, STIFF CLAY
Cyclic Loading Effects on Suction Bucket Foundations
Offshore Wind Turbines



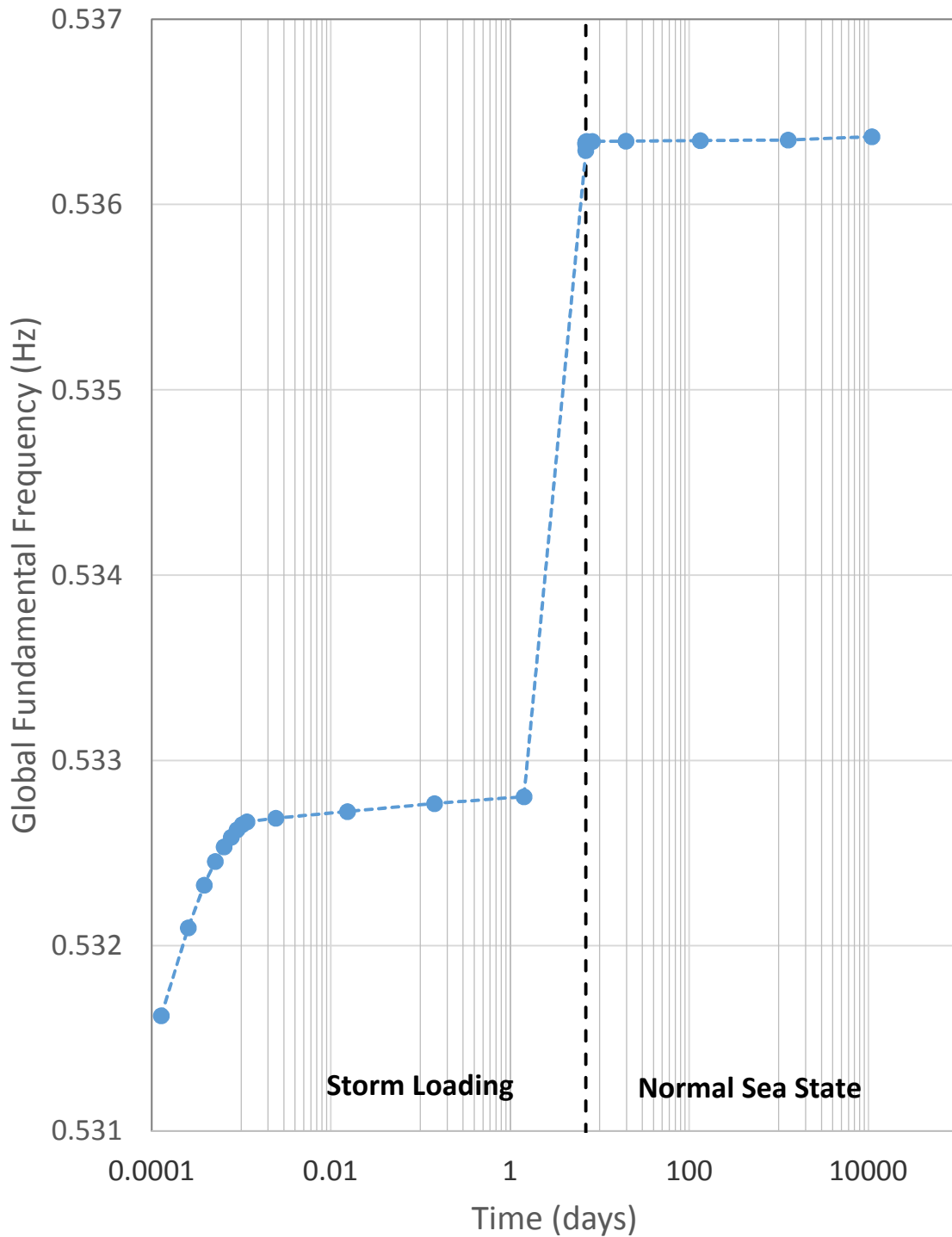
MAXIMUM TOTAL ROTATION VS. TIME – MONOCAISSON, STIFF CLAY
Cyclic Loading Effects on Suction Bucket Foundations
Offshore Wind Turbines



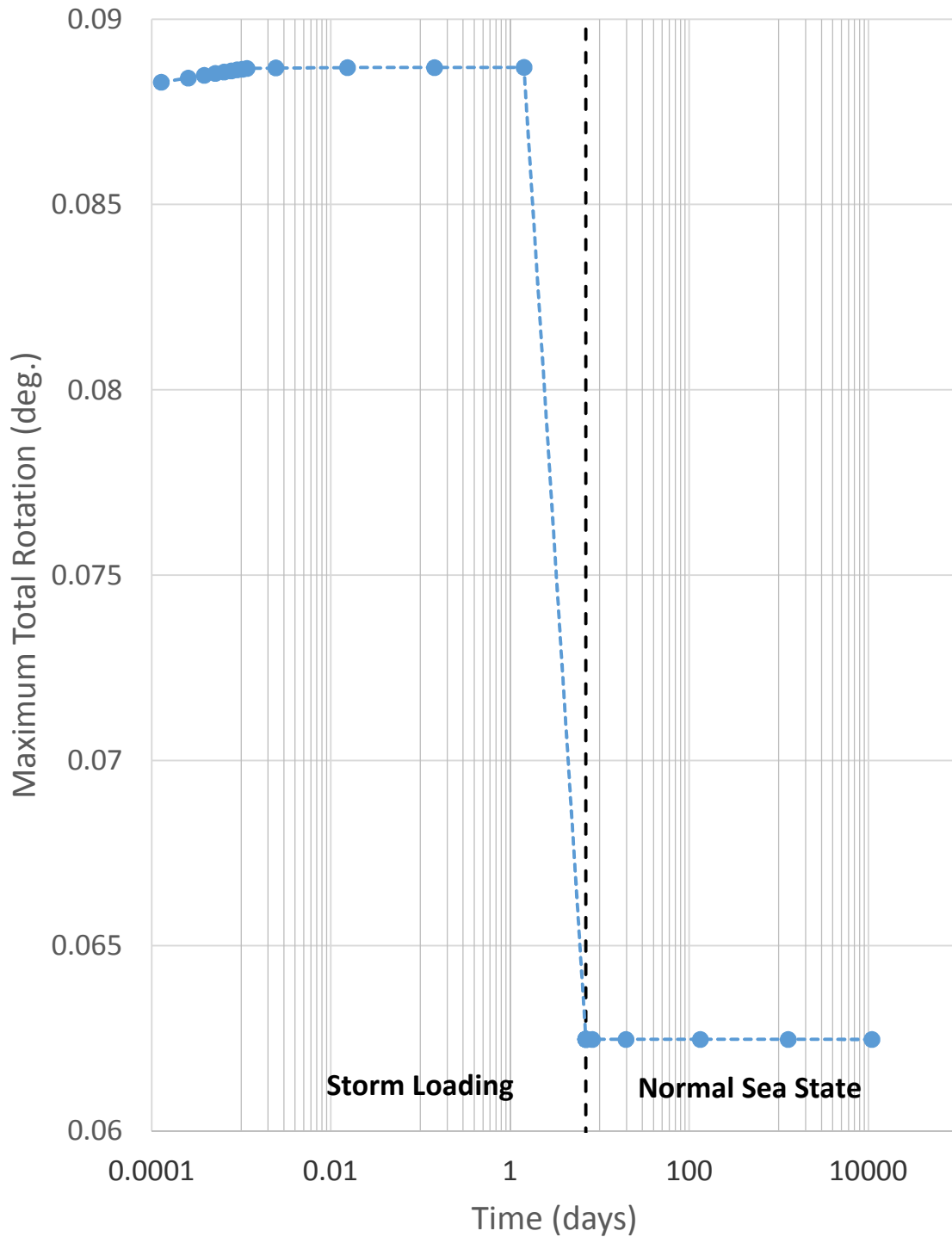
DEGRADATION INDEX CONTOURS – MONOCAISSON, DENSE SAND
Cyclic Loading Effects on Suction Bucket Foundations
Offshore Wind Turbines



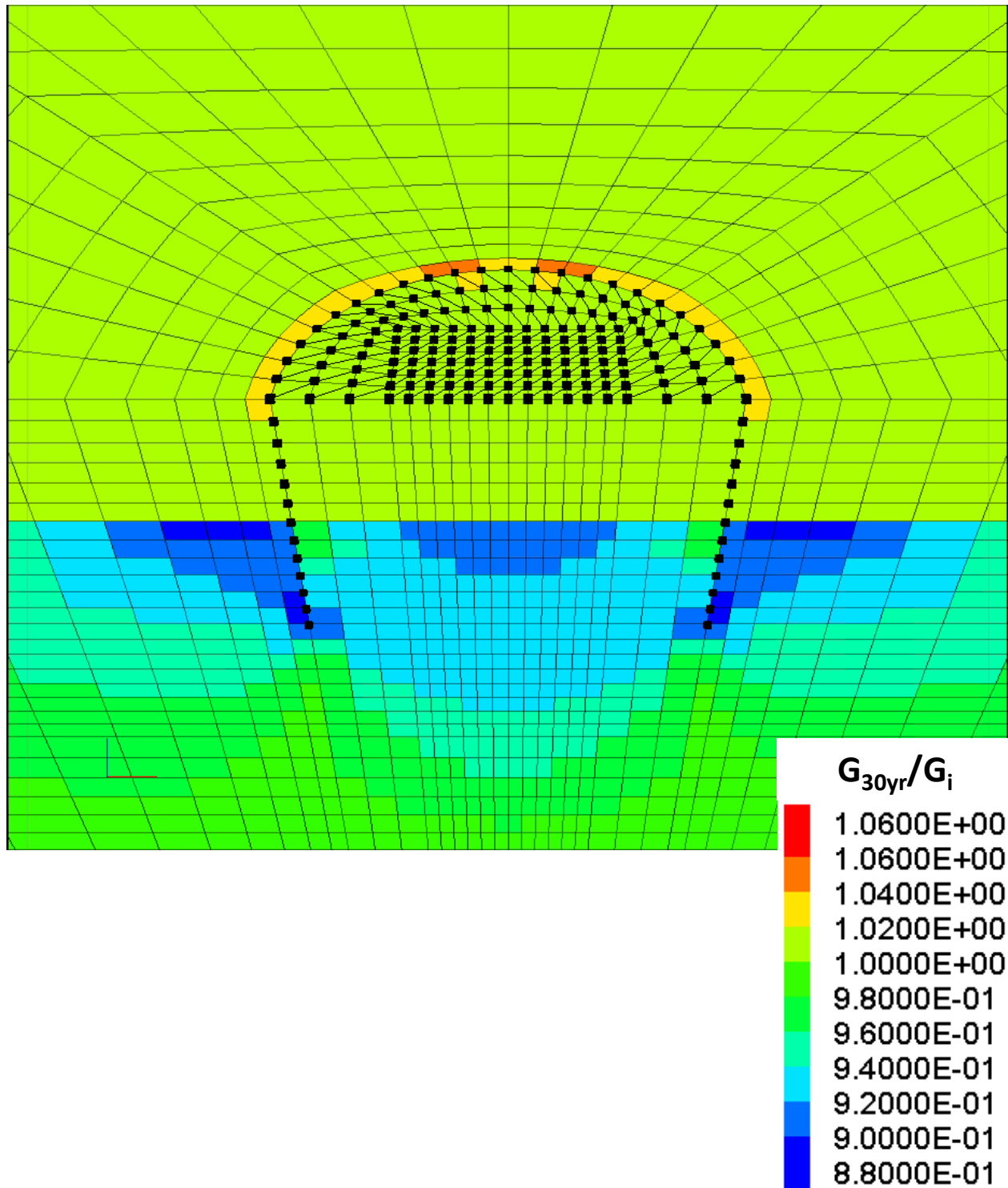
ROTATIONAL STIFFNESS VS. TIME – MONOCAISSON, DENSE SAND
Cyclic Loading Effects on Suction Bucket Foundations
Offshore Wind Turbines



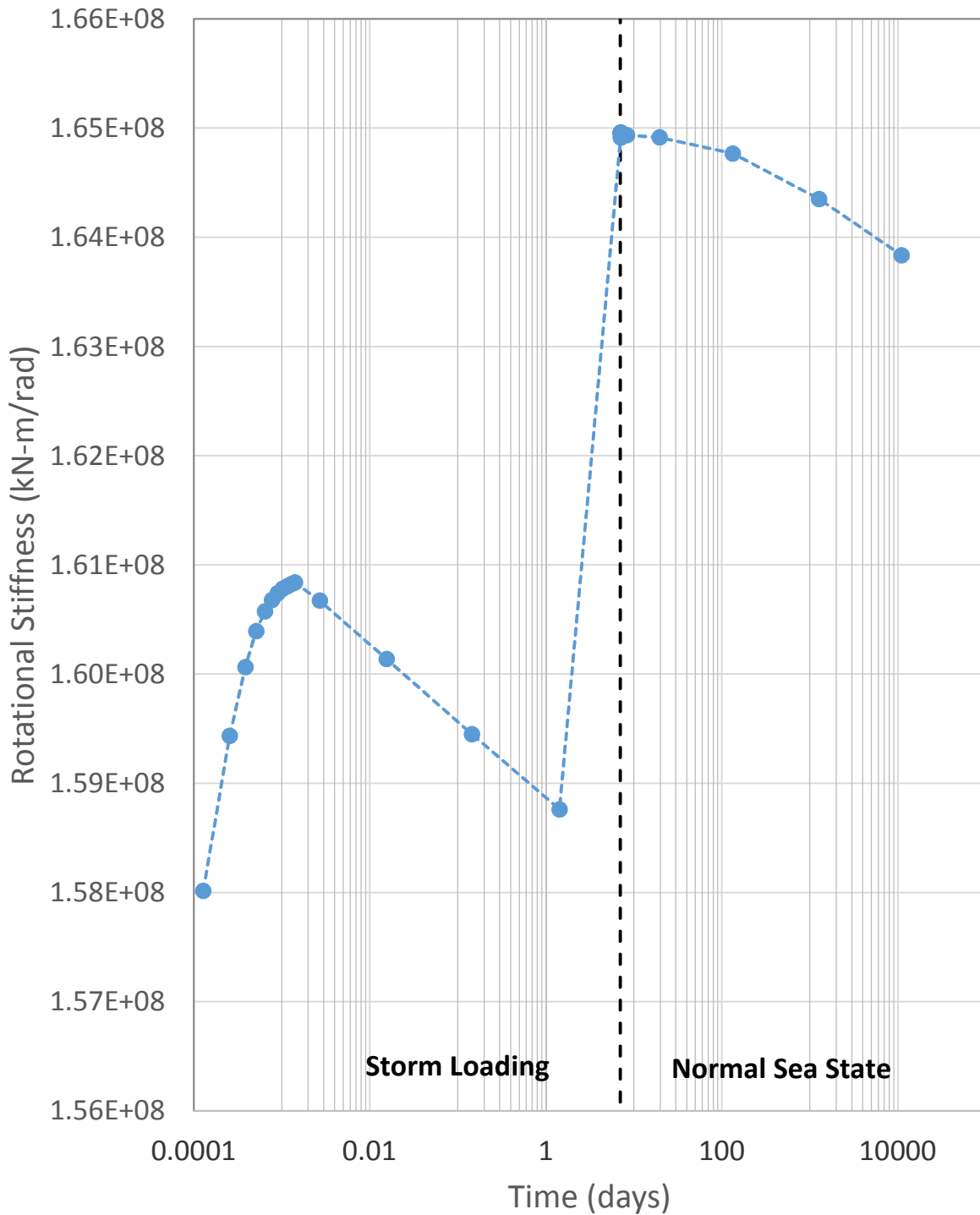
GLOBAL FUNDAMENTAL FREQUENCY VS. TIME – MONOCAISSON, DENSE SAND
Cyclic Loading Effects on Suction Bucket Foundations
Offshore Wind Turbines



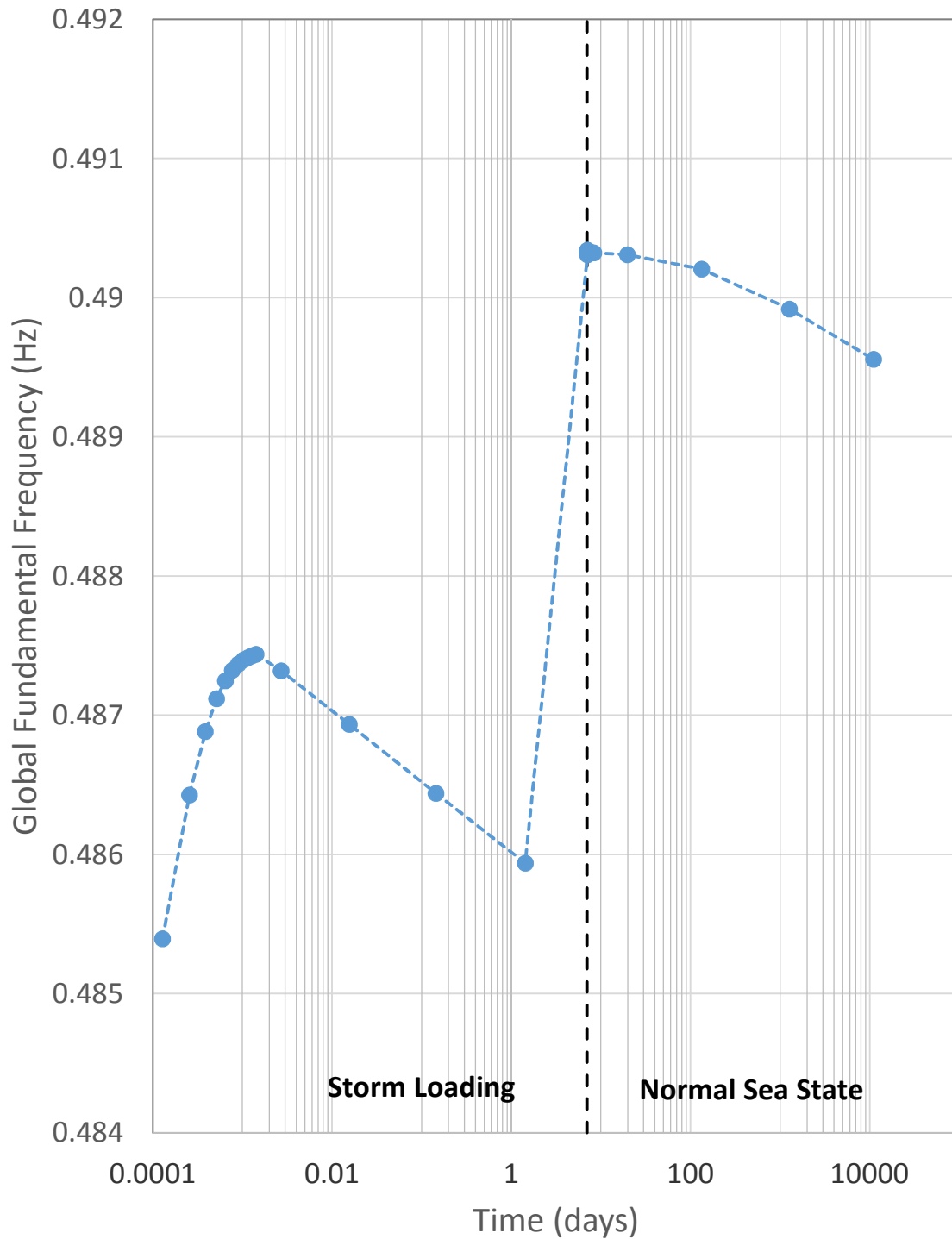
MAXIMUM TOTAL ROTATION VS. TIME – MONOCAISSON, DENSE SAND
Cyclic Loading Effects on Suction Bucket Foundations
Offshore Wind Turbines



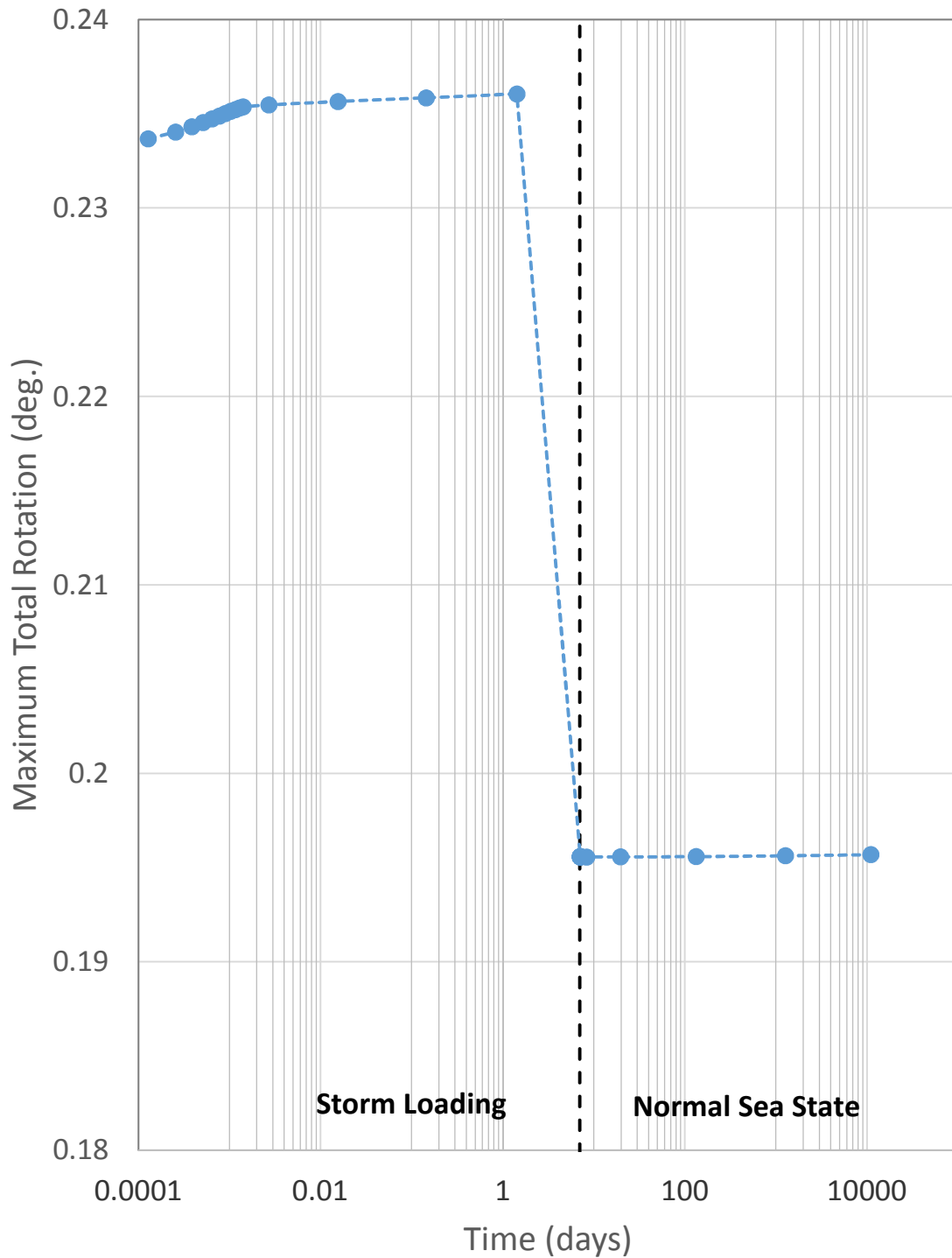
DEGRADATION INDEX CONTOURS – MONOCAISSON, INTERLAYERED
Cyclic Loading Effects on Suction Bucket Foundations
Offshore Wind Turbines



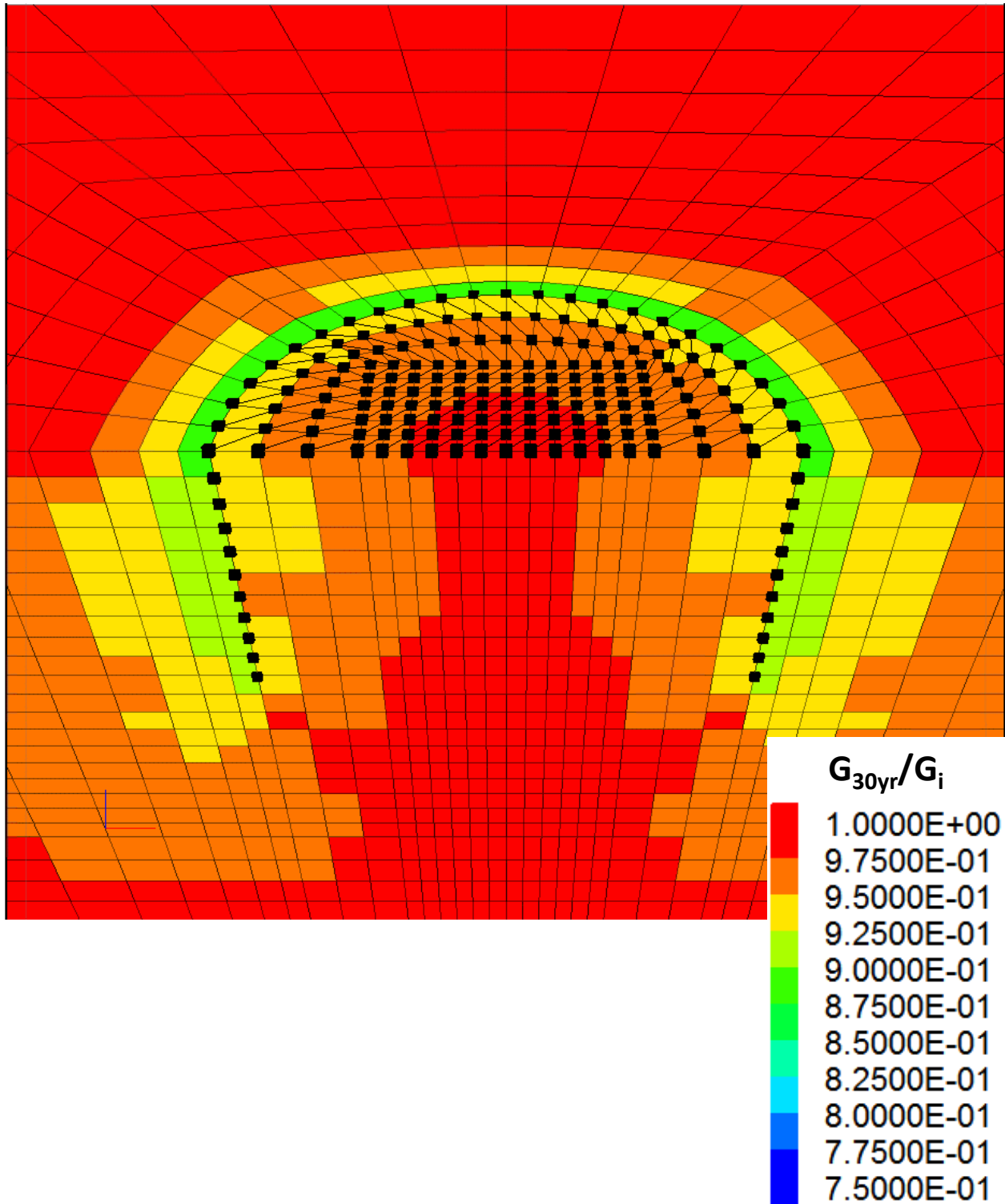
ROTATIONAL STIFFNESS VS. TIME – MONOCAISSON, INTERLAYERED
Cyclic Loading Effects on Suction Bucket Foundations
Offshore Wind Turbines



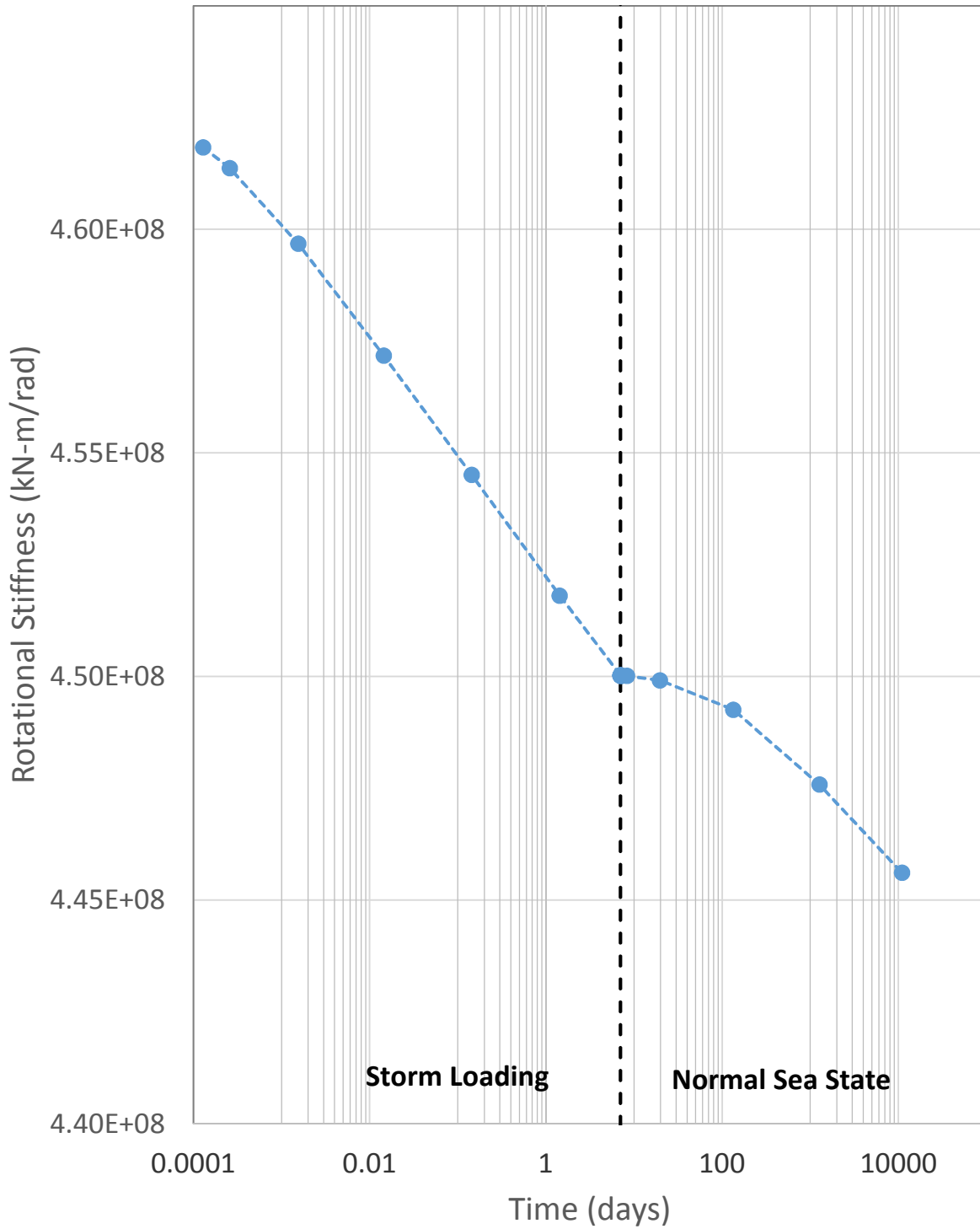
GLOBAL FUNDAMENTAL FREQUENCY VS. TIME – MONOCAISSON, INTERLAYERED
Cyclic Loading Effects on Suction Bucket Foundations
Offshore Wind Turbines



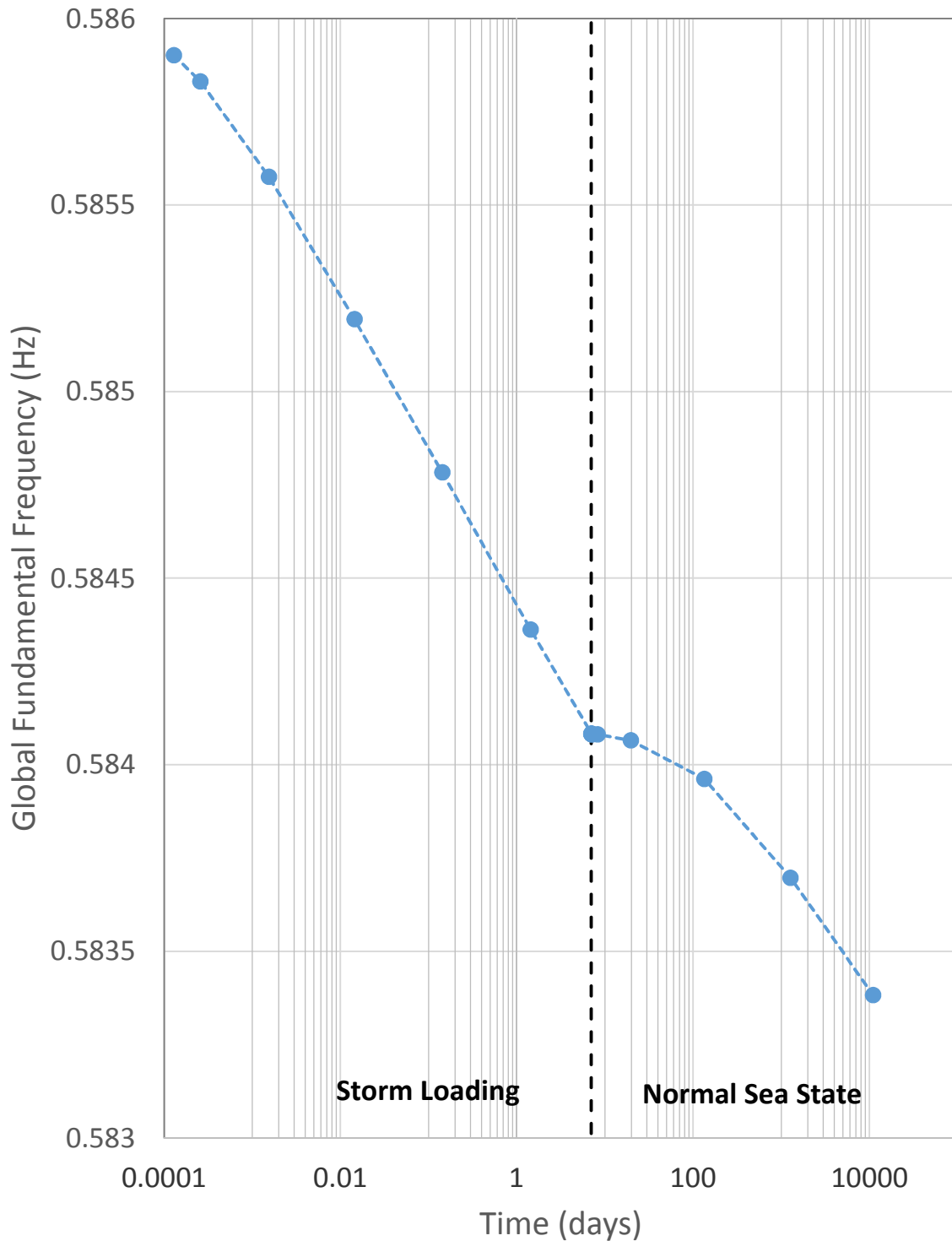
MAXIMUM TOTAL ROTATION VS. TIME – MONOCAISSON, INTERLAYERED
Cyclic Loading Effects on Suction Bucket Foundations
Offshore Wind Turbines



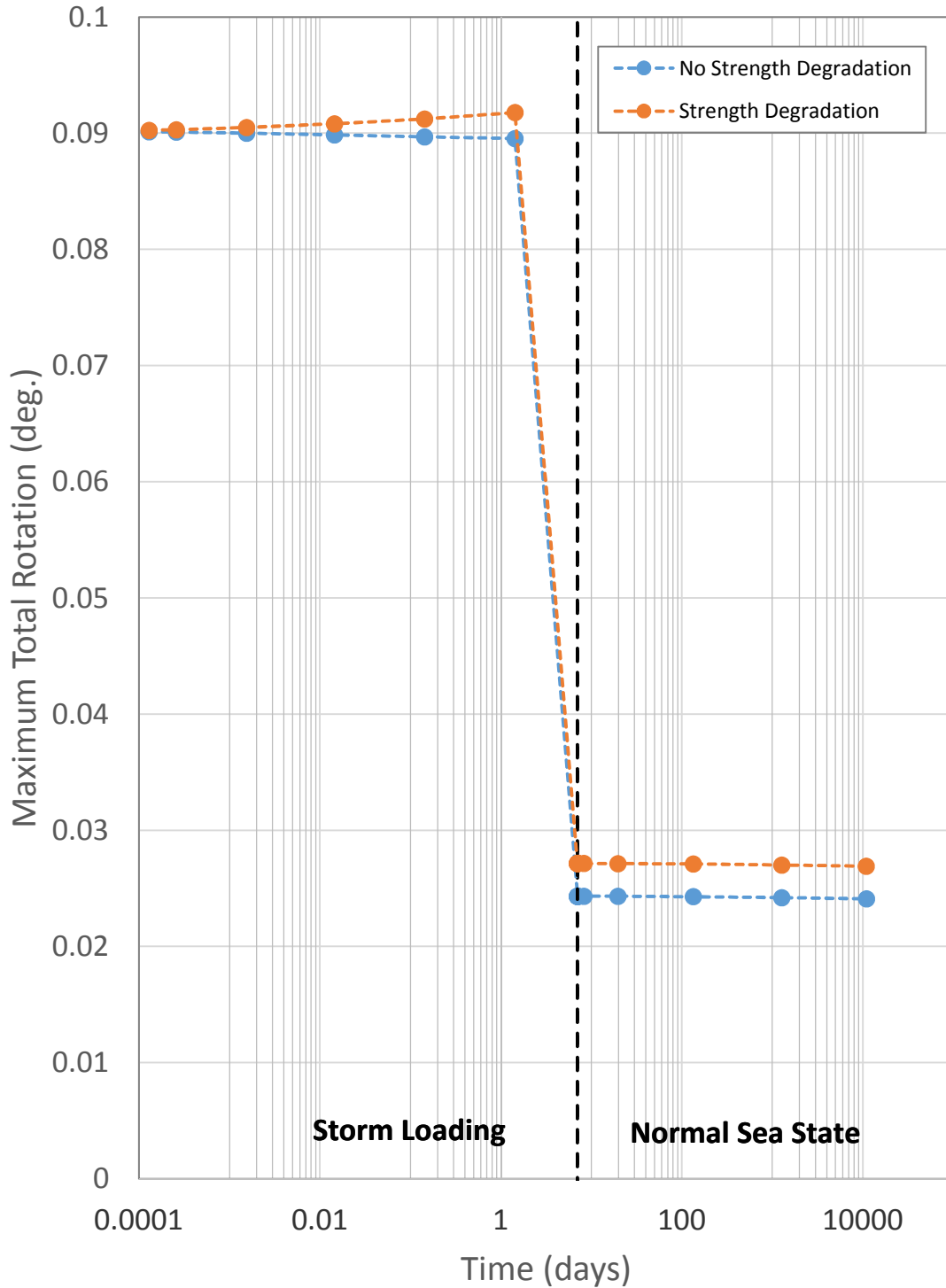
DEGRADATION INDEX CONTOURS – TETRAPOD, SOFT CLAY
Cyclic Loading Effects on Suction Bucket Foundations
Offshore Wind Turbines



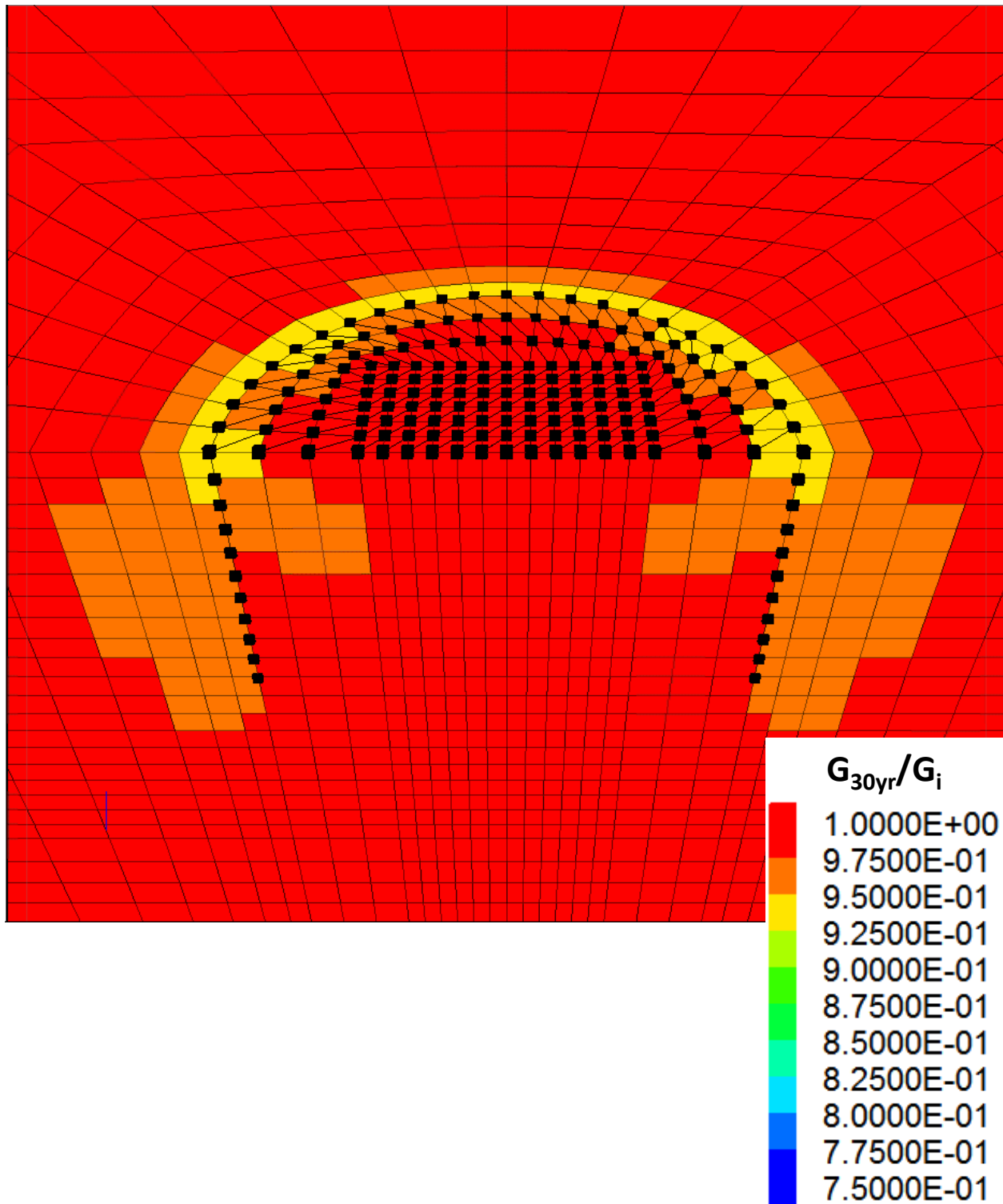
ROTATIONAL STIFFNESS VS. TIME – TETRAPOD, SOFT CLAY
Cyclic Loading Effects on Suction Bucket Foundations
Offshore Wind Turbines



GLOBAL FUNDAMENTAL FREQUENCY VS. TIME – TETRAPOD, SOFT CLAY
Cyclic Loading Effects on Suction Bucket Foundations
Offshore Wind Turbines

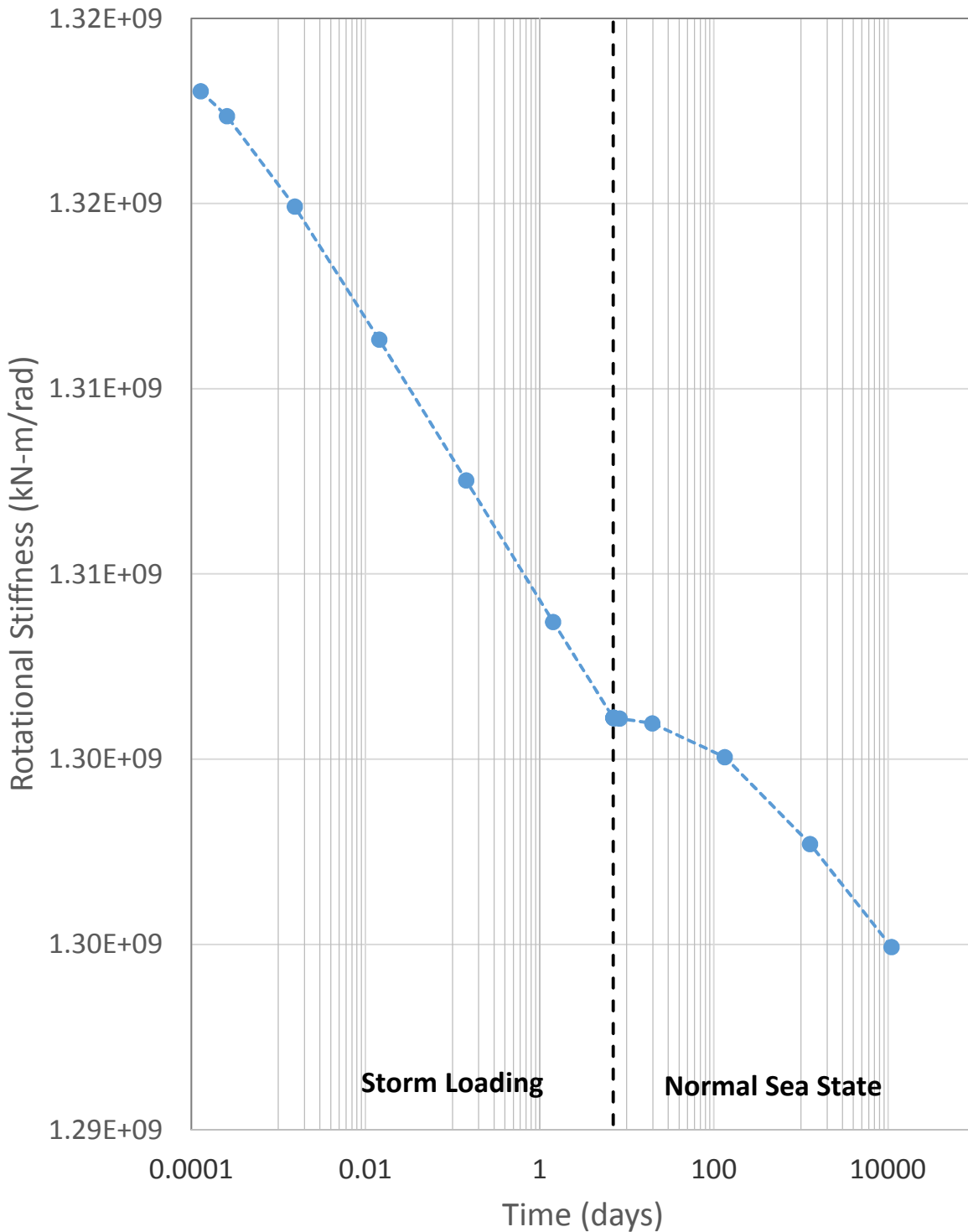


MAXIMUM TOTAL ROTATION VS. TIME – TETRAPOD, SOFT CLAY
Cyclic Loading Effects on Suction Bucket Foundations
Offshore Wind Turbines

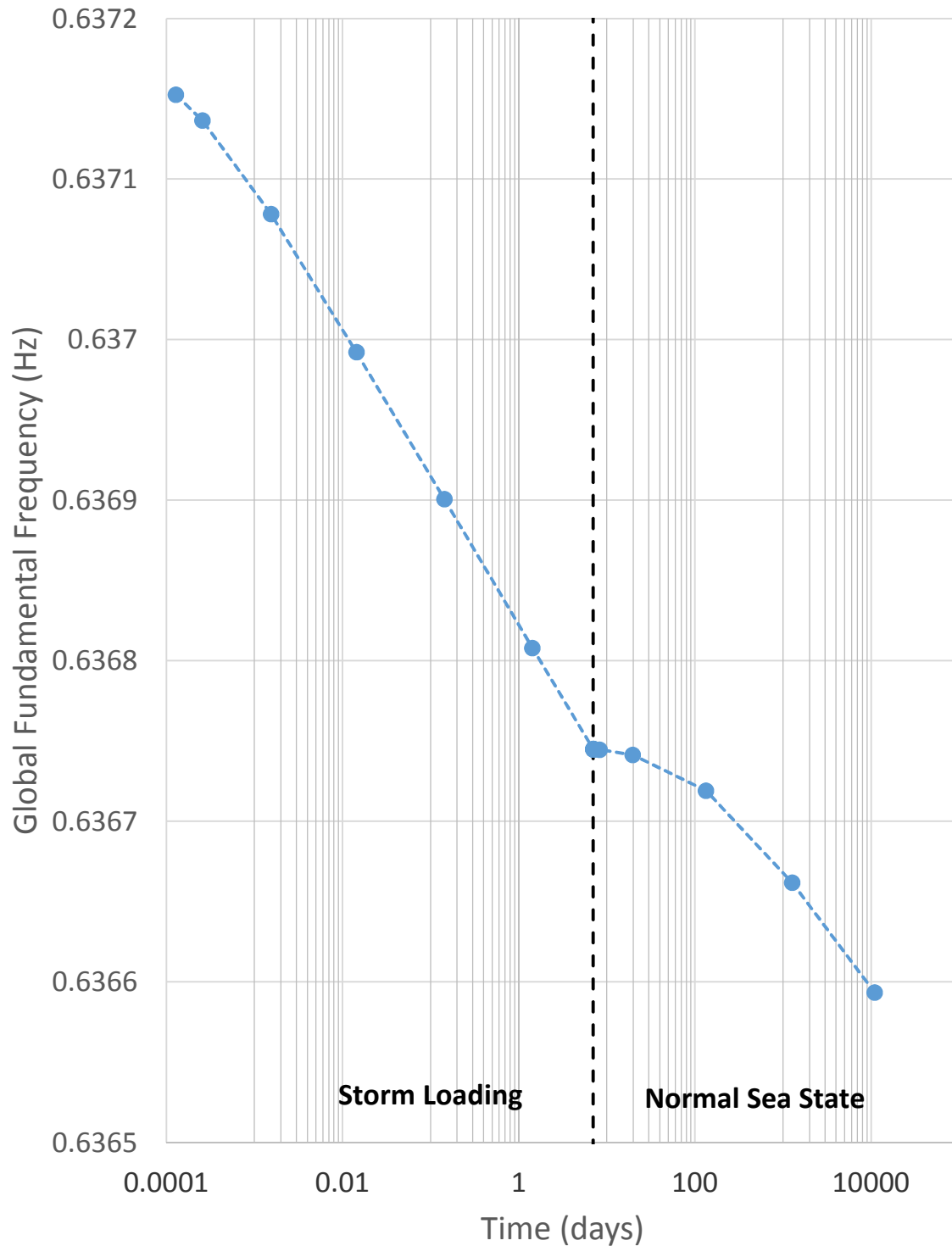


DEGRADATION INDEX CONTOURS – TETRAPOD, STIFF CLAY
Cyclic Loading Effects on Suction Bucket Foundations
Offshore Wind Turbines

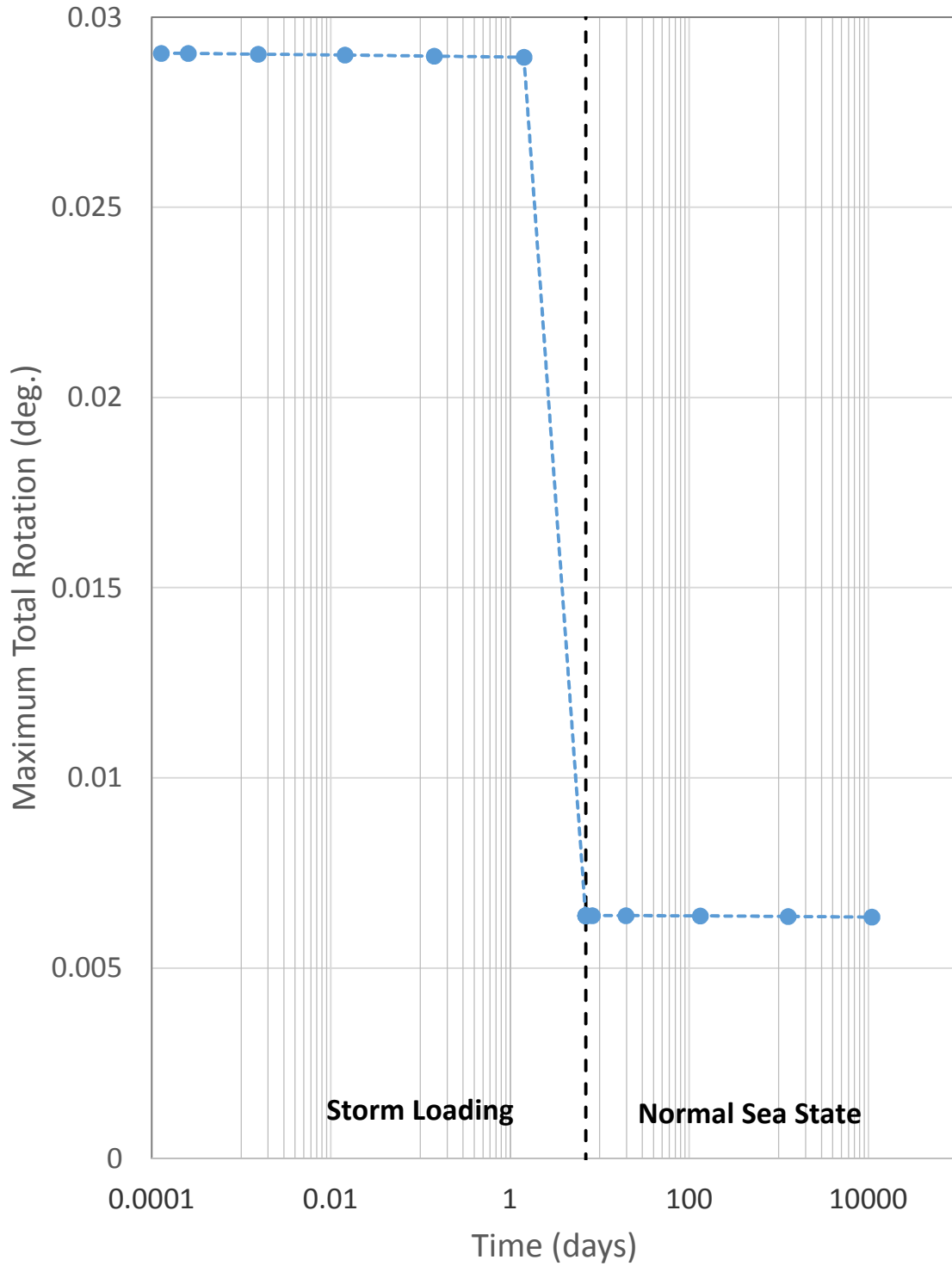
FIGURE 4.3-5



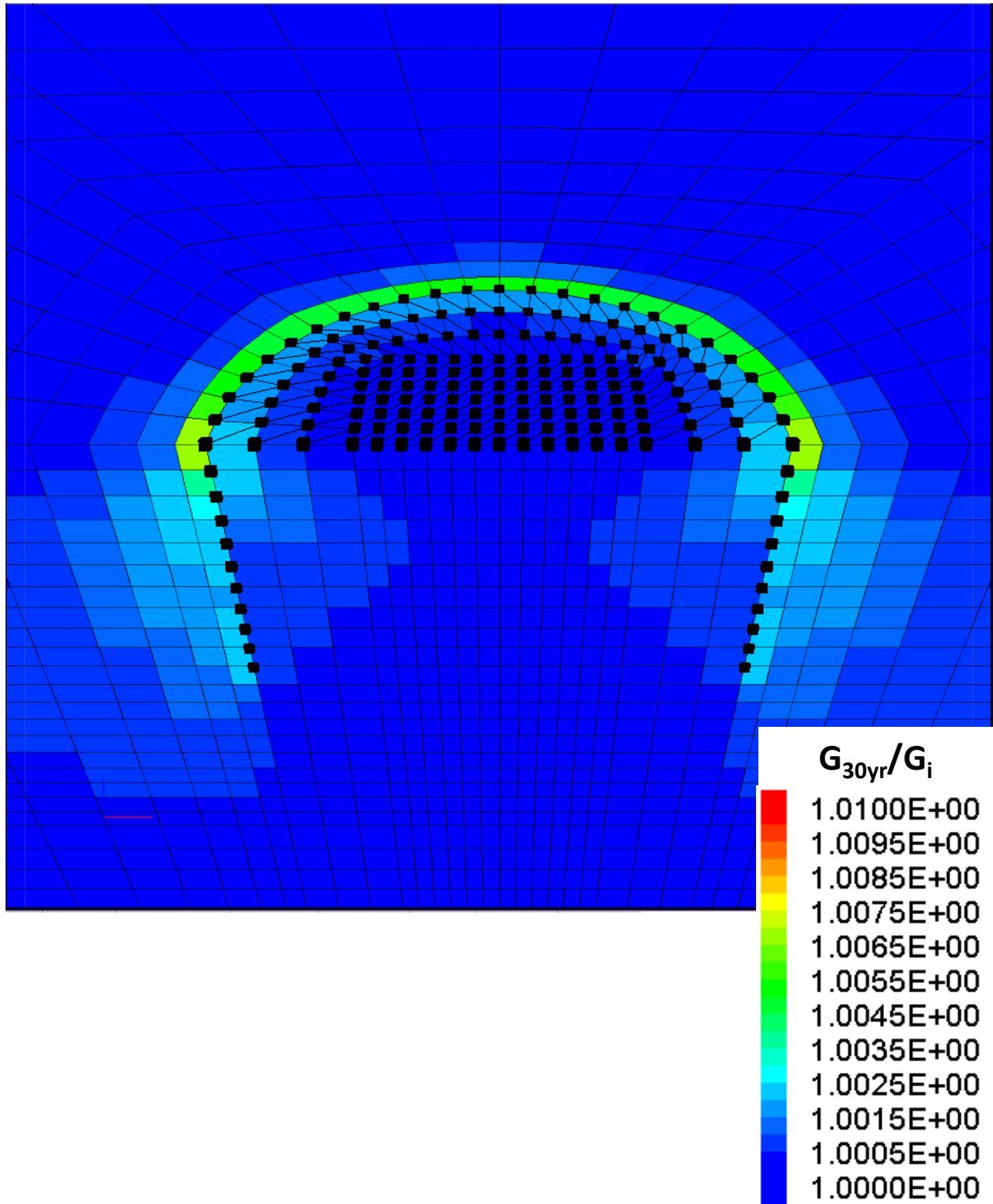
ROTATIONAL STIFFNESS VS. TIME – TETRAPOD, STIFF CLAY
Cyclic Loading Effects on Suction Bucket Foundations
Offshore Wind Turbines



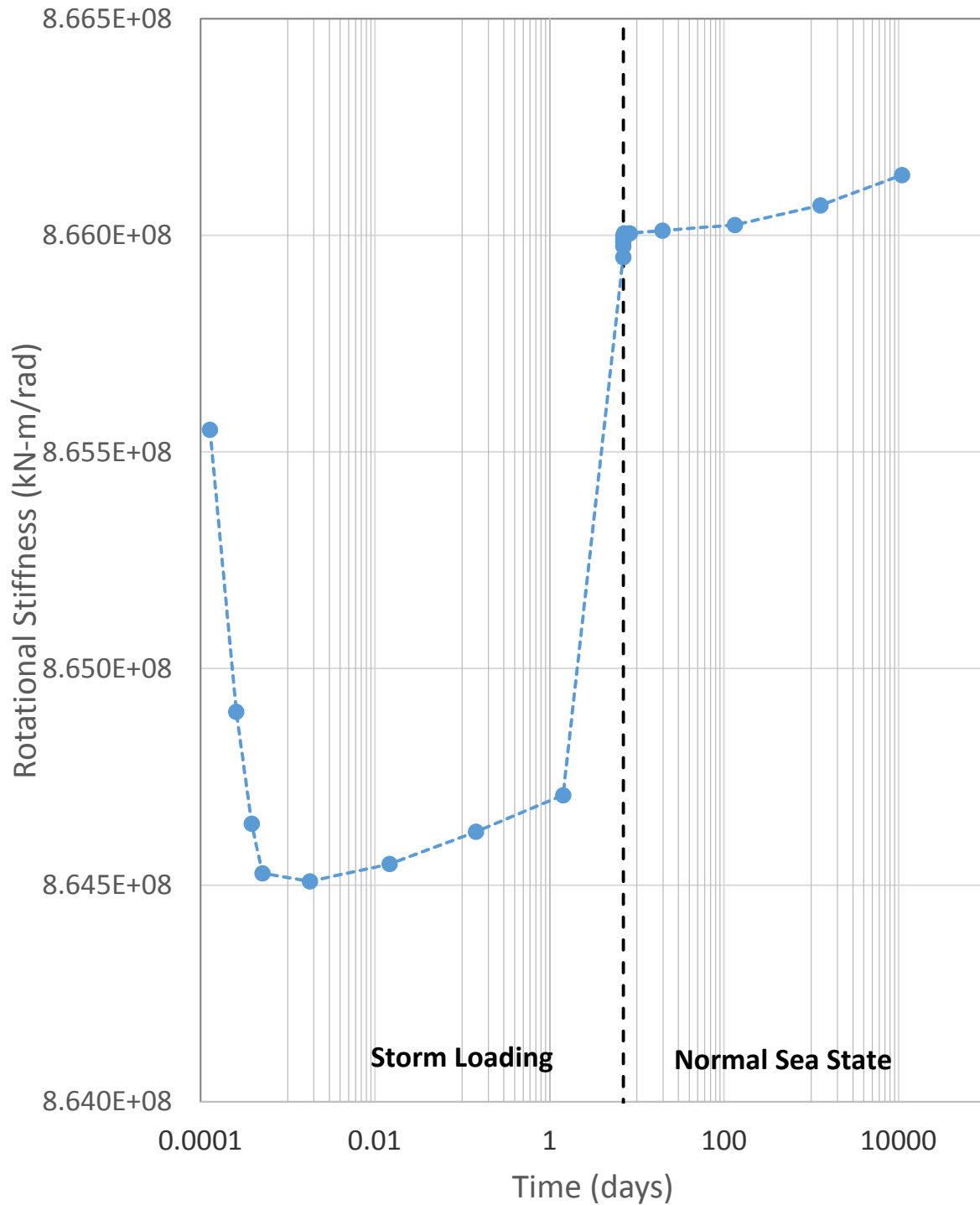
GLOBAL FUNDAMENTAL FREQUENCY VS. TIME – TETRAPOD, STIFF CLAY
Cyclic Loading Effects on Suction Bucket Foundations
Offshore Wind Turbines



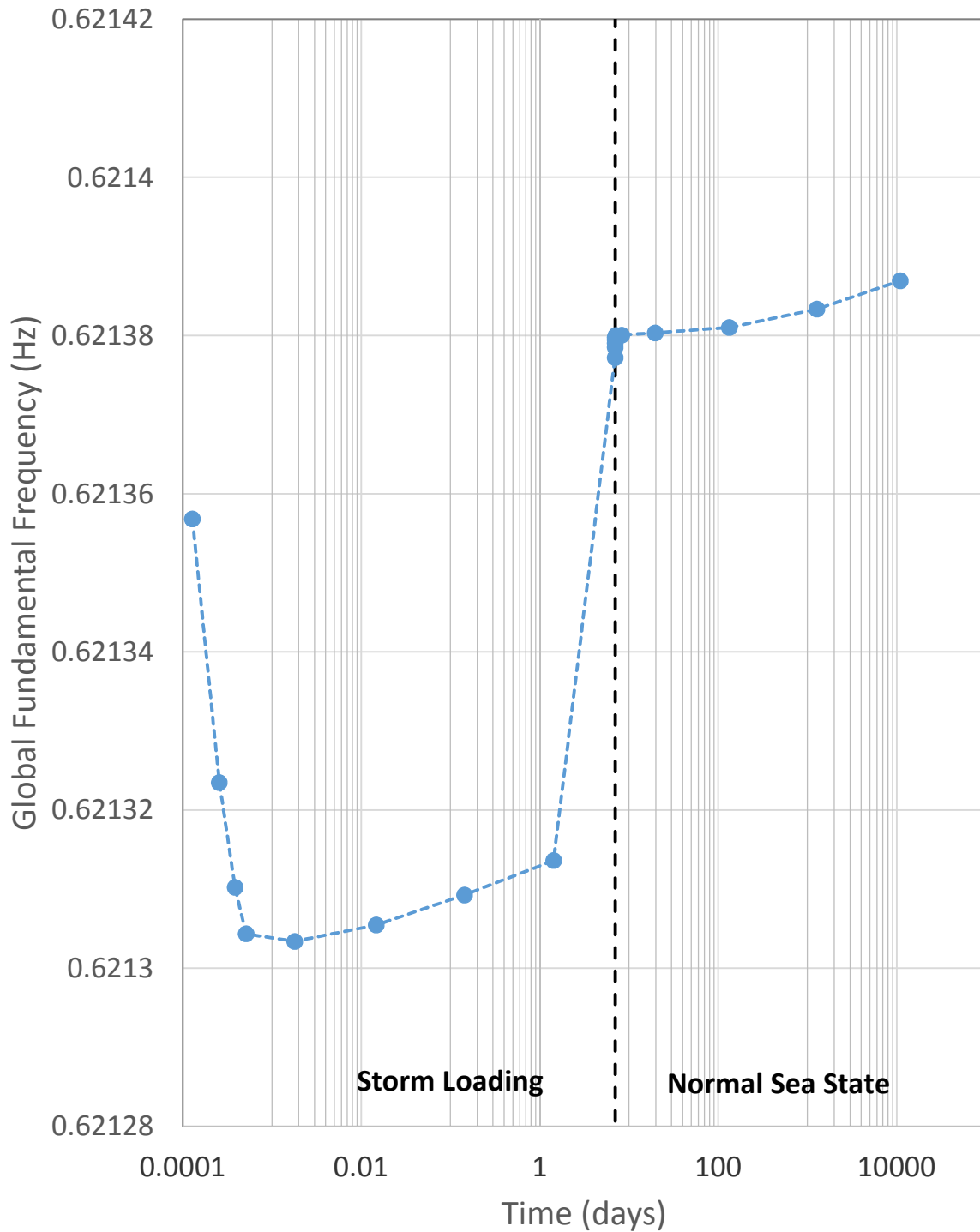
MAXIMUM TOTAL ROTATION VS. TIME – TETRAPOD, STIFF CLAY
Cyclic Loading Effects on Suction Bucket Foundations
Offshore Wind Turbines



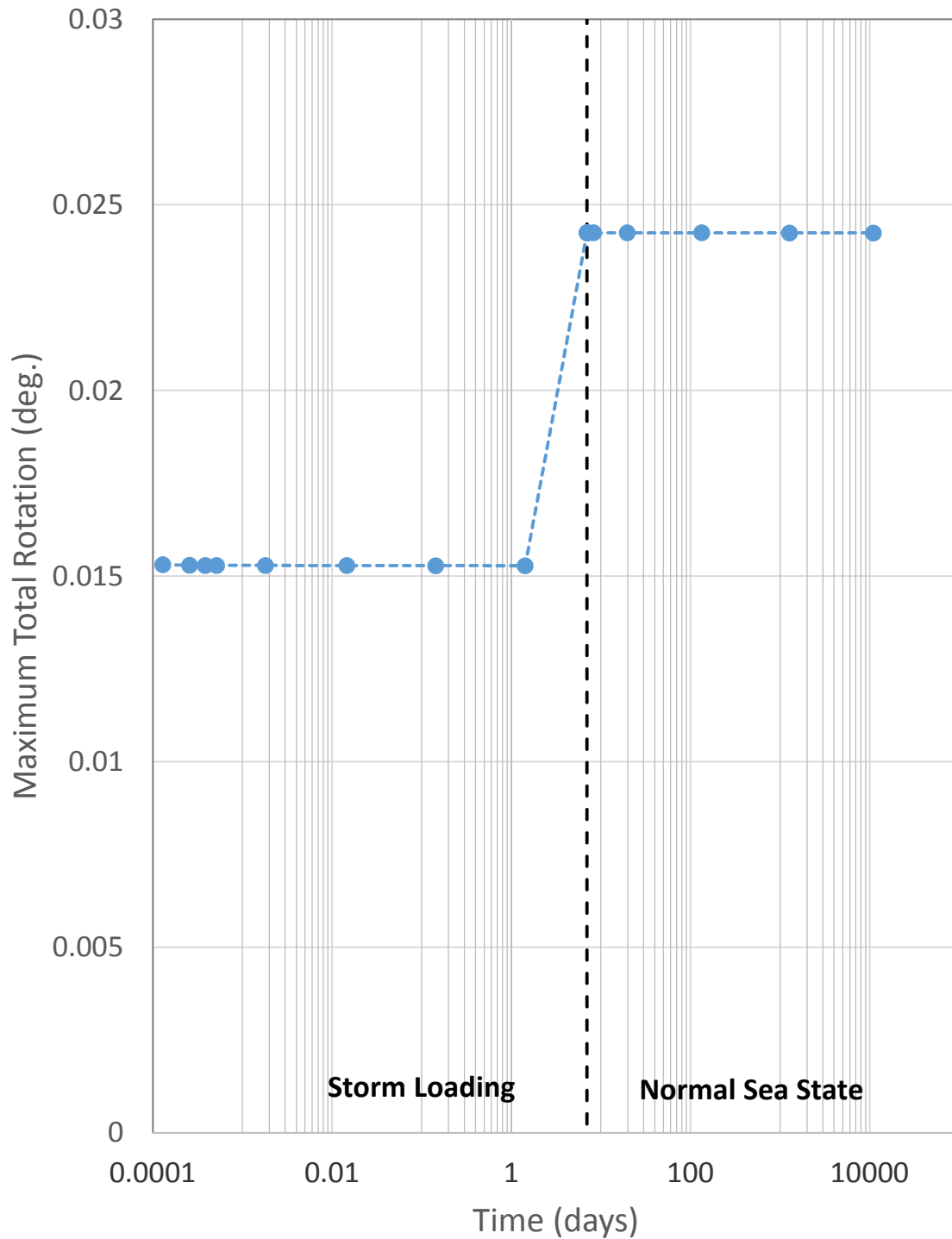
DEGRADATION INDEX CONTOURS – TETRAPOD, DENSE SAND
Cyclic Loading Effects on Suction Bucket Foundations
Offshore Wind Turbines



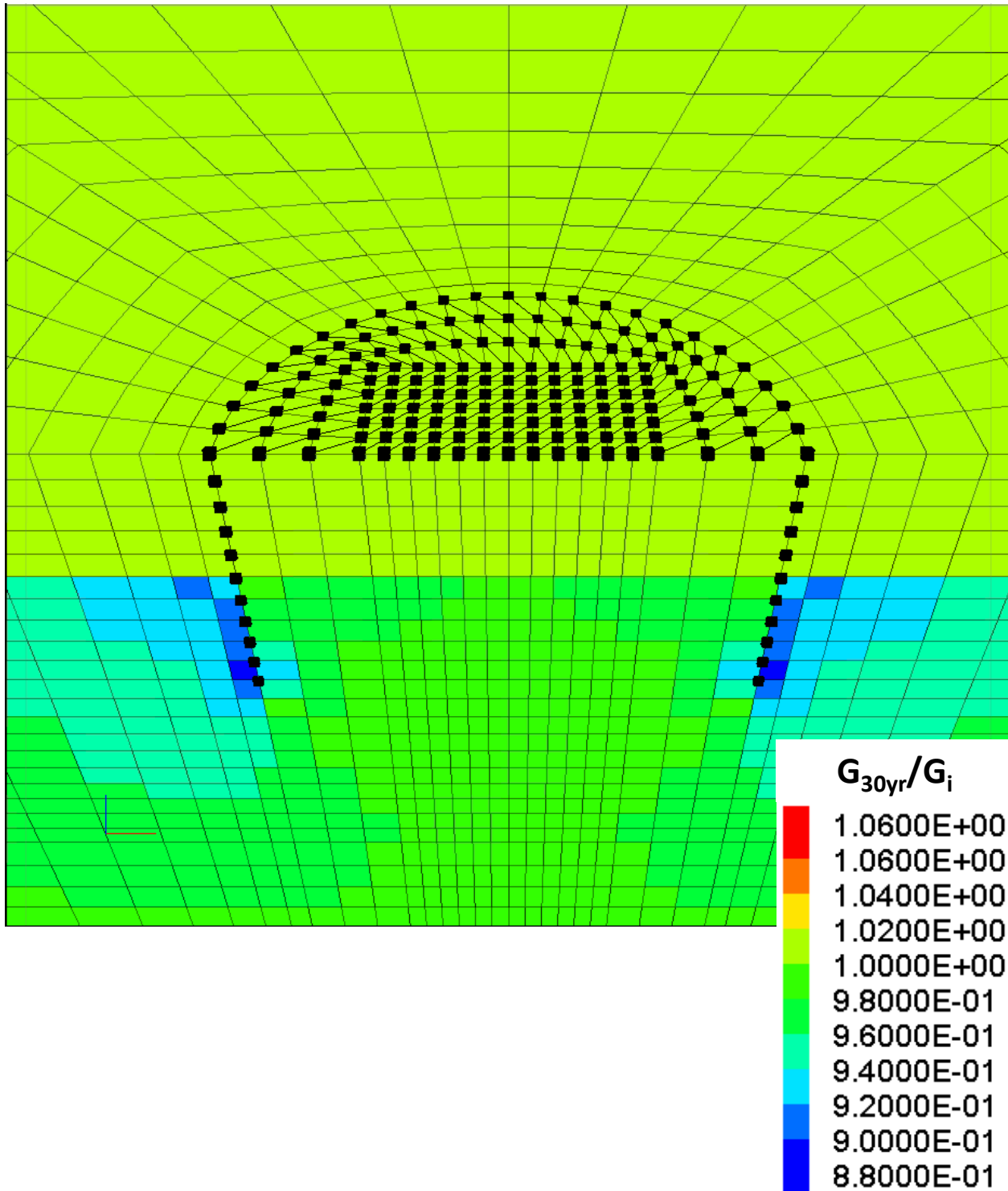
ROTATIONAL STIFFNESS VS. TIME – TETRAPOD, DENSE SAND
Cyclic Loading Effects on Suction Bucket Foundations
Offshore Wind Turbines



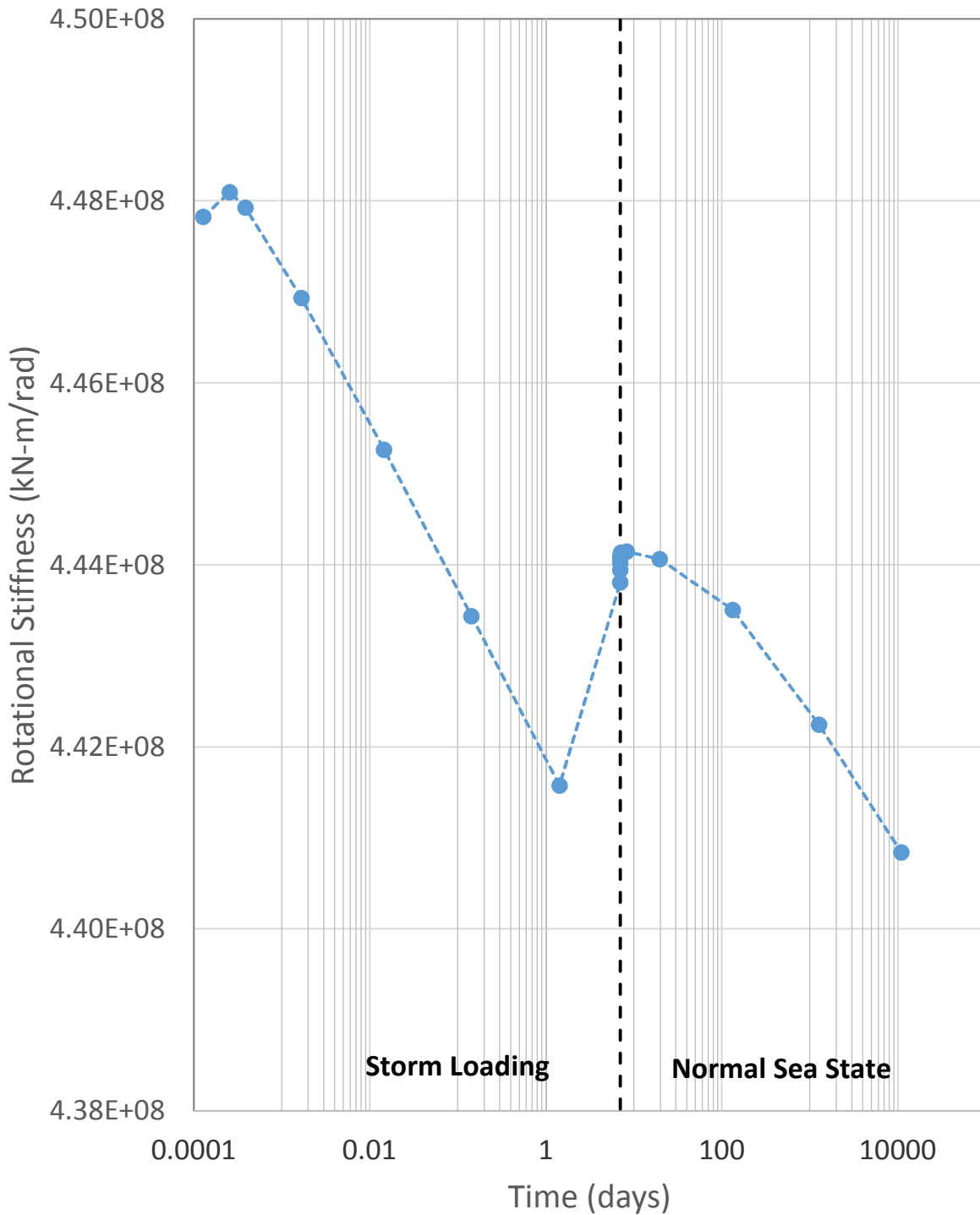
GLOBAL FUNDAMENTAL FREQUENCY VS. TIME – TETRAPOD, DENSE SAND
Cyclic Loading Effects on Suction Bucket Foundations
Offshore Wind Turbines



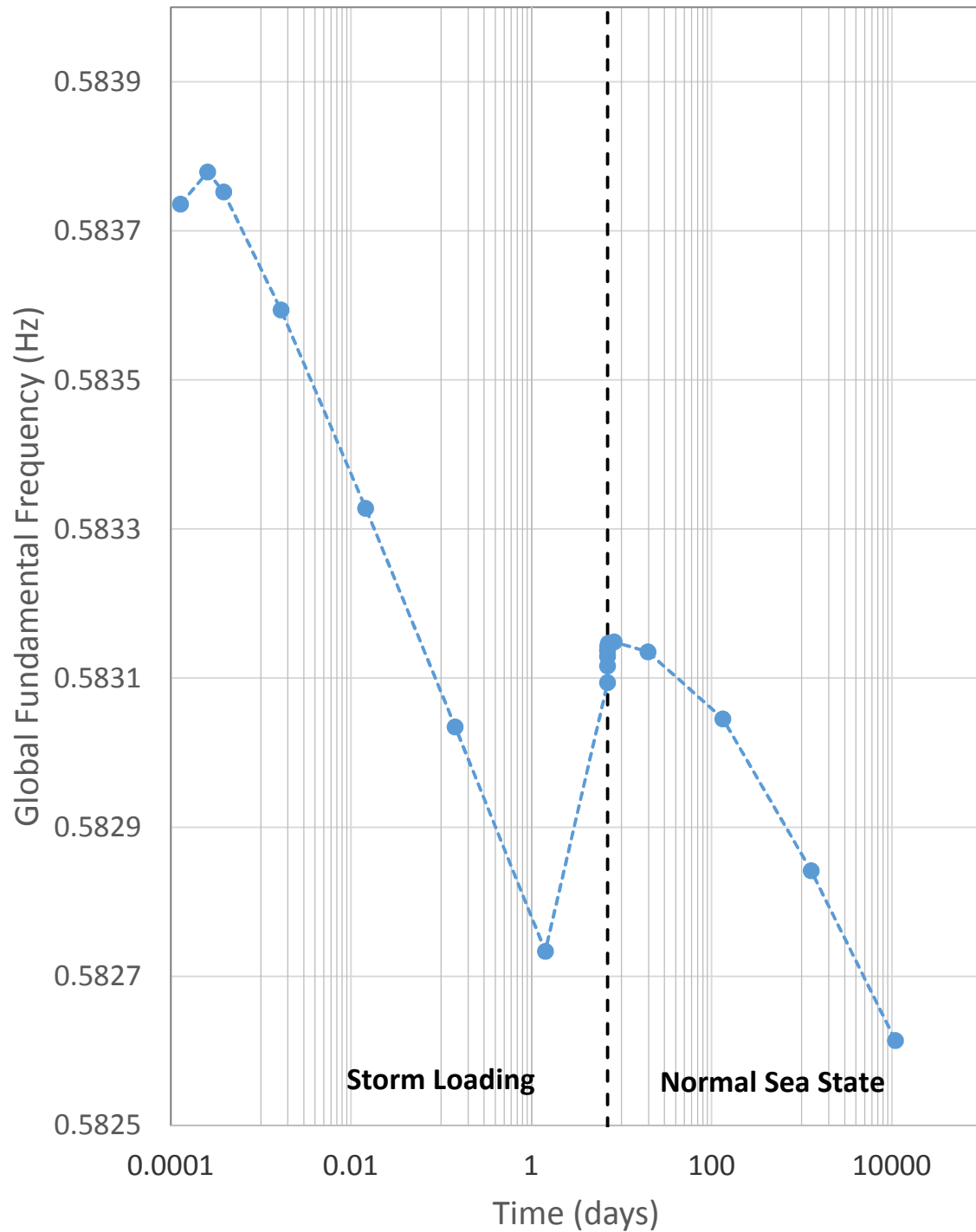
MAXIMUM TOTAL ROTATION VS. TIME – TETRAPOD, DENSE SAND
Cyclic Loading Effects on Suction Bucket Foundations
Offshore Wind Turbines



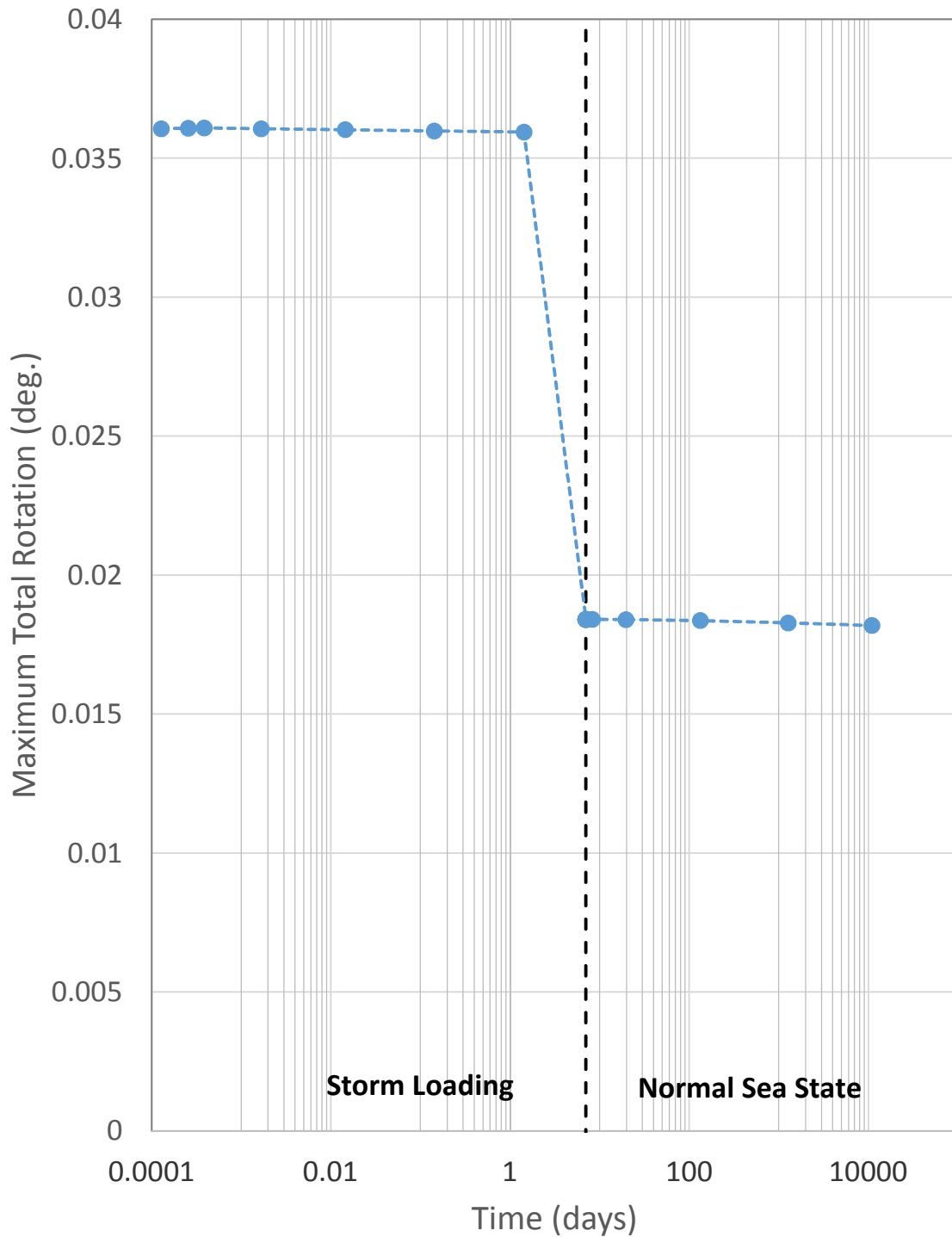
DEGRADATION INDEX CONTOURS – TETRAPOD, INTERLAYERED
Cyclic Loading Effects on Suction Bucket Foundations
Offshore Wind Turbines



ROTATIONAL STIFFNESS VS. TIME – TETRAPOD, INTERLAYERED
Cyclic Loading Effects on Suction Bucket Foundations
Offshore Wind Turbines



GLOBAL FUNDAMENTAL FREQUENCY VS. TIME – TETRAPOD, INTERLAYERED
Cyclic Loading Effects on Suction Bucket Foundations
Offshore Wind Turbines



MAXIMUM TOTAL ROTATION VS. TIME – TETRAPOD, INTERLAYERED
Cyclic Loading Effects on Suction Bucket Foundations
Offshore Wind Turbines

SECTION 5.0



5.0 DEVELOPMENT OF PRELIMINARY DESIGN GUIDELINES

5.1 CYCLIC DESIGN CONSIDERATIONS

For conventional driven piles, cyclic effects are considered by means of degraded p-y and t-z springs, which generally provide lower-bound soil resistance for both sands and clays. With the degraded pile springs, designers can estimate the required pile penetration depth, the potential upper-bound pile deflection, and settlement under design cyclic loads. It is noted that p-y and t-z springs were developed based on pile load tests with much smaller diameter (D) and higher length/diameter (L/D) ratios compared to suction buckets. In addition, failure mechanisms between conventional piles and suction buckets are quite different, which impedes the use of conventional pile springs for suction buckets.

For the suction bucket foundation, developing such a “lower-bound” cyclic foundation stiffness could be feasible; however, the limited data on cyclic soil behavior and model experiments makes this a difficult task. The proposed laboratory tests ([Section 6.0](#)) are developed to fill these data gaps and provide more information to develop such a bounding foundation stiffness. The findings from the literature review presented in [Section 2.0](#) and the results from the limited numerical analyses cases presented in [Section 4.0](#) suggest that key factors affecting cyclic suction bucket performance include the following:

1. Subsurface conditions and soil properties and cyclic response;
2. Loading conditions including loading frequency and amplitude, and number of loading cycles; and
3. Foundation type and dimensions (e.g., single bucket- vs. multi-support buckets).

As stated in [Section 2.1](#), although current design guidelines require the evaluation of cyclic loading effects on foundation performance, detailed procedures or methodologies for suction buckets are not presented in those guidelines. Our findings showed that cyclic loads affect the foundation stiffness, system frequency, and cyclic and permanent foundation displacements. However, the magnitudes of these effects highly depend on the combination of the aforementioned three key factors.

5.1.1 Subsurface Conditions and Soil Properties

Based on the small-scale and field experiments reviewed as part of this study, cohesive soils (i.e., clay) are generally more susceptible to stiffness and strength degradation than cohesionless soils (sands), provided that sand is fully drained. In clays, soil stiffness degradation is primarily associated with disturbance in the soil structure and the development of excess pore pressures during primarily undrained loading conditions (e.g., Vucetic and Dobry, 1988). For sands, cyclic degradation effects are primarily a function of relative density and whether loading is applied primarily in a drained or undrained manner. If loading frequency is low enough such that loading conditions are primarily drained, then cyclic densification is likely to occur. Conversely, if loading is primarily undrained, then the development of excess pore pressures may lead to stiffness and strength reduction. In general, the magnitude of stiffness and strength degradation are a function of cyclic shear strain amplitude and number of loading cycles. Overall larger degradation is associated with larger shear strain amplitudes and/or number of loading cycles. For clays, soil degradation also depends on OCR and PI, with higher degradation generally associated with smaller OCR and lower PI values.



For clays, cyclic stiffness degradation results in an overall reduction in foundation stiffness and system frequency with an associated increase in both the total and cyclic foundation displacements. The effect of cyclic strength degradation is an increase in total foundation displacements; however, it does not significantly affect foundation stiffness and frequency for the cases analyzed in this study.

For dense sands under fully drained conditions (generally anticipated at low loading frequency), the effect of cyclic loading is a small increase in foundation stiffness and system frequency and an associated decrease in cyclic foundation displacements over time (or number of cycles). Fabric breakdown may occur after a significant number of cycles resulting in an eventual reduction in foundation stiffness. Strength degradation effects appear to be negligible assuming fully drained conditions.

It should be noted that the effect of soil stiffness and strength degradation also depends on: a) foundation dimension and foundation type; b) loading amplitude, duration and bias; and c) superstructure properties (e.g., tower vibration frequency, self-weight, and blade frequency).

5.1.2 Loading Conditions

Throughout the design life of the wind turbine (typically 20~30 years), the foundation may be subjected to the following static, cyclic, and extreme loads:

- Permanent loads: 1) masses of structure and equipment, 2) hydrostatic pressure;
- Variable loads: 1) personnel, 2) installation, and 3) crane operation;
- Environmental loads: 1) wind, 2) wave, 3) current, 4) ice, and 5) earthquake;
- Operating loads: 1) turbine rotation, 2) blade aerodynamics;
- Accidental loads: 1) explosion, 2) ship impact/collision, and 3) rare, large breaking wave; and
- Deformation loads: 1) temperature, 2) built-in deformation, and 3) settlement of foundation.

For the cyclic foundation design, environmental loads, including wind and wave loads and their impacts towards foundation performance, are of the highest importance and should be considered. For the current study, the performance of suction buckets subjected to normal sea state and storm loads were analyzed. Their magnitude, loading frequency, and foundation performance over large number of cycles were presented in [Section 4.0](#).

While performing the cyclic foundation design, wind and wave loads shall be site-specific considering the site conditions such as water depth, current, seasonal effects, and structural factors such as wind tower properties or blade properties. Proper load combinations should be applied for different design limit states (i.e., ULS, SLS, and FLS) and verify with their specific performance criteria.

5.1.3 Foundation Type

[Table 2.6-1](#) presented OWT projects with suction bucket foundation. Depending on site condition (e.g., water depth), two types of suction bucket foundation can be adopted: 1) Mono-bucket, and 2) Multi-buckets (tripod and tetrapod).

The loading mechanism of the foundation soils depends on the type of foundation. As shown on [Figure 5.1-1](#), mono-bucket foundations are subject primarily to vertical and horizontal loads and bending moments. Hence, rotational foundation response is the primary response mechanism. Multi-bucket foundations are subjected to vertical and horizontal loads, and hence, axial foundation response



is more important. The results from numerical analyses presented in [Section 4.0](#) suggest that cyclic foundation performance is highly dependent on the type of loads applied – overturning moments (for mono-bucket) generally induce rotational displacements and vertical loads (for multi-bucket) generally induce vertical settlements. While performing the cyclic foundation design, representative load mechanisms should be applied depending on the site-specific foundation type.

5.2 FOUNDATION PERFORMANCE CHECKLIST

To incorporate the effect of cyclic loading into suction bucket design, cyclic performance for the suction bucket should be verified against the following items:

- Cyclic stability of suction bucket;
- Cyclic settlement, horizontal displacement, and rotation;
- Cyclic foundation stiffness and associated system frequency; and
- Cyclic soil reactions on foundation.

5.2.1 Cyclic Stability of Suction Bucket Foundation

Cyclic soil strength degradation can affect the stability of the suction bucket foundation system. Analyses performed in this study showed that, depending on the degree of soil strength degradation, total foundation displacements post-degradation can be significant. For the strength degradation model and loading regime assumed in this study, total system rotations including strength degradation are approximately twice as large as without consideration of strength degradation. The effect can be further quantified for the purpose of design recommendations through a larger number of parametric analyses.

5.2.2 Cyclic Settlement and Displacement

The effect of cyclic stiffness degradation on peak foundation displacement is generally small for the cases analyzed. Therefore, depending on the allowable deformations, the effect of cyclic stiffness degradation on OWT performance for the service limit state may be small. Again, this effect can be better quantified for the purposes of design based on a wider range of parametric evaluations.

5.2.3 Cyclic Foundation Stiffness and Frequency

To avoid potential resonance due to cyclic environmental loads (wind and wave) and interference of system response with operational loads (i.e., rotor and blade passing), the allowable range of working frequency for offshore wind turbines is relatively narrow. For suction bucket design against cyclic environmental loads, estimating the fundamental frequency and potential change in frequency due to long-term cyclic loads is essential. The potential change in system frequency over the period of wind turbine design life should be evaluated considering the effects of soil stiffness degradation for the actual subsurface conditions encountered (e.g., different treatment of sands vs. clays may be required).

In general, for clay subsurface conditions initial system frequency should be designed closer to the upper allowable bound to ensure that system frequency decrease due to soil stiffness degradation will not cause resonance.

For dense sand conditions, assuming drained response, soil stiffness “degradation” may increase the foundation stiffness and associated frequency. For such conditions, the initial system frequency should be closer to the lower allowable frequency range.



If the ratio of structure-to-foundation stiffness is larger than about one order of magnitude, then the effect of soil stiffness degradation on system frequency is likely negligible.

5.2.4 Cyclic Soil Reactions on Skirt and Top Plate

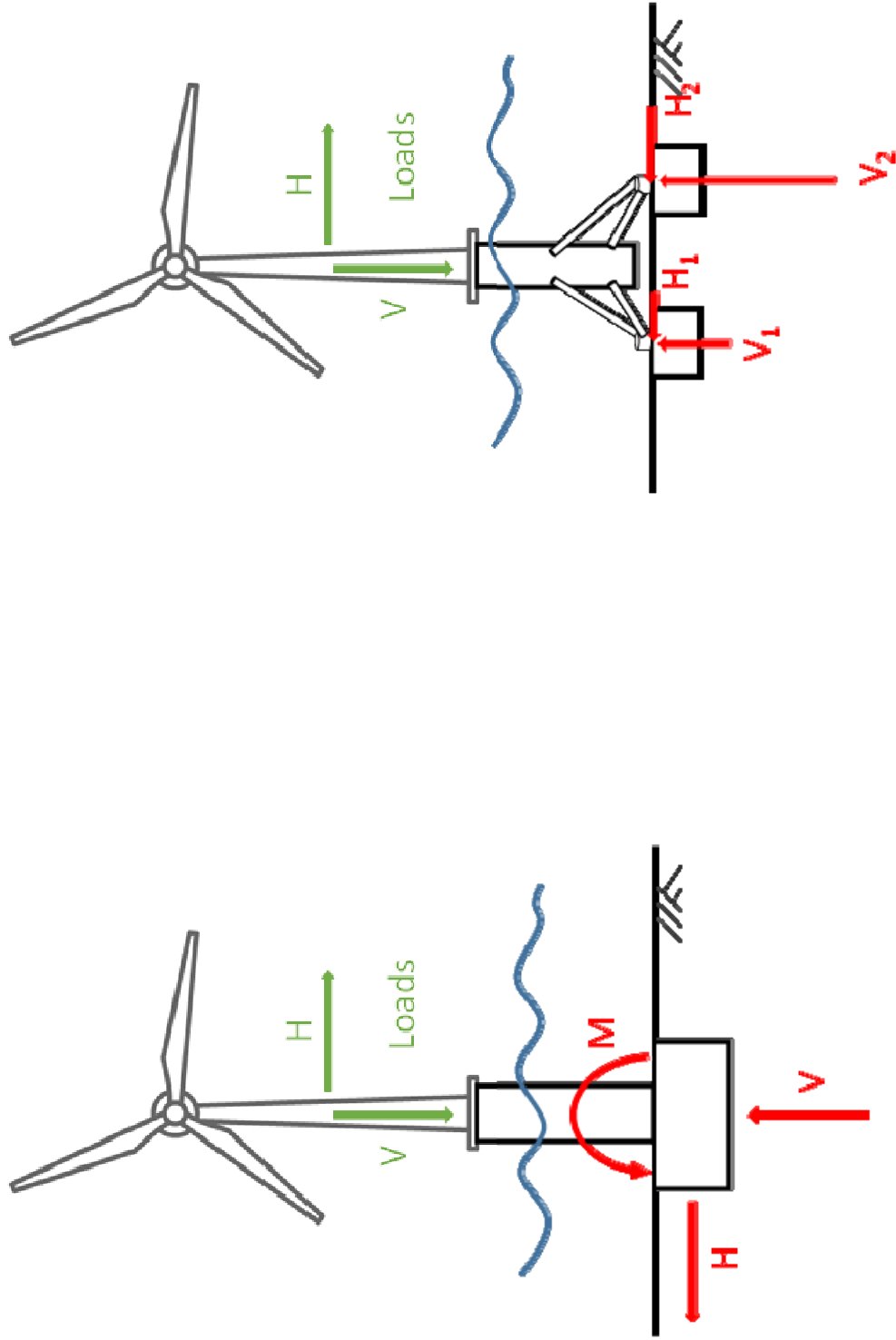
During cyclic loading, the distribution of soil reactions against structural members also varies cyclically. When designing the thickness and properties of the structural members, the maximum soil reactions shall be considered. The design should recognize the possibility that soil pressure in bucket in sand may be higher than if cyclic degradation was not considered.

5.2.5 Design Considerations

A summary of design considerations to assess cyclic foundation performance is presented in [Table 5.2-1](#) below:

Table 5.2-1: Cyclic Suction Bucket Foundation Design Considerations

Design Considerations	Primarily Affected by	Check List	Analytical Model Input Parameters	Foundation Design
<ul style="list-style-type: none"> Cyclic Capacity 	<ul style="list-style-type: none"> Cyclic soil strength 	<ul style="list-style-type: none"> Vertical, lateral, moment, and torque capacities Group effects (for multi-bucket) 	<ul style="list-style-type: none"> Static and cyclic soil properties <ul style="list-style-type: none"> Loading combination Soil-foundation interface properties Superstructure properties Foundation properties 	<ul style="list-style-type: none"> Foundation geometry (diameter, depth) Foundation self-weight Spacing (for multi-bucket)
<ul style="list-style-type: none"> Cyclic Displacement 	<ul style="list-style-type: none"> Cyclic soil stiffness and strain 	<ul style="list-style-type: none"> Vertical, lateral, and rotational cyclic displacements 		
<ul style="list-style-type: none"> Cyclic Stiffness/Damping 	<ul style="list-style-type: none"> Cyclic soil stiffness Foundation dimension 	<ul style="list-style-type: none"> Cyclic foundation stiffness Cyclic foundation damping Fundamental frequency 		
<ul style="list-style-type: none"> Cyclic Soil Reaction Stress 	<ul style="list-style-type: none"> 	<ul style="list-style-type: none"> Soil stresses on skirt 		<ul style="list-style-type: none"> Top plate thickness Skirt wall thickness



Multi-pod Caisson

Mono Caisson

LOADING MECHANISM – MONOCAISSON VS. MULTICAISSON
 Cyclic Loading Effects on Suction Bucket Foundations
 Offshore Wind Turbines

FIGURE 5.1-1

SECTION 6.0



6.0 RECOMMENDATIONS FOR LABORATORY TESTING AND FUTURE STUDIES

6.1 LIMITATIONS OF EXISTING STUDIES AND DATA GAPS

The findings from the literature review performed for this study suggest a number of data gaps both in element level and laboratory model experiments. These include the following:

- Small number of cycles compared to actual design loads: in general, published studies are limited to about 1,000 cycles, with only a very small number performed for ~100,000 cycles;
- Strain amplitude – element test data are lacking for small shear strain amplitudes that are representative of a majority of design loading conditions;
- Limited small scale tests in clays – there are a very small number of available scale model tests for clays, potentially due to additional difficulties in testing procedures (e.g., more handling in the centrifuge) compared to sands; and
- Limited small scale tests in saturated sands – there are a very small number of available scale model tests in saturated sands, and hence assessment of drainage conditions representative of actual in-situ conditions.

The goal of the additional elemental and small-scale model testing proposed in this section is to provide information to reduce these data gaps.

6.2 RECOMMENDATIONS FOR FUTURE LABORATORY TESTING

The purpose of the proposed testing program is to develop a database that can be used to further assess feasibility of the suction bucket concept. Our recommendations for future tests are developed to target the subsurface conditions generally encountered in the US east coast waters. Overall, we recommend high quality, well instrumented small scale model testing to provide additional understanding of the primary mechanisms of OWT system response under a large number of loading cycles, supplemented by laboratory testing on an element level to characterize cyclic soil behavior and stiffness and strength degradation.

Soils encountered at offshore wind turbine sites vary widely in terms of soil types and engineering properties. [Table 6.2-1](#) summarizes the subsurface conditions for various offshore wind turbine (OWT) projects along the US east coast from Fugro's in-house project database. As shown, soils encountered at current developed or to-be-developed project sites consist mainly of sands of various thickness or sands overlying clays. For the sands, the relative densities are generally around 75 percent with peak friction angles of about 35 degrees and can be classified as generally "dense sand". For the clays, the plasticity indices (PI) were about 30 with undrained shear strength ranging between 40 to 100 kPa and can be classified as "firm to stiff clay".



Table 6.2-1: Soil Classification Properties for US East Coast Offshore Wind Turbine Projects

Project	Location	Soil Stratigraphy in Upper 15 Meters	Clay Properties			Sand Properties	
			PI	Su (kPa)	OCR	Rd	ϕ
Bay State Windfarm	Offshore Massachusetts	3~15 m sand overlying clay	30	60	-	77±10	~34
Cape Wind	Offshore Massachusetts	Primarily sand	-	-	-	75±10	~37
VOWTAP	Offshore Virginia	5 m sand overlying clay	30±15	40~100	1~6	75±10	~30
Deepwater Block 7033	Offshore New Jersey	Primarily sand	-	-	-	75±10	35±5
Bluewater Block 6325	Offshore Delaware	10 m sand overlying clay	-	-	-	70±10	~35
Bluewater Block 6936	Offshore New Jersey	Primarily sand with thin clay layer	-	-	-	75±10	~35
Deepwater	Offshore Rhode Island	Primarily sand	-	-	-	70±10	~34
Garden State	Offshore New Jersey	12 m sand overlying firm clay	-	-	-	-	~35

6.2.1 Elemental Cyclic Soil Behavior

Both cyclic simple shear and cyclic triaxial tests have been used previously to estimate soil strength and stiffness properties. To better address the elemental soil data gaps, well-documented cyclic experiments with both clayey and sandy soils are recommended. Considering that the majority of cyclic loads within soils are in the form of simple shear, we suggest that cyclic simple shear (CSS) tests be used.

For the clays, we propose a testing program primarily targeted to augment the dataset used by Vucetic and Dobry (1988) and provide data that can be used to extrapolate their proposed model to very large numbers of cycles, small shear strains typical of anticipated conditions, and establish a lower degradation limit if warranted. Other specifications for the CSS tests are listed in Table 6.2-2 below:



Table 6.2-2: Recommendation for Laboratory Cyclic Soil Elemental Tests

Material	Sand	Clay
Test type	Cyclic Simple Shear	Cyclic Simple Shear
Stress/Strain Control	Stress controlled	Stress controlled
Index Property	Rd = 75%	PI = 30
OCR	1, 2, 4	1, 2, 4
# of cycles	Ranging, Min. 100,000 cycles	Ranging, Min. 100,000 cycles
Cyclic Stress Level	various	various
Drainage Condition	Fully saturated, undrained	Fully saturated, undrained

6.2.2 Laboratory Model Experiments

Small-scale model experiments can be performed to shed light on the predominant mechanisms governing the cyclic response of OWT suction bucket foundations and provide a basis for numerical model calibration and validation. Given the general absence of small scale model tests for clays, we recommend that such tests be performed to advance our understanding of how soil response during a large number of loading cycles affects the foundation and structural system response. Additionally, given the very different potential cyclic response in sands depending on the drainage conditions, we recommend that model tests be conducted for saturated sand conditions with the primary goal of examining the drainage conditions and assessing whether a decrease or increase in stiffness is more likely to occur. For the case of the sand, centrifuge testing is preferable over 1-g testing as in-situ stresses, which govern the sand behavior, are appropriately simulated in the centrifuge. For the case of clay, both centrifuge and 1-g experiments could be considered.

Specifically, considering the data gaps and general soil condition in US east coastal area, testing setups in Table 6.2-3 are recommended:

Table 6.2-3: Recommendation for Laboratory Model Experiments

Soil Type	Water condition	Relative Density (Rd)	Plasticity Index (PI)	Cyclic Loading Mechanism	Loading Frequency (Hz)	# of cycles	Foundation Type
Sand	Fully Saturated	75	-	V, H, M	0.1	100,000 ~ 300,000	Mono- and Multi-buckets
Clay	Fully Saturated	-	30	V, H, M	0.1	100,000 ~ 300,000	Mono- and Multi-buckets



6.3 RECOMMENDATIONS FOR ADDITIONAL ANALYTICAL STUDIES

Additional analytical studies can help expand the number of cases analyzed in this study for the purpose of confirming the preliminary findings presented herein, generalizing the recommendations, and developing more quantitative design guidance. In particular, the following items should be considered.

6.3.1 Design Soil-Load Combinations

The results of the current study are limited in terms of the number of combinations of foundation design, soil type, and load conditions that have been analyzed; however, the study has developed a methodology for assessing the effects of a significant number of load cycles within a reasonable analysis run time. Additional combinations are required to provide a more complete analytical basis, which can then be used to develop more specific design guidance. We recommend that future studies be performed for compatible conditions where the foundation dimensions have been developed for the specific subsurface conditions and loading combinations.

6.3.2 Definition of “Threshold” Limits

It will be very useful for the foundation design team to understand the combinations of cyclic load amplitude and cyclic count that fall below the threshold limit of soil degradation (i.e., these are the combination of loads where cyclic degradation can be ignored). As recommended in Section 6.2, the strain threshold should be better estimated with the new testing program. The effect of the strain threshold towards cyclic suction bucket performance should also be evaluated for additional load cases discussed in Section 6.3.1.

6.3.3 Assessment of Degradation for Actual Foundations

The results of the current study are limited to some extent given that the foundation was not specifically developed for a set of site specific conditions and then analyzed for cyclic degradation as would be the case in an actual design process. It is suggested that a site specific example be developed with either a mono-bucket or multi-bucket design for a representative east coast site. The bucket diameter, spacing, and penetration depth would be developed for all of the applicable IEC and API load cases currently required by BOEM. This design would then be assessed for cyclic degradation following the same procedures defined in the current study. Such a study would help to provide a more complete example for designers to reference and would be based on bucket properties that are not under or over-designed for the conditions at the site.

6.3.4 Assessment of Cyclic Wind Loads

If it is determined that the amplitudes associated with cyclic wind loads are large enough to induce some amount of cyclic degradation, additional study should include rotor loads as a contributing source of cyclic load.



7.0 REFERENCES

- American Bureau of Shipping (ABS), "Guide for Building and Classing, Floating Offshore Wind Turbine Installations," January 2013 (updated July 2014), New York, United States.
- American Bureau of Shipping (ABS), "Guide for Building and Classing, Bottom-founded Offshore Wind Turbine Installations," January 2013 (updated July 2014), New York, United States.
- Andersen, K.H. & Berre, T. (1999), "Behavior of a dense sand under monotonic and cyclic loading," ECSMGE XII Geotechnical Engineering for Transportation Infrastructure, Proc., Vol. 2., Balkema, Rotterdam, 1999.
- Andersen et al. (1988), "Cyclic soil data for design of gravity structures," Journal of Geotechnical Engineering, Vol. 114, No. 5, May 1988.
- Andersen, K.H. (2015), "Cyclic soil parameters for offshore foundation design," Frontiers in Offshore Geotechnics III – Meyer (Ed.), London, UK.
- Andersen K.H. (2009), "Bearing capacity under cyclic loading – offshore, along the coast, an on land - The 21st Bjerrum Lecture, Oslo, Norway November 2007," published on the NRC Research Press Web, May 2009.
- Andersen, K.H. & Høeg, K. (1991), "Deformations of soils and displacements of structures subjected to combined static and cyclic loads," X ECSMFE, Firenze, Proc., (4): 1147–1158.
- Bhattacharya et al. (2013), "Dynamics of offshore wind turbines supported on two foundations," Proceedings of the institution of civil engineers, Geotechnical Engineering 166, April 2013, Issue GE2.
- Bundesamt Fur Seeschifffahrt Und Hydrographie (BSH), "Standard – Design of Offshore Wind Turbines," December 2007.
- Bundesamt Fur Seeschifffahrt Und Hydrographie (BSH), "Standard for Geotechnical Site and Route Surveys," 2008.
- Byrne B.W. and Houlsby G.T. (2004), "Experimental investigations of the response of suction caissons to transient combined loading," Journal of Geotechnical and Geoenvironmental Engineering, Vol. 130, No. 3, March 1, 2004.
- Byrne, P. M. (1991). A cyclic shear-volume coupling and pore pressure model for sand. Second International Conference on Recent Advances in Geotechnical Earthquake Engineering and Soil Dynamics, St. Louis Missouri.
- Cox et al. (2014), "Centrifuge study on the cyclic performance of caissons in sand," International Journal of Physical Modelling in Geotechnics, Vol. 14, Issue 4, 2014.
- Danish Energy Agency (DEA), "Recommendation for Technical Approval of Offshore Wind Turbines," December 2001.
- Det Norske Veritas (DNV), "Design of Offshore Wind Turbine Structures, DNV-OS-J101," Oslo, Norway, May 2014.



- Det Norske Veritas (DNV), "Design of Floating Wind Turbine Structures, DNV-OS-J103," Oslo, Norway, June 2013.
- Det Norske Veritas (DNV), "Offshore Substations for Wind Farms, DNV-OS-J201," Oslo, Norway, November 2013.
- Dyvik et al. (1989), "Model tests of gravity platforms I: Description," *Journal of Geotechnical Engineering*, Vol. 115, No. 11, November 1989.
- Erbirch et al. (2016), "Numerical Modeling of Seismically Induced Settlement for Ichthys Riser Support Structure," *Offshore Technology Conference, OTC-26778-MS*
- Fugro Consultants (2014), "Site characterization and geotechnical engineering analysis, VOWTAP demonstration project, offshore Virginia, outer continental shelf," prepared for Dominion Resources, May 2015.
- Germanischer Lloyd (GL), "Guideline for the Certification of Offshore Wind Turbines," Hamburg, Germany, Edition 2005.
- Guo et al. (2013), "Undrained deformation behavior of saturated soft clay under long-term cyclic loading," *Soil Dynamics and Earthquake Engineering* 50 (2013), 28-37.
- Houlsby, G. T., and Byrne, B. W. (2000). "Suction caisson foundations for offshore wind turbines and anemometer masts." *Wind Eng.*, 24(4), 249–255.
- Houlsby, G. T., Ibsen, L. B., and Byrne, B. W. (2005). "Suction caissons for wind turbines." *Proc., Int. Symp. on Frontiers in Offshore Geotechnics*, Taylor & Francis Group, London, 75–94.
- Houlsby et al. (2005), "Field trials of suction caissons in clay for offshore wind turbine foundations," *Geotechnique* 55, No. 4, 287-296.
- Houlsby et al. (2006), "Field trials of suction caissons in sand for offshore wind turbine foundations," *Geotechnique* 56, No. 1, 3-10.
- Ibsen, L. B., Liingaard, S., and Nielsen, S. A. (2005). "Bucket foundation, astatus." *Proc., Copenhagen Offshore Wind*, EWEA, Brussels, Belgium.
- International Electrotechnical Commission (IEC), "Wind Turbines – Part 1: Design Requirements, IEC 61400-1," August 2005.
- International Electrotechnical Commission (IEC), "Wind Turbines – Part 3: Design Requirements for Offshore Wind Turbines, IEC 61400-3, Edition 1.0," February 2009.
- Itasca (2015), "FLAC3D Fast Lagrangian Analysis of Continua in 3 Dimensions, User's Guide",
Itasca Consulting Group Inc., version 5.01
- Kelly et al. (2006), "A comparison of field and laboratory tests of caisson foundation in sand and clay," *Geotechnique* 56, No. 9, 617-626
- Kelly et al. (2006), "Transient vertical loading of model suction caissons in a pressure chamber," *Geotechnique* 56, No. 10, 665-675.



- Kim et al. (2014), "Investigation of monotonic and cyclic behavior of tripod suction bucket foundations for offshore wind towers using centrifuge modeling," *Journal of Geotechnical and Geoenvironmental Engineering*, 140, 2014.
- Lee et al. (2016), "Foundation Design and Installation for the Ichthys Riser Support Structure," *Offshore Technology Conference*, OTC-26786-MS
- Liingaard, M. (2006), "Dynamic behavior of suction caissons," PhD Thesis, Aalborg University, December 2006.
- Mortezaie, A., & Vucetic, M. (2016). Threshold Shear Strains for Cyclic Degradation and Cyclic Pore Water Pressure Generation in Two Clays. *Journal of Geotechnical and Geoenvironmental Engineering*, 142(5), 04016007.
- Nippon Kaiji Kyokai (NKK), "ClassNK Guidelines for Offshore Floating Wind Turbine Structures," Tokyo, Japan, 2012.
- Vucetic, M. & Dobry, R. (1988), "Degradation of marine clays under cyclic loading," *Journal of Geotechnical Engineering*, Vol. 114, No. 2, February 1988.
- Wichtmann, T., & Triantafyllidis, T. (2004). Influence of a cyclic and dynamic loading history on dynamic properties of dry sand, part I: cyclic and dynamic torsional prestraining. *Soil Dynamics and Earthquake Engineering*, 24(2), 127-147.
- Wichtmann, T. Niemunis, A., Triantafyllidis, Th. (2010), "On the elastic stiffness in a high-cycle accumulation model for sand: comparison of drained and undrained cyclic triaxial tests," *Canadian Geotechnical Journal*, Vol. 47, No. 7, 2010.
- Yasuhara et al. (1982), "Cyclic Strength and Deformation of Normally Consolidated Clay," *Japanese Society of Soil Mechanics and Foundation Engineering, Soils and Foundations*, Vol. 22, No. 3, September 1982.
- Yasuhara et al. (1992), "Effects of Cyclic Loading on Undrained Strength and Compressibility of Clay," *Japanese Society of Soil Mechanics and Foundation Engineering, Soils and Foundations*, Vol. 32, No. 1, March 1992.
- Zhu et al. (2013), "Long-term lateral cyclic response of suction caisson foundations in sand," *Journal of Geotechnical and Geoenvironmental Engineering*, Vol. 139, No. 1, January 2013.